Cape Peninsula
University of Technology

Bio-oxidation of ferrous iron at low temperature conditions in a packed bed column bioreactors

by

Chukwunonso Emmanuel Chukwuchendo

Thesis submitted in fulfillment of the requirements for the degree

Masters of Engineering: Chemical Engineering

in the Faculty of Engineering

at Cape Peninsula University of Technology

Supervisor: Prof T.V. Ojumu

November 2016

DECLARATION

I, Chukwunonso Emmanuel Chukwuchendo, declare that the contents of this thesis represent my own unaided work and that the thesis has not previously been submitted for academic examination towards any qualification. Furthermore, it represents my own opinions and not necessarily those of the Cape Peninsula University of Technology.

…… …….

Signed Date

ABSTRACT

The oxidation of microbial ferrous iron is an important sub-process in the bioleaching process. Several studies focussing on microbial ferrous iron oxidation have been investigated and reported in various studies. These studies were carried out using stirred tank bioreactors and shake flasks at optimum conditions. However, these studies could not describe the context of heap bioleach system. Packed column system may describe heap bioleaching, and most studies on microbial ferrous iron oxidation were performed under flooded conditions, which do not represent solution flow dynamics in a heap situation.

Biooxidation of ferrous iron oxidation kinetics of *Acidiobacillus ferrooxidans* was studied in a packed-bed bioreactor to investigate the kinetics in a system that mimics the solution flow dynamic of a heap bioleach operation at low-temperature conditions. This was done in a batch mode operation, with glass marble (15 mm) as reactor packing. The pH of the bioreactor was maintained at pH 1.35 ± 0.05 and aeration at 500 ml/min. Unstructured models known as Monod and Hansford were used to describe the experimental data in determining the kinetics of bio-oxidation.

The effect of low temperature on the kinetic parameters was investigated at 6, 7, 8, and 10°C. The results of the kinetics obtained upon analysing experimental data showed that the maximum microbial ferrous iron oxidation rate, $r_{Fe^{2+}}^{max}$ and kinetic constant, $K_{Fe^{2+}}$ increased linearly as temperature increased within the temperature range investigated. The maximum microbial ferrous iron oxidation rates, $r_{Fe^{2+}}^{max}$, determined in this study within the temperature (6, 7, 8 and 10°C) range studied are 1.078, 1.300, 1.554 and 1.656 mmol/L.h. Similar studies on microbial ferrous iron conducted in stirred tank reactors, reported a rate of 0.025 mmol/L.h at 4°C. With the aid of Arrhenius equation, it was possible to show the relationship between microbial oxidation rate and temperature. An activation energy (E_a = 65.7 kJ/mol) was obtained, indicating a limitation in biochemical reaction at low temperatures.

In addition, the bioreactor was observed to be clear of ferric precipitate at low temperature for the culture of *Acidiobacillus ferrooxidans* during the course of experiments. At maximum solution redox potential, the effect of low temperature on Fe(III) precipitate in a packed column bioreactors was studied. The solution in the bioreactor upon reaching its maximum solution redox potential was allowed to operate for additional 36 hours at every 6 hours interval of sampling. Experimental data generated during this investigation was described by rate

equation. The results showed a linear increase in rate constant kinetics with an increase in temperature. The fit was observed to be first order due to higher kinetic constants obtained in first order compared to second order. Fe(III) precipitate that precipitated in solution with the lowest precipitate (1.90 g/L) was recorded at 8°C at the average rate of 1.507 mmol/L.h.

However, it was noted that despite the solution in the bioreactor reaching its maximum redox potential, the rate continued to increase in all the tested temperatures. Fe(III) precipitate evaluated during the 36 hours was found to be insignificant due to a shorter time of operation. The data generated during the study of Fe (III) was also described by Arrhenius equation. The activation energy value of 77.1 kJ/mol and a frequency factor of 1.82 X 10^9 mmol Fe^{3+}. h^{-1} were obtained during the investigation.

This study on microbial ferrous iron oxidation at low temperature by *Acidiobacillus ferrooxidans* can be improved in a simulated heap bioleach system as compared to stirred tank reactors. It also showed that the formation of Fe precipitate within the walls of the bioreactors will occur after several periods of operation.

DEDICATION

This thesis is dedicated first, to my Creator for being with me throughout my journey as a student in South Africa. My Creator is good is good, I am blessed for taking refuge in him. To my mother, whose endless prayers, love and encouragement brought about strength. I also dedicate this thesis to my siblings for their moral support, and for their fully support on this journey. It is specifically dedicated to my late father, Chief Ichie R. A. Chendo, whose principles and wisdom have been my bedrock. It is sad that you are not alive to witness this great height of academic success. Above all, I am immensely grateful for all you gave me.

"Comparison is capable of destroying your chances to be great in life, discover your pace and walk the path to greatness"

Rotimi Williams

ACKNOWLEDGMENT

I am sincerely appreciative to all those who contributed to the accomplishment of my thesis:

- My Creator for the courage he afforded me and for helping me to persevere throughout the period of this study
- Prof TV Ojumu whose supervisory role, insightful criticisms, wise advice, patience and encouragement contributed to my completing this thesis.
- Prof SKO Ntwampe for his advice towards the completion of this thesis
- Dr. V Okudo whose advice and encouragement sustained me through this journey
- Dr. B Godongwana for his contribution on the kinetics aspect of this study
- Mr. R Ademola, whose input contributed to the success of this thesis
- Mr. A Bester and Mrs H Small for their technical assistance throughout this study
- Mr. B Mabika, an intern whose assistance contributed during experimental runs for this study.
- A big thank you to my friends and family for keeping me motivated.
- A special thank you to my brothers PA Chendo and PO Chendo for their financial and moral support. I appreciate you two.
- A special thank you to my nephews (Uchenna and Ebube) and nieces (Chinyere and Chisom) for being patient during my busy times.
- Ms CN Ben whose encouragement and prayer serves as a catalyst to seeing the completion of this study.
- My family for their love, prayers and encouragement.
- A big thank to my brother AE Iwuchukwu for his assistance during the hard times.
- All my postgraduate colleagues and the Chemical Engineering staff for their support and assistant.

LIST OF PUBLICATION AND PRESENTATION

Oral presentation

1 **Chukwuchendo, E. C** and Ojumu, T. V. 2016. Biooxidation of ferrous iron oxidation at low-temperature conditions in a packed column bioreactor. Hydrometallurgy Conference 2016, Cape Town, South Africa, 01 – 03 August 2016

2 **Chukwuchendo, E. C** and Ojumu, T. V. (2017). Microbial ferrous ion oxidation versus ferric ion precipitation at low-temperature condition. International Bio-hydrometallurgy Symposium, 24 -27 September 2017, TU Bergakademie Freiberg/Germany **(Accepted)**

Poster presentation

1 **Chukwuchendo, E. C** and Ojumu, T. V. 2016. Biooxidation of ferrous iron oxidation at low-temperature conditions in a packed column bioreactor. Hydrometallurgy Conference 2016, Cape Town, South Africa, 01 – 03 August 2016

Journal publication

1 **Chukwuchendo, E. C** and Ojumu, T. V. (2017). Investigation of microbial ferrous ion oxidation at low-temperature conditions in a packed column bioreactor (To be submitted).

TERMS AND CONCEPTS CITED

Bioleaching: Bioleaching refers to the dissolution of metals from their ores in solution, which is facilitated/catalysed by certain microorganisms, e.g. bacteria and archaea.

Heap bioleaching: Heap bioleaching is a mineral processing technology whereby large piles of low-grade, crushed ores or rock are leached with various chemical solutions that extract valuable minerals facilitated by microorganisms**.**

Jarosite: Jarosite is a basic hydrous sulfate of iron with a chemical formula of $XFe_3(SO_4)_2(OH)_6$, where X = K^+ (potassium jarosite), Na^+ (natrojarosite), NH_4^+ (ammoniojarosite), or H_3O^+ (hydronium Jarosite). This sulfate mineral is formed in ore deposits by the oxidation of iron sulfides.

Mesophilic bacteria: These are most common iron-oxidising and sulphur-oxidising

Micro-organisms found in commercial bioleaching processed at optimum temperatures below 40 °C.

Packed-bed bioreactor: A packed-bed bioreactor is a hollow pipe that is filled with a packing material (eg glass beads, Raschig rings) that mimic a typical heap system.

TABLE OF CONTENTS

LIST OF FIGURES

LIST OF TABLES

NOMENCLATURE

Symbol	Description	Unit
a	Gas-liquid interfacial area per unit volume of fluid	$m^2.L^{-1}$
$a_{Fe^{2+}}$	Activities of species ferrous-iron	$mmol.L^{-1}$
$a_{Fe^{3+}}$	Activities of species ferric-iron	$mmol.L^{-1}$
A_h	The gas-liquid interfacial area at a height h	m^2
a_h	Specific interfacial area at height h	m^2
a_i	Activity of species i	$mmol.L^{-1}$
C_{AL}	Oxygen concentration in the broth	$mmol.L^{-1}$
C^*_{AL}	Solubility of oxygen in the broth	$mmol.L^{-1}$
C_X	Cell concentration	$mmol\ C.L^{-1}$
C_{X_0}	Initial bacteria concentration	$mmol\ C.L^{-1}$
$[E]$	Concentration of the enzyme	$mmol.L^{-1}$
E_a	Activation energy	$kJ.mol^{-1}$
E_h	Standard redox potential	mV
E'_h	Solution potential	mV
$[ES]$	Concentration of the enzyme-substrate complex	$mmol.L^{-1}$
$[E_T]$	Total concentration of the enzyme	$mmol.L^{-1}$
F	Faraday's constant	$Coulomb.mol^{-1}$
$[Fe^T]$	Total iron	$mmol.L^{-1}$
$[Fe^{2+}]$	Ferrous-iron concentration	$mmol.L^{-1}$
$[Fe^{3+}]$	Ferric-iron concentration	$mmol.L^{-1}$

K_0	Frequency factor	mmol Fe^{2+}.L^{-1}
K_d	Specific death rate constant	h^{-1}
k_1	First order rate constant	h^{-1}
k_2	Second order rate constant	M^{-1} h^{-1}
$K_{1,ES}$	Rate constant for enzyme-substrate complex formation	L.mmol$^{-1}h^{-1}$
$K_{2,ES}$	Rate constant for reverse enzyme-substrate complex formation	L.mmol$^{-1}h^{-1}$
$K_{3,ES}$	Rate constant for product formation	L.mmol$^{-1}h^{-1}$
$K'_{Fe^{2+}}$	Affinity constant	Dimensionless
$K_{Fe^{2+}}$	Ferrous iron based affinity constant	mmol Fe^{2+} .L^{-1}
$K_{Fe^{3+}}$	Ferric iron based affinity constant	mmol Fe^{3+} .L^{-1}
K_L	Liquid phase mass transfer coefficient	$m.s^{-1}$
K_m	Michaelis-Menten constant	mmol Fe^{2+} .L^{-1}
$m_{Fe^{2+}}$	Maintenance coefficients based on ferrous-iron	mmol. (mol C)$^{-1}$ .h^{-1}
n	Number of moles of electrons transferred in the half reaction	Dimensionless
N_A	The rate of O_2 and CO_2 transfer from gas to liquid	$mmol.s^{-1}$
$q_{Fe^{2+}}$	Microbial specific ferrous-iron utilisation rate	mmol. (mol C)$^{-1}h^{-1}$
$q^{max}_{Fe^{2+}}$	Maximum microbial ferrous-iron utilisation rate	mmol (mol C)$^{-1}h^{-1}$
q_{O_2}	Microbial specific oxygen utilisation rate	mmol (mol O)$^{-1}h^{-1}$
$q^{max}_{O_2}$	Maximum microbial specific oxygen utilisation rate	mmol (mol O)$^{-1}h^{-1}$
R	Universal gas constant	J.mol$^{-1}K^{-1}$

R^2	Regression coefficient	Dimensionless
rCO_2	Oxygen utilisation rate	mmol CO_2.L^{-1} h^{-1}
$r_{(ES)}$	Net rate of formation of the enzyme-substrate complex	L.$mmol^{-1}h^{-1}$
$-r_{Fe^{2+}}$	Ferrous-iron oxidation rate	mmol.$L^{-1}h^{-1}$
$r_{Fe^{2+}}^{max}$	Maximum ferrous-iron oxidation rate	mmol.$L^{-1}h^{-1}$
$-r_{O_2}$	Oxygen utilization rate	mmol.$L^{-1}h^{-1}$
r_X	Cell production rate	mmol.$L^{-1}h^{-1}$
$[S]$	Substrate concentration	mmol.L^{-1}
T	Absolute temperature	K
$Y_{Fe^{2+}}$	Microbial yield on ferrous iron	mmol C.(mmol Fe^{2+})$^{-1}$
$Y_{Fe^{2+}X}^{max}$	Maximum microbial yield on ferrous iron	

Greek Symbols

μ	Specific growth rate	H
μ_{max}	Maximum specific growth rate	h^{-1}
γ_i	Activity coefficient	Dimensionless

LIST OF ABBREVIATIONS

Abbreviation	Description
ADP	Adenosine diphosphate
AMD	Acid mine drainage
ARD	Acid rock drainage
At.	*Acidothiobacillus*
ATP	Adenosine triphosphate
BDS	Barium Diphenylamine Sulphonate
CSTR	Continuous stirred tank reactor
CycA1	Cytochrome-cA1
Cyc1	Cytochrome-c1
Cyc2	Cytochrome-c2
E	Enzyme
EDTA	Ethylenediaminetetraaacetic acid
EPS	Exopolysaccharide layer
ES	Enzyme-substrate
Ib	Pound
L.	*Leptospirillum*
OZ	Ounce
P	Product
PLS	Pregnant leaching solution
S	Substrate
SHE	Standard hydrogen electrode
SSE	Sum of squares error
UCT	University of Cape Town
USA	United State of America

Chapter 1: Introduction

1.1 Background

Bioleaching has been defined as a technology that involves the extraction of metallic compounds from ores and concentrates by the use of biocatalyst under normal pressure and temperature between 5-90°C (Tekin et al., 2014). The process is simple, efficient and it is also an environmentally friendly method to process ores. It has also been successfully applied for the recovery of valuable minerals such as copper, cobalt and other minerals. This process of extraction comprises the solubilisation of components from complex solid phase to liquid (Bosecker, 1997). It is also applied in the pre-treatment method for refractory gold ores, where it is utilized in removing intrusive metal sulfides before cyanidation (Chowdhury, 2012, Ojumu et al., 2008, Rohwerder et al., 2003).

Various bioleaching techniques such as stirred tank, heap or dump have been applied to the mineral extraction of different ores in the mining industries. Tank bioleaching is operated at optimum conditions, and its operating variables are controllable. Due to high operating cost and the diminution of high-grade ores that may be involved in tank bioleaching, the use of both heap and dump bioleaching for low-grade ores become alternative to the leaching of low grade and run-of-mine (ROM) ores (Chowdhury, 2012, Ngoma, 2015). Microbial ferrous iron oxidation is reported by several researchers as a sub-process in bioleaching of sulfide minerals.

Microbial ferrous iron oxidation is achieved by a sequence of cyclic reactions comprising both direct and indirect processes. The purpose of microorganisms is to catalyse the oxidation of ferrous-iron (Fe^{2+}) to ferric-iron (Fe^{3+}) in acidic medium (Dopson et al., 2007), and the oxidation of sulfur compounds to sulfur or sulfates. The resulting ferric ion, Fe^{3+}, is an oxidizing agent that serves as a lixiviant for the oxidation of metal sulfides. While the reduced ferrous ion, Fe^{2+}, is regenerated in a cyclic bioleaching process by indirect mechanisms (Mazuelos et al., 2001).

Most studies on microbial oxidation of ferrous ion were conducted at near optimum conditions for microbial performance. Although limited studies conducted at low temperatures were also investigated with the use of stirred tank and flask shakes, where operating conditions are controllable (Ahonen and Tuovinen, 1989, Dopson et al., 2007, Kupka et al., 2007). These cannot be compared to heap bioleaching in terms of the fluid dynamics in bioleach heap. The wide range of operating conditions (e.g. pH, temperature, etc) for the microbial ferrous iron oxidation that was investigated by Ojumu et al. (2009) may also not be applicable to the heap, especially where prevailing conditions were at the extremes. It has been recorded that zone of temperatures less than 10^{o}C may be found in such bioleach heaps (Ojumu et al., 2009, Ongendangenda and Ojumu, 2011). Moreover, overall relatively high rates of mineral oxidation

were reported at a temperature lower than 21^{o}C due to the fact that ferric iron remained in solution despite pH increment above 1.6 but precipitated at higher temperatures (Dopson et al., 2007, Kupka et al., 2007).

It is clear that temperature has a major effect on the formation of ferric ion precipitates in biological iron oxidation (Ahonen and Tuovinen, 1989, Dopson et al., 2007). In lower temperature conditions, it is understood that precipitate formation will decline compared to high-temperature conditions (Ahonen and Tuovinen, 1989). Although, a limited number of authors have investigated ferric ion precipitate formation at low-temperature conditions which were conducted in batch reactors. It was observed that cultures that oxidized ferrous iron at low temperature were clear of precipitates during active oxidation, but precipitate occurs after several months operations (Ahonen and Tuovinen, 1989, Kupka et al., 2007), which may have implication in the context of bioleach heap. These studies may not mimic the real bioleach heap situations and the fact that the kinetics of the precipitates were not reported may be due to insignificant ferric precipitation over a short period of time.

Hence, it is important to investigate microbial ferrous iron oxidation under cold temperature condition and more importantly, to investigate the kinetics of ferric ion precipitation in a system that can reasonably mimic bioleach heap, such as a packed-bed bioreactor. This is necessary to facilitate design and kinetic prediction of processes that may be operating under this non-optimum condition, especially in a reactor configuration, which can mimic, reasonably, the solution flow dynamics relevant to bioleach heap.

1.2 Research objectives

The objective of this study was to investigate the kinetics of microbial ferrous ion oxidation and the resulting ferric ion precipitation by a strain of mesophilic bacteria *Acidiobacillus ferrooxidans* in a temperature controlled packed-bed bioreactor. This is to understand the effects of temperature on the kinetics in a system that simulates bioleach heap condition.

In specific terms, this study will investigate:

- The kinetics of ferrous ion bio-oxidation by *Acidiobacillus ferrooxidans* at 10, 8, 7 and 6°C in a packed-bed bioreactor
- The kinetics of the resulting ferric ion precipitation in the system described in (a) above
- The effects of temperatures (10, 8, 7 and 6°C) on both kinetics with a view to determining the activation energy of both processes

1.3 Research design and methodology

Experiments on ferrous iron bio-oxidation were performed at a fixed pH and aeration rate using a temperature controlled packed-bed bioreactor. The methodology was adapted from (Chowdhury and Ojumu, 2014). The experiment set-up was airtight when assembled, and the column was packed with inert materials to simulate inert mineral ore. An inoculum containing predominately *Acidithiobacillus ferrooxidans* was used and the ferrous-iron concentration in the growth medium, 5 $g.L^{-1}$ Fe^{2+} added as $FeSO_4$. $7H_2O$ was chosen to simulate a heap bioleach situation.

The solution was then fed to the packed-bed reactor from the top of the column using a peristaltic pump and aerated from the bottom to simulate the dynamic flow of the solution. Contrary to the previous studies (Chowdhury, 2012, Chowdhury and Ojumu, 2014, Wanjiya, 2013), the effluent from the bottom of the bioreactor was recycled back into the reactor from the top, to enhance mixing, and as such the reactor is operated effectively as a batch system**.** The redox potential was monitored using CRISON GLP 21 meter and samples were collected from the recycle stream and analysed in order to determine the total iron concentration and ferrous by titration.

1.4 Delineation of study

This study was exclusive to microbial ferrous-iron oxidation by *Acidithiobacillus ferrooxidans* in a packed-bed bioreactor at low temperature. In this study, the oxidation of other minerals by ferrous iron and the intra- and inter-particle diffusion are assumed to have no effect on the oxidation kinetics. The experimental trials were conducted in a packed-bed bioreactor that simulates the flow dynamics of heap situation and glass balls was used as the inert packing material.

1.5 Significance of the study

The research investigated the microbial ferrous iron oxidation under cold condition in packed column bioreactor system that was operated in a similar conditions as bioleach heap. This is to evaluate the kinetics under such system, it also quantified the amount of Fe(III) (jarosite) formed under the same condition. Results from this study could provide an understanding of the expected slow kinetics and the significance of the precipitate, which may be useful in design consideration of bio heap systems.

1.6 Thesis outline

This thesis is divided into seven chapters that are structured as follows:

Chapter 1 comprises a summary of the background to the research project, the problem statement as well as the research objectives which defines the purpose of the study. In addition to this, there are discussions of the findings of previous studies that are in contrast to the process of heap bioleaching. Lastly, there is an outline of the significance of the study, the research design and methodology adapted for the study.

Chapter 2 provides a brief historical description about heap bioleaching through a literature review. The literature review includes studies done on the application of heap bioleaching, the chemistry and mechanism of bioleaching, and the types of microorganisms involved. It provides an account of the microbial growth and kinetics of ferrous-iron oxidation with effects of operating conditions**.** This chapter also provides a brief overview of jarosite formation. In addition, it discusses relevant factors (e.g. pH, temperature, aeration, packing size, jarosite) affecting microbial ferrous-iron oxidation kinetics.

Chapter 3 describes the detailed experimental rig and approach used in this study. It also offers an account of the theoretical calculations involved in substrate consumption and the detailed method used in quantifying the jarosite formed.

Chapter 4 & 5 present the study's experimental results and analysis. While Chapter 4 specifically discusses the effects of changes in temperature, chapter 5 focuses on the effects of ferric iron precipitate in the packed-bed bioreactor. The experimental data obtained was correlated to an appropriate rate equation reported in literature.

Chapter **6** summarises the main points of the study by highlighting the unique aspects, articulating the conclusions reached as well offering recommendations for future work to complement the objectives met in this study. While chapter **7** is a list of the references cited in the thesis.

Chapter 2: Literature Review

In this chapter, the historical background of heap bioleaching, the microorganisms involved in the process as well as the established mechanisms are discussed. Moreover, the literature review provides a critical evaluation of microbial ferrous iron oxidation and bioleaching techniques as relation to the conditions that are applicable to heap bioleaching. The literature review is necessary identify the knowledge gaps that currently exist in literature and to highlight the significance of the study.

2.1 Heap bioleaching

In Seville, which is situated in the south of Spain, copper and silver were discovered by Romans and Pre-Romans from an existing located deposit. The extraction of copper from its ore through the process of bioleaching and the precipitation of copper from the resultant solution through treatment with metallic iron is an ancient technology (Ehrlich, 2001). In heap bioleaching, the mineral sulfides are crushed, agglomerated, placed in engineered piles; sprayed above the top with acidic leach liquor and aeration is provided to the system (heap) from the bottom (Dopson et al., 2007). The microorganisms present catalyse mineral breakdown and the soluble metal is collected at the bottom of the heap. The technology was practiced by the Chinese about 100–200 BCE. Although the leaching of copper ore and cementation were also known in Europe and Asia during the second century, the technology may have been in existence prior to this civilization. Moreover, it is unknown whether this knowledge originated from China or was brought to China (Ehrlich, 2001).

Quebrada Blanca operation which is situated in northern Chile is an example of a commercial bioleach application. The location of this commercial bio-leach plant is at an elevation of 4400 m on the Alti Plano. Information about eleven copper bio-heap leach plants and one in-situ bioleaching operation commissioned in 1980 is given in Table 1. Also, a large scale of copper was extracted at the Rio Tinto mine, which later became Rio Tinto due to the red colour imparted to the water by the high ferric iron concentration**.** Although, this dissolved ferric iron (and the less easily seen dissolved copper) is due to natural microbial activity (Rawlings, 2002)

At Rio Tinto, heap leaching was established and a process of copper leaching from partially roasted ore was developed in 1752 (Ehrlich, 2001). The process was considered to be a natural phenomenon, as the involvement of microorganisms in the mineral leaching for the extraction of copper was not known by the miners until recently because there was no general knowledge of the existence of microorganisms until the mid-seventeenth century. (Bosecker, 1997, Wanjiya, 2013, Ojumu et al., 2008, Ehrlich, 2001, Rawlings, 2002).

Table 1: Commercial copper bio-heap leach plants (Brierley and Brierley, 2001)

Plant	Size (t/day)	Years in operation
Lo Aguirre, Chile	16, 000	1980 - 1996
Gunpowder's Mammoth Mine, Australia	In-situ[a]	1991 – present
Mt. Leyshon, Australia	1370	1992 – in closure (1997)
Cerro Colorado, Chile	16, 000	1993 – present
Girilambone, Australia	2000	1993 – present
Ivan-Zar, Chile	1500	1994 – present
Quebrada Blanca, Chile	17, 300	1994 – present
Andacollo, Chile	10, 000	1996 – present
Dos Amigos, Chile	3000	1996 – present
Cerro Verde, Peru	15, 000	1996 – present
Zaldivar, Chile	≈ 20, 000	1998 – present
S&K Copper Project, Myanmar	15, 000	1998 – present

[a] ≈ 1.2 million tonne ore body.

The process of bio-hydrometallurgy began with the bioleaching of copper from sub-marginal grade, run-of-mine material (Brierley and Brierley, 2001, Chowdhury, 2012). This process has been successfully applied since the 1950s for the processing of oxides and sulfides in dumps (Panda et al., 2012). However, bio-hydrometallurgical expansion into the recovery of other metals (except copper) only occurred during the mid-1980s, when the first commercial plant for pre-treatment of refractory gold-bearing concentrate was commissioned at the Fairview operation in South Africa (Olson et al., 2003). This brought about an expansion of bio-hydrometallurgy into the recovery of metals. The plant is used for treating refractory arsenopyrites/pyrite gold-bearing concentrate, in large stirred tanks and aerated, continuous flow reactors have been in operation since 1986.

The processes for copper and refractory gold pre-treatment are designed to stimulate the activity of microorganisms (Brierley and Brierley, 2001, Olson et al., 2003). Commercial plants that use similar aerated stirred tank processes treat concentrates that are prepared from ores to enrich the gold and sulfide content (Olson et al., 2003). The shutdown of the Youanmi bio-oxidation pretreatment plant and delay in the start-up of Newmont's commercial bio-oxidation heap pretreatment process reflect the impact of these processes on the price of gold (Brierley and Brierley, 2001).

From Figure 2.1, it can be seen that most bio-hydrometallurgical innovations have been commercially implemented during times of low metal prices, indicating that the mining industry

is more inclined to apply bio-hydrometallurgical processes during leaner times (Brierley, 2010). About 16 000 tons of ore per day were processed in the Lo Aguirre mine in Chile. The recovery of gold ranges from 60 – 80% of the contained value is subject to mineralogy and particle size used.

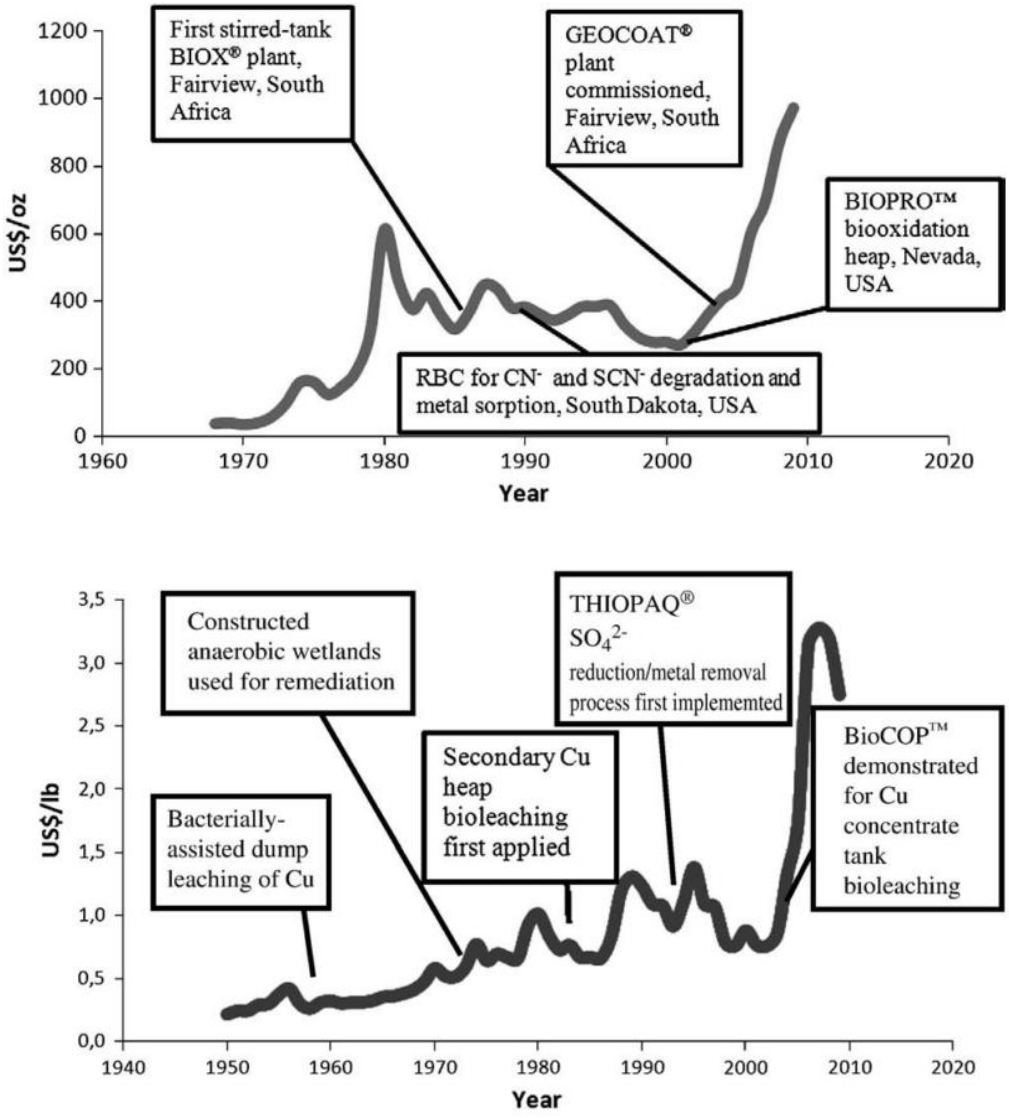

Figure 2.1: Cumulative average gold price (US$/oz) from 1968 through 2009 and average copper price (US$/lb) from 1950 through 2008, with significant bio-hydrometallurgical applications (Brierley, 2010).

2.2 Application of bioleaching techniques

The application of heap bioleaching in industry shows its significance in the recovery of metals that have metal concentrations of below 0.5% (w/w) (Bosecker, 1997). The treatment of precious and base metals in bioleaching is applied through three main forms in the industrial categories. These include stirred tank, irrigated dump, and the heap process. These are processes controlled in treating of low-grade sulfide mineral ores involving secondary minerals (Wanjiya, 2013). The operating cost associated with stirred tank bioleaching is very high.

Therefore, it is applied in the leaching of high-grade ore concentrates and the use of highly aerated continuous flow reactors, that are placed in series (as shown in Figure 2.2) is applied in the treatment of minerals in stirred tank procedures.

The mineral feed needs to be in the form of a finely milled concentrate, the concentrate from the stock is then diluted to 20% solids by mass before being fed to the primary tank. The overflow stream is connected from tank to tank until microbial oxidation of the mineral concentrate is complete (Ojumu et al., 2009). However, in a continuous flow with a cascade of tanks, there is variation in conditions, such as the concentrations of soluble metals and metalloids as a result of increasingly extensive mineral oxidation. This can impact on diversity and numbers of indigenous microbial species. The operation of the stirred tank reactor is limited in the restriction of its application to the treatment of mineral when moderate volumes of ore are to be processed. Yearly, about 11,000 tons of gold concentrates are bio-oxidized in reactors (Van Aswegen et al., 2007, Ojumu et al., 2009).

Heap, dump, and in-situ bioleaching are examples of irrigation based leaching processes**.** The heap bioleaching method is similar to dump leaching, however, the process is designed to be more efficient (Rawlings, 2002, Bosecker, 1997). This involves the crushed ore being acidified with sulphuric acid and agglomerated in rolling drums to bind fine particles to coarse particles. The agglomerated ore is irrigated using acid ferric-iron solution which contains bacteria and subsequently with recycled heap reactor effluent. This agglomerated ore is then stacked between 2 to10 m high on irrigation pads (Rawlings, 2002), lined with high-density polyethylene in order to avoid loss of solution. The operation of the system is achieved by irrigating them from the top in a continuous or intermittent mode (Wanjiya, 2013).

The mineral particles that are fed to the heap system are larger and mainly constitute the inert matrix having small valuable minerals. During the construction of heap leaching, aeration pipes may be included to enforce aeration and catalyse the process of bioleaching (Rawlings, 2002). The small particle size and the introduction of aeration from underneath is a fundamental distinction between dump and heap bioleaching as shown in Figure 2.2. The coupling of dump leaching, copper oxide heap leaching and industrial microbiology in the past decades has produced a positive commercial process for bio-heap leaching of secondary copper (primarily chalcocite and covellite) ores. This has also been the case for the technical demonstration of sulfidic refractory precious metal ore bio-heap leaching (Brierley and Brierley, 2001).

In order to achieve efficient microbial leaching, the process is carried out in enormous heaps of sulphide material, allowing water to dissolve the metal sulphates and migrate via the heap base, where they are removed, through a drainage system into collection ponds as pregnant leach solution (PLS) (Bosecker, 1997, Pantelis and Ritchie, 1990, Ojumu et al., 2009). The metal of economic interest is removed from the PLS through a suitable process and the barren

solution is recycled to the top surface of the heap for re-use (Ojumu et al., 2009, Petersen and Dixon, 2007, Chowdhury, 2012). The practicing of the leaching occurred in a large basin consisting about 12 000 tons of ore.

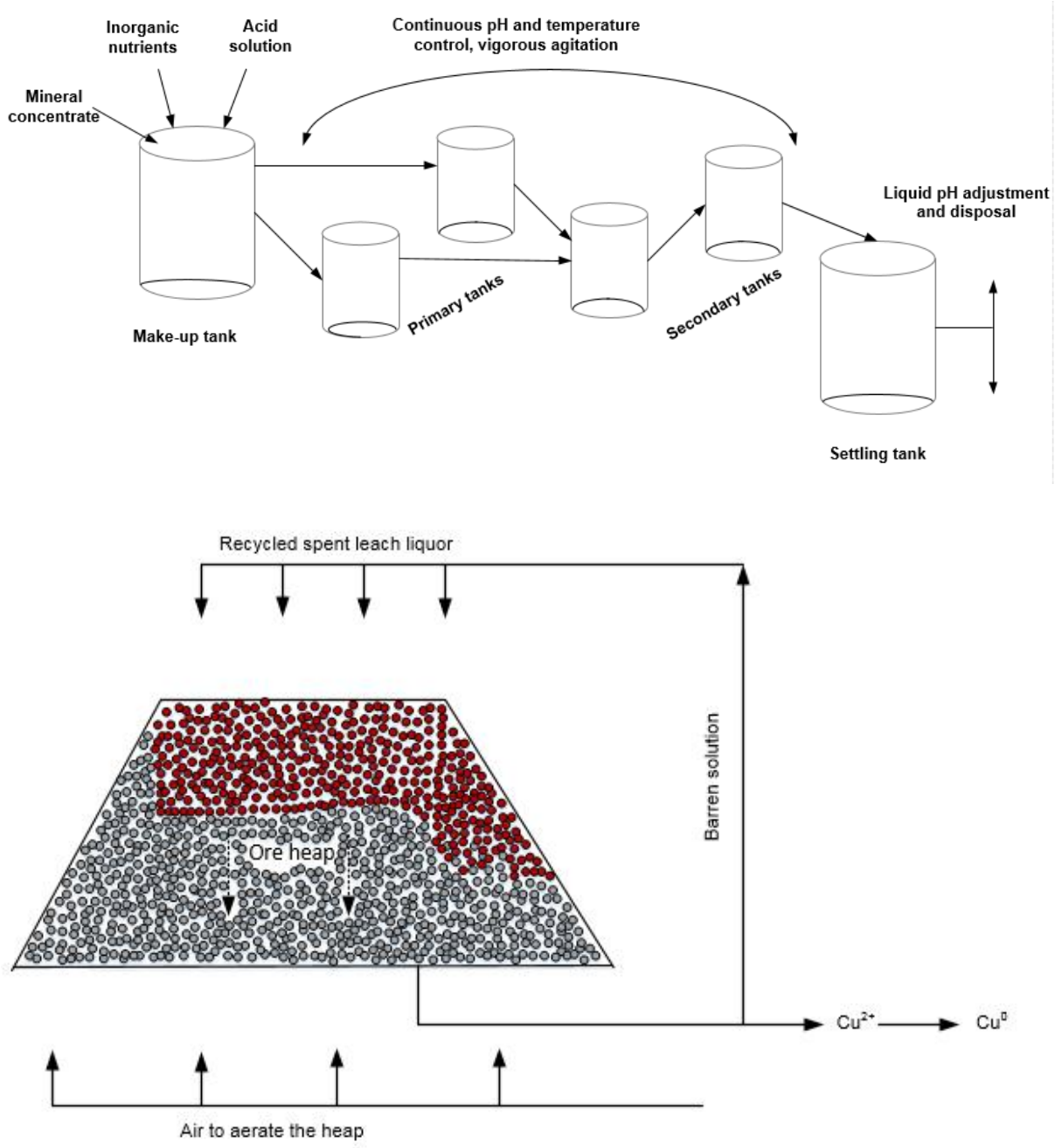

Figure 2.2 Schematic diagram of the tank and irrigated heap bioleaching processes modified after Rawlings (2002).

Although heap bioleaching offers some advantages when considering its design and operation simplicity as well as its low operating cost, however, it is severely limited in its operation. Some

of the operating conditions become uncontrollable due to the construction and heterogeneous nature of the system. This could result in an occurrence of extreme conditions such as hot spots, a high concentration of total dissolved solids (TDS), low rate of oxygen and carbon dioxide transfer, poor solution distribution and high pH (Petersen and Dixon, 2004).

In-situ bioleaching is employed in unrestrained and underground mines where conventional techniques cannot be applied to the ore deposits as a result of low grade, small deposits or both. Other advantages of the in-situ process include shorter mine development times, lower mining infrastructure costs and the isolation of personnel from both broken ore and other radiation hazards. However, the process of in-situ requires sufficient permeability of the ore body, if there is no sufficient porosity in the ore, the ore should then be fractured by explosives to enable the injected solution flow through the deposit without any hindrance. Shortcomings to this process includes permeability problems experienced in the process, the precipitation of secondary minerals, that any outflow of the pregnant leaching solution is prevented from the entire ore body and the risk of contamination of the ground water due to poor solution control (Brandl, 2008, Murr and Brierley, 1978, Schnell, 1997).

Commercial application of in-situ, dump and heap bioleaching for metal recovery has been reported widely (Brierley, 1999, Brierley and Brierley, 2001, Domic, 2007, Kinnunen and Puhakka, 2005). Subsequently, the application of heap bioleaching in numerous other metals in the near future is promising, this is as a result of the inexpensive operational and construction costs associated with this process as well as its ability to handle substantial amounts of ore.

2.3 Chemistry of bioleaching

It has been reviewed and reported that mineral bioleaching processes comprise of chemical and microbial oxidation reactions, whereby ferric iron and protons form part of the reactant of the leaching reaction. These reactions are: (i) the chemical attack of sulfide minerals with ferric irons, (ii) the microbial oxidation of reduced ferrous to ferric iron, and (iii) the elemental sulfur to sulphuric acid (Wanjiya, 2013, Ojumu et al., 2006). The main use of microorganisms during microbial oxidation of ferrous ion is to generate/regenerate the leaching agents and to enable the reaction by creating reaction space in which the leaching occurs.

$$2MS + 4Fe^{3+} \rightarrow 2M^{2+} + 4Fe^{2+} + 2S^{0} \quad (2.1)$$

$$4Fe^{2+} + O_2 + 4H^{+} \rightarrow 4Fe^{3+} + 2H_2O \quad (2.2)$$

$$2S^{0} + 3O_2 + 2H_2O \rightarrow 2SO_4^{2-} + 4H^{+} \quad (2.3)$$

The bio-dissolution of metals involve direct metabolic attachment of bacterial cell on the mineral surfaces through the chemical oxidation of reduced sulfur to sulfate by generated microbial Fe^{3+} (Kim et al., 2008). The two mechanisms involved in bioleaching are known as direct and indirect bacterial leaching. However, in the indirect process, the cycling of Fe^{3+}/Fe^{2+}, coupled by the bacteria is imperative in order to maintain an environment of high redox potential that is needed for efficient leaching. The process of bioleaching is entirely based on the activity of *At.ferrooxidans, L.ferrooxidns,* and *T.thiooxidans,* as they convert heavily soluble metal sulfide through the oxidation of biochemical reactions into water-soluble metal sulfates (Bosecker, 1997). The following reactions are of extreme importance in bioleaching mechanism.

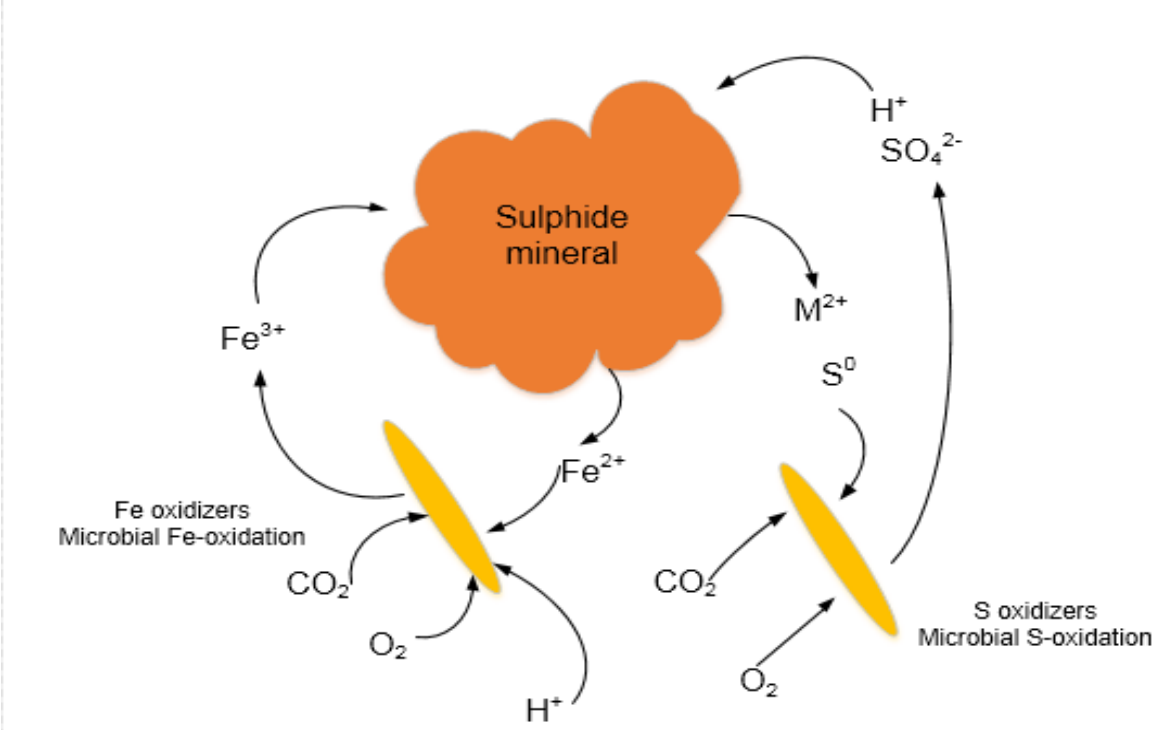

Figure 2.3: A schematic representation of bioleaching mechanism modified after Hansford and Vargas (2001).

2.3.1 Direct bacterial leaching

By definition, this involves physical contact of the bacteria cell with the respective surface of the mineral sulfide, while the oxidation of the sulfate occurs without detecting any occurring intermediate (Bosecker, 1997, Sand et al., 2001). This process also entails the oxidation of pyrite to ferrous sulfate as seen in the following reactions.

$$4\,FeS_2 + 14\,H_2O \xrightarrow{bacteria} 4\,FeSO_4 + 4\,H_2SO_4 \qquad 2.4$$

$$4\,FeSO_4 + O_2 + 2\,H_2SO_4 \xrightarrow{bacteria} 2\,Fe_2(SO_4)_3 + 2\,H_2O \qquad 2.5$$

However, the direct bacterial oxidation of pyrite is best summarised by the following reaction

$$4FeS_2 + 15O_2 + 2H_2O \xrightarrow{bacteria} 2Fe(SO_4)_3 + 2H_2SO_4 \quad 2.6$$

It has been revealed through investigations that the following non-iron metal sulphides can be oxidized by *A.ferooxidans* in direct interaction: covellite (CuS), chalcocite (Cu_2S), sphalerite (ZnS), galena (PbS), molybdenite (MoS_2), stibnite (Sb_2S_3), cobaltite (CoS), millerite (NiS) (Bosecker, 1997). In order to describe direct bacterial leaching, the following reaction is imperative, where MeS represents the metal sulfide.

$$MeS + 2O_2 \xrightarrow{bacteria} MeSO_4 \quad 2.7$$

Moreover, evidence exists to support the claim that bacteria has to be in contact with the mineral surface, but the mechanism of attachment and the initiation of metal solubilisation needs complete understanding (Bosecker, 1997). This is due to its lack of justification (Sand et al., 2001, Rohwerder and Sand, 2007). However, the attachment of the bacteria does not occur at the whole of the mineral surface, but at specific sites where crystal limitation exist and the metal, solubilisation occurs due to electrochemical interactions (Bosecker, 1997).

2.3.2 Indirect bacterial leaching

In indirect bacterial leaching, the ferric iron is produced as a result of bacteria growth, which serves as lixiviant for the oxidation sulfide mineral, and it can be regenerated in a cyclic bioleaching process (Bosecker, 1997, Mazuelos et al., 2001). The metal solubilisation is described according to equation 2.8 below. To maintain sufficient iron in solution, chemical oxidation of metal sulfide has to occur in an acid atmosphere at a pH less than 5.0. The *Acidothiobacillus ferrooxidans or L.*ferrooxidans can re-oxidize the resulting ferrous ion to ferric state, as in Equation 2.8 (Silverman, 1967, Bosecker, 1997) and this could take place in the process of oxidation (Bosecker, 1997).

$$MeS + Fe_2(SO_4)_3 \xrightarrow{bacteria} MeSO_4 + 2FeSO_4 + S^o \quad 2.8$$

2.4 Micro-organisms involved in bioleaching

Microorganisms play an important role in the extraction of minerals from the ores. They also effect the kinetics of reaction within the bioleaching processes. They are acidophilic in nature and survive under acidic conditions. In addition, they have the ability to oxidize ferrous iron (Fe^{2+}) to ferric iron (Fe^{3+}) in the presence of atmospheric oxygen as well as carbon dioxide (Alemzadeh et al., 2009) and oxidize elemental sulfur to sulphuric acid (H_2SO_4).

Respectively, the oxidation of ferrous iron to ferric ion and sulfur to sulphuric acid appears to be the main function of acidophilic microorganisms (Das et al., 1998). Their growth can occur

in inorganic medium with low vales of pH and they tolerate metals with high ion concentrations. The resulting product (Fe^{3+}), is a chemical oxidant, that is employed in treating acidic mine effluent processes for hydrogen sulfide removal from sour gasses (Alemzadeh et al., 2009). In this process, hydrogen sulfide is achieved through two different steps; the first is the chemical oxidation of the sulfide by Fe^{3+} and the bacterial regeneration of Fe^{3+} as a leaching agent (Yujian et al., 2007).

Acidophilic microorganisms with dynamic effect in the oxidation of Fe (II) to Fe (III) and sulfur to H_2SO_4 are *Acidianus*, *Thiobacillus*, *Leptospirillium*, and *Sulfolobus*. *Acidianus* species are spherical with the tetrahedron, pyramid disc or saucer shaped lobes. Whereas *Thiobacillus* species are rod-shaped, gram-negative, non-spore forming and *mesophilic,* excluding the *Thermophilic Thiobacilli* that is capable of growing at a higher temperature (Das et al., 1998).While *Leptospirillium* species are spiral-shaped, with non-spore forming and gram negative, and the species of *Sulfobacillus* are gram positive in contrast with *Leptospirillium* species, and they are rod-shaped with tapered ends, which can grow at a higher temperature (Das et al., 1998).

Furthermore, the slow rate of reaction of bioleaching restricts its commercial application. Wanjiya (2013) outlined that these reactions are responsible for controlling kinetic reaction, hence, their role in bioleaching can never be underrated(Wanjiya, 2013). Microorganisms involved in the reaction are described according to their performance. These microorganisms are categorized into three sub-groups, such as mesophiles, moderate thermos-acidophiles and extreme thermos-acidophiles (Das et al., 1998).

2.4.1 Mesophiles

Mesophiles are microorganisms that grow at normal room temperature (28-37^{o}C). The most popular and widely used strains among the mesophiles are *Acidithiobacillus ferrooxidans*. Even though there has been an isolation of strains of *Acidithiobacillus ferrooxidans* from various sources, as the majority of these strains illustrated an optimum growth condition of pH 1.5-2.5 (Das et al., 1998). Investigation shows that mesophilic iron oxidizers have also been isolated from the environment that has variations in extreme annual temperature, but ensures a lower substantial activity at lower temperatures approaching 5^{o}C (Kupka et al., 2007). Mesophiles grow at a temperature of up to 45^{o}C, and depending on the experimental condition, the activation energy of *Acidithiobacillus ferrooxidans* varies from 34 to 96 kJ /mol (Franzmann *et al*, 2005).

Reviews show that *Leptospirillium ferrooxidans* are incapable of oxidizing sulfur to sulfate, for this reason, it is combined with *Acidithiobacillus ferrooxidans* in order to oxidize Fe (II) and sulfur. Even though *Thiobacillus ferrooxidans* acquired the same shape as *Thiobacillus*

thiooxidans (Franzmann *et al*, 2005), it has been reported that *Thiobacillus thiooxidans* cannot oxidize Fe (II) as well. The energy acquired by the bacterium comes from the oxidation of sulfur and sulfur compound to sulfate.

2.4.2 Moderate thermophiles

Moderate thermophiles are microorganisms that grow at a temperature up to 60^{o}C. *Sulfobacillus thermosulfidooxidans* is a moderate thermophile, which is used extensively in the industry due to its ability to oxidize both sulfur and iron (Das et al., 1998, Franzmann et al., 2005, Wanjiya, 2013). With the leaching experiments performed at higher temperature, the kinetic of bioleaching by moderate thermophiles has appeared to be faster when compared to mesophiles

2.4.3 Extreme thermophiles

These microorganisms are an important strain which belongs to the genus *Sulfolobus,* they are capable of growing at a temperature of 60^{o}C (Das et al., 1998, Franzmann et al., 2005, Wanjiya, 2013). Few of the isolated *Sulfolobus* species are *S. acidocaldarius*, *S. sofataricus, S. Brierley, S. ambioalous*, and all of these strains display features such as;

- Optimal growth temperature of 65 – 70^{o}C
- Growth that occurs in anaerobic condition, following the ability to reduce sulfur
- Growing in aerobic condition coupled together with sulfur oxidation
- The ability to oxidize Fe (II) to Fe (III) and sulfur to sulfate

2.5 Mechanism of ferrous iron oxidation

The presence of microorganisms in the oxidation of minerals has been beneficial in leaching processes. Most microbial leaching consists of the oxidation of iron and sulfur. It has been reported that in order to achieve effectiveness in bioleaching operations, iron oxidizing bacteria vastly depend on the oxidation rate process, which has been in the application of bioenergetics of growth of *Acidothiobacillus ferrooxidans* on ferrous iron (Chowdhury, 2012, Ojumu et al., 2008). The same mechanism was assumed to be applied for other iron oxidizing bacteria and archaea (Ojumu et al., 2008), knowing that the cell structure of two microbes differs.

The coupling of ATP synthesis and ferrous as well as iron oxidation in *Acidothiobacillus ferrooxidans* (Ingledew (1986), was elucidated using chemiosmotic theory. It was noted that the mechanism of ferrous iron oxidation involves oxidation of the transfer of electrons through an energy-transducing membrane, to the production of energy-rich molecules. The energy

obtained by microorganisms result from the oxidation of ferrous iron or reduced sulfur (Ojumu et al., 2008, Nemati et al., 1998, Chowdhury, 2012, Crundwell, 1997). This is achieved by ferrous being the electron donor during the microbial respiratory mechanisms under acidic condition, with the utilization of oxygen as an oxidant (Dempers, 2000, Ojumu et al., 2008).

During the conversion of ferrous iron to ferric iron, only one mole of the electron is released and this signifies that a large amount of ferrous iron will, in turn, produce a large amount of energy (Wanjiya, 2013, Rawlings, 2002).

The performance by *Acidithiobacillus ferrooxidans* has challenges in maintaining the internal pH of the cell close to neutral. The pH of the cytoplasm was reported to be around the pH of 6.5 to 7. This suggests that the maintenance of pH is not exclusively due to the energy conservation in the bacteria, but probably a relic of the measurement (Crundwell, 1997). During active growth, the pH is close to 4.5, the ATP synthase of *Thiobacillus ferrooxidans* becomes similar in structure and function to that of mitochondria, chloroplasts and other bacteria (Crundwell, 1997). The illustration below is the half reactions resulting from the metabolic activities of the microorganisms, as well as ferrous to ferric iron oxidation and electron acceptance by the oxygen (Ojumu et al., 2008, Chowdhury, 2012).

$$2Fe^{2+} \rightarrow 2Fe^{3+} + 2e^{-}$$ (Oxidation) E_h = +770 mV 2.9

$$2e^{-} + 0.5O_2 + 2H^{+} \rightarrow H_2O$$ (Reduction) E_h = -1120 mV 2.10

Overall reaction

$$2Fe^{2+} + 0.5O_2 + 2H^{+} \rightarrow 2Fe^{3+} + H_2O + Energy$$ E_h = -350 mV 2.11

The overall reaction, as shown above, consumed Fe^{2+} (ferrous iron), O_2 (oxygen) and H^+ (hydrogen), producing Fe^{3+} (ferric iron), H_2O (water) and energy for the carbon dioxide (CO_2) fixation and cell growth (Chowdhury, 2012, Wanjiya, 2013). The generated electrons arising from the oxidation of ferrous iron (Equation 2.8) occurs on the periplasmic side of the membrane cell and are transported along the electron transport chain to the terminal oxidase, where they reduce oxygen to water on the cytoplasmic side of the cell membrane (Crundwell, 1997). The concentration of protons is reduced outside the cytoplasm of the cell as well. A proton pump would be required (Equation 2.9) if the oxygen half reaction occurred outside the cell envelope.

The mechanism for energy conservation in *Thiobacillus ferrooxidans* as shown in Figure 2.4 involves the flow of electrons from ferrous iron at membrane surface to a cytoplasmic cytochrome through copper that contains a protein called rusticyanin (Nemati et al., 1998).

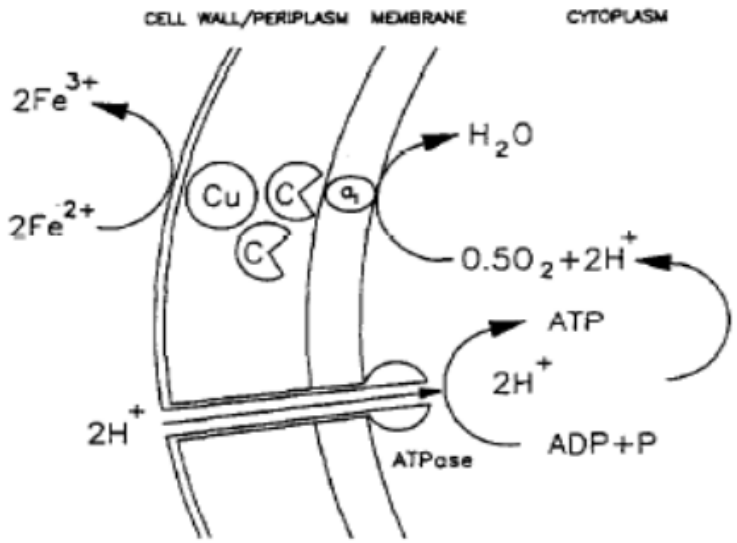

Figure 2.4: Fe2+ oxidizing chain of Acidothiobacillus ferrooxidans (Nemati et al., 1998). Cu refers to Rusticyanin; C, cytochrome c; αI, cytochrome αI.

The available energy from the oxidation of ferrous ions by oxygen must exceed or equal the required energy for adenosine diphosphate (ADP) phosphorylation. A proton electrochemical gradient, which is generated by the energy available from ferrous iron oxidation across the cell membrane is responsible for ADP phosphorylation drive (Crundwell, 1997). According to Wanjiya (2013), an energy carrier of ADP to adenosine triphosphate (ATP) within the cell physiology is achieved due to the variations in the cytomplastic and solution pH. With ATP formation where there is translocation of protons from the solution to the cytoplasm. This reveals the importance of ferrous iron oxidation as an energy generation process for the bacteria, which holds the basis for their growth and survival (Wanjiya, 2013, Chowdhury, 2012, Ojumu et al., 2008, Crundwell, 1997).

The protons channeled across the cell membrane influence the electrochemical potential associated with the formation of ATP. The membrane is impervious to protons and the transfer of protons occur via these channels (Ojumu et al., 2008). The wall of the outer cell membrane of *Acidothiobacillus ferrooxidans* consists of a high molecular weight c-type cytochrome (Cyc2), which serves as the primary electron acceptor. This remains in its oxidized state (see Figure 2.5), which is ready to receive electron from ferrous iron even if there are short-term oxygen fluctuations (Rawlings, 2002), the electron is then passed to the second cytochrome (Cyc1) in the periplasm through rusticyanin and then onto c cytochrome oxidase as shown below (Ojumu et al., 2008).

Rusticyanin which is the most important oxidant in the oxidation of ferrous ion is a blue copper that is present in high concentration (roughly 5% of the cell protein) in the cell envelop of

Acidothiobacillus ferrooxidans (Crundwell, 1997, Dempers, 2000). It contains protein that is moderately small but has a remarkably high redox potential. Although the presence of rusticyanin increases the rate of reduction of rusticyanin by ferrous iron as reported by Crundwell (1997), it is believed that an unknown enzymatic component (X) arbitrates the electron transfer from ferrous iron to rusticyanin (Nemati et al., 1998). The chemical energy that is released in the ferrous iron oxidation process is used in the fixation of dissolved CO_2 via Calvin reductive pentose phosphate cycle, and from the thermodynamics consideration.

In order to provide enough redox potential energy (ΔG calculated to be -8.1 kcal mol^{-1}) required for the phosphorylation of ADP to ATP (ΔG estimated to be -8.9 to 16 kcal mol^{-1}), at least 2 moles of Fe^{2+} must be oxidized (Ingledew, 1982, Ojumu et al., 2008). The oxidation of ferrous iron is essential to produce $NAD(P)^+$ for CO_2 fixation and other anabolic processes by transfer of electrons from Fe^{2+}(Ojumu et al., 2008).

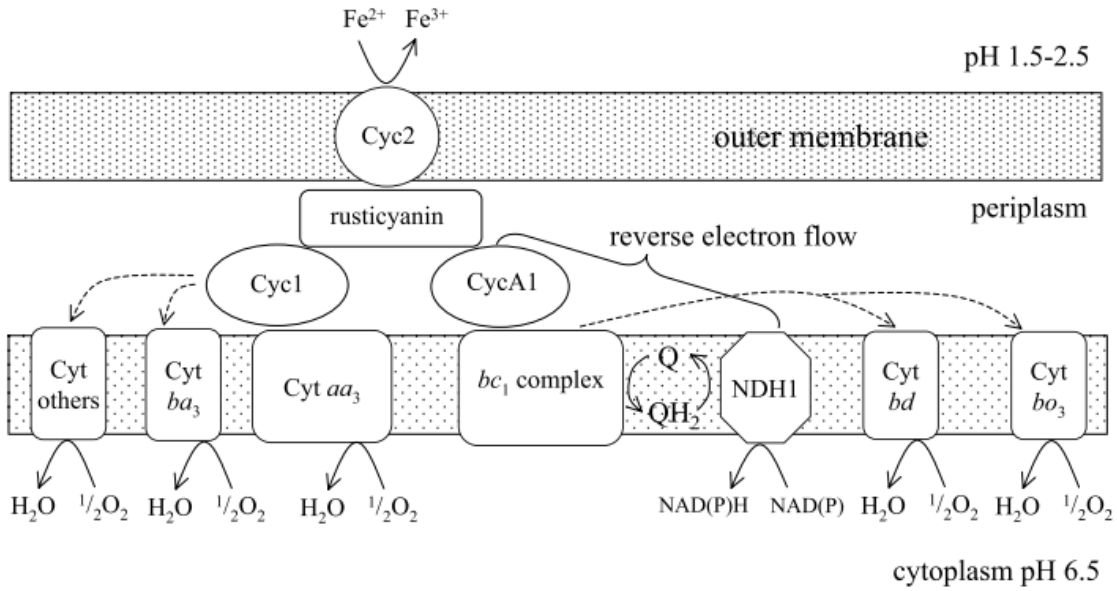

Figure 2.5: Model of iron oxidation electron transport pathway of Acidothiobacillus ferrooxidans showing the transfer of an electron from the membrane-located cytochrome c to rusticyanin and then along one of two paths (Rawlings, 2002).

2.6 Microbial growth and ferrous iron kinetics

The microbial cell growth results from hundreds of enzymatically catalysed reactions, several of which are controlled by the cell to ensure that nutrients are not wasted (Blanch, 1981). Such reactions have been shown to occur not only within the cell complex as reported by Blanch (1981). It is not surprising that microbial growth models commence with lumped models that define the major biotic and abiotic variables (Blanch, 1981). Several classification schemes for models of microbial growth have also been reported. The foremost classification is based on

the integrity of the individual cell. It focuses on the constitutive kinetics models for microbial growth from the simple, unstructured model to a brief overview of models, which describe intracellular kinetics. The most widely used unstructured model for the substrate consumption rate is the Monod Equation (Zeng and Deckwer, 1995).

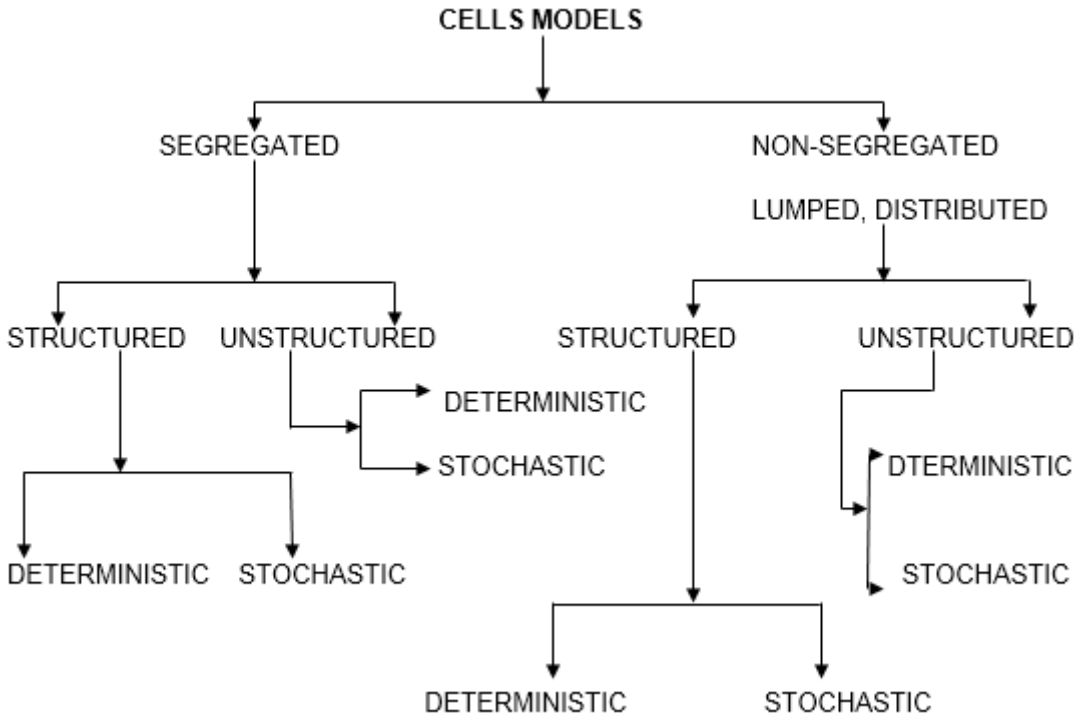

Figure 2.6: Classification of models for microbial growth adapted from (Blanch, 1981)

The unstructured models have been reported to be the most popular, as they comprise of the most basic observation in relation to microbial growth and they are simple and easy to use (Zeng and Deckwer, 1995). Moreover, unstructured models view cells as an entity in a solution, which interacts with the environment, whereby the rate of reaction is only related to biomass concentration (Mrwebi, 2004). Therefore, these models attempt to describe the kinetics of the cell growth based on cell and nutrient profiles.

During the bioleaching of sulfide minerals, microorganisms are critical for the oxidation of ferrous iron to ferric iron. The ferrous iron oxidation was reported by Dempers (2000) to be the rate controlling sub-process in the bioleaching of sulfide minerals. This hypothesis facilitated the use of kinetics bacterial ferrous iron oxidation combined with the kinetics of chemical ferric leaching (Dempers, 2000) to effectively model the bioleaching of pyrite and arsenopyrite. It is, therefore, evidence to support the notion that microbial ferrous iron oxidation is a vital sub-process in the bioleaching of sulfide minerals.

Microbial growth kinetic has its root in the Michaelis-Menten model for the interaction of enzyme substrate kinetics (equation 2.11-2.13). According to the model, enzyme-substrate complex ES is formed when the enzyme E combines with the substrate. The enzyme complex then decomposes, forming product P and free enzyme E. The elementary assumption behind Michaelis-Menten enzyme kinetics is that the formation of enzyme-substrate complex is reversible, whereas the formation of product and the free enzyme is irreversible (Ojumu et al., 2008).

$$E + S \xrightarrow{K_1} ES \qquad 2.12$$

$$ES \xrightarrow{K_2} E + S \qquad 2.13$$

$$ES \xrightarrow{K_{3,ES}} P + E \qquad 2.14$$

Where:

K_1 = rate constant for complex formation

K_2 = rate constant for reverse complex formation, and

K_3 = rate constant for product formation

The rate law for the above equations (2.12-2.14) are:

$$r_{2.11(S)} = K_1[E][S] \qquad 2.12a$$

$$r_{2.12(S)} = -K_2[ES] \qquad 2.13a$$

$$r_{2.13S)} = -K_3[ES] \qquad 2.14a$$

According to Fogler (1999), the net rate of disappearance (equation 2.15) of the substrate, $-r_{(ES)}$ and the net rate of formation (equation 2.16) of the enzyme-substrate complex are represented by the following:

$$-r_{(ES)} = K_1[E][S] - K_2[ES] \qquad 2.15$$

$$r_{(ES)} = K_1[E][S] - K_2[ES][ES] \qquad 2.16$$

Assumption made for the enzyme adsorption and desorption of the substrate is that they occur so rapidly that at equilibrium, the rate of formation of the enzyme-substrate complex is zero.

With $r_{(ES)}$ = 0, therefore:

$$[ES] = \frac{K_1[E][S]}{K_2 + K_3} \quad 2.17$$

By substituting equation 2.17 into 2.15 and re-arranged, equation 2.18 is obtained.

$$-r_{(ES)} = \frac{K_1 K_3[E][S]}{K_1 + K_3} \quad 2.18$$

In the absence of denaturation, the total concentration of the enzyme in the system [E_T] is constant and equal to the sum of the concentrations of the free, unbounded enzyme [E] and the enzyme-substrate complex [ES] (Chowdhury, 2012), such that:

$$[E_T] = [E] + [ES] \quad 2.19$$

By substituting equation 2.17 into 2.19 and re-arranged, equation 2.20 is obtained.

$$[E] = \frac{[E_T](K_{2,ES} + K_{3,ES})}{K_{2,ES} + K_{3,ES} + K_{1,ES}[S]} \quad 2.20$$

By substituting equation substituting equation 2.20 into 2.17, it can be shown that the rate equation for a single substrate enzymatic reaction is expressed as in equation 2.21.

$$-r_{(ES)} = \frac{K_1 K_3[E_T][S]}{K_1[S] + K_2 + K_3} \quad 2.21$$

With $K_m = \frac{K_{2,ES} + K_{3,ES}}{K_{1,ES}}$, equation 2.21 reduces to equation 2.22, a form of the Michaelis-Menten equation.

$$-r_{(ES)} = \frac{K_3[E_T][S]}{K_m + [S]} \quad 2.22$$

Let K_3 be represented by V_{max}, the maximum rate of reaction for a known enzyme concentration, and when substitute into equation 2.22, the following form of Michaelis-Menten equation is obtained:

$$-r_{(ES)} = \frac{V_{max}[S]}{K_m + [S]} \quad 2.23$$

The contribution of the substrate concentration [*S*] in the denominator can be neglected if [*S*] is adequately small (K_m >>[S]), as shown in equation 2.24. With respect to the limiting substrate concentration, the kinetics then becomes the first order, at which the microorganisms multiply. At a very high substrate concentration when 100% of the enzyme is in the busy state, K_m is

relatively small under these conditions, the reaction rate then follows a zero order as described in equation 2.25.

$$-r_{(ES)} \cong \frac{V_{\max}[S]}{K_m} \quad 2.24$$

$$-r_{(ES)} \cong V_{\max} \quad 2.25$$

In a batch reactor, microbial growth can be expressed as shown in equation 2.26 and reduces to equation 2.27 as $\mu >> K_d$.

$$r_X = \frac{dx}{dt} = (\mu(s) - K_d)X \quad 2.26$$

$$r_x = \frac{dx}{dt} = \mu(s)X \quad 2.27$$

In which

X = concentration of microorganisms,

S = concentration of growth limiting substrate,

$\mu(s)$ = specific growth rate defined by the Michaelis-Menten equation,

K_d = decay rate coefficient.

It is common to evaluate the growth rate from the substrate utilization, which highlights the difficulties in measuring the cell concentration. This stoichiometry for cell growth is considered complex due to the diversity of microorganisms, nutrient media used and environmental conditions (pH, aeration rate, temperature, and redox potential). The stoichiometric equation can be in the form as shown in equation 2.28. The growth rate is generally related to the substrate utilization rate by the growth yield, Y_{SX}. This is defined as the amount of biomass produced per amount of substrate consumed. The yield coefficient for cells and substrate is represented by equation 2.28.

$$Cells + Substrate \rightarrow More\ cells + \text{Pr}\ oduct \quad 2.28$$

$$Y_{SX} = \frac{amount\ of\ biomass\ produced}{amount\ of\ biomass\ consumed} = \frac{r_X}{-r_S} \quad 2.29$$

For the concentration of limiting substrate, the specific growth rate kinetics of ferrous iron oxidation may be stated according to Equation 2.30, which is the kinetics of microbial ferrous iron oxidation derived from the Monod Equation (Monod, 1942).

$$\mu = \frac{\mu_{max}\left[Fe^{3+}\right]}{K_{Fe^{2+}} + \left[Fe^{2+}\right]} \quad 2.30$$

Where

μ = specific growth rate, h^{-1}

μ_{max} = maximum specific growth rate, h^{-1}

$\left[Fe^{2+}\right]$ = concentration of the limiting substrate, g L^{-1}

K_{Fe}^{2+} = the affinity constant, g L^{-1}

The low value of K_{Fe}^{2+} shows that the affinity of the microorganism is strong towards the limiting substrate and vice versa. This affinity is also called Michaelis-Menten constant. Microbial growth rate, r_X (mmolC.L.h^{-1}) is directly proportional to its concentration, C_X as shown in equation 2.31, which has been previously defined (see Equation 2.27):

$$r_X = \frac{dC_X}{dt} = \mu C_X \quad 2.31$$

If the growth yield is based on the amount of ferrous iron consumed, thus biomass yield on ferrous-iron coefficient can be obtained from the ratio of the rate of biomass produced to the rate of ferrous-iron utilization $r_{Fe^{2+}}$. A similar equation can be written for biomass yield on oxygen consumption (see equation 2.32 and 2.33).

$$-r_{Fe^{2+}} = \frac{1}{Y_{Fe^{2+}X}} r_X \quad 2.32$$

$$-r_{O_2} = \frac{1}{Y_{O_2X}} r_X \quad 2.33$$

Where r_{O_2} and Y_{O_2} are the rate of oxygen consumption and the biomass yield on oxygen. Both equations (2.32 and 2.33) have been found to be insufficient in terms of explaining the observed trends in microbial growth. Also, they have been adjusted to include terms, accounting for the presence of endogenous respiration (Ojumu et al., 2008) or energy used by existing cells, which is equivalent to a maintenance energy requirement that may justify the yield variation in the growth rate (Chowdhury, 2012).

The consumption of energy by microbes during substrate utilization according to Pirt (1965) are firstly, the energy required for maintenance processes within the microbe, which are non-growth associated processes, like cell motility, turnover of cell material, membrane potential,

internal pH and other metabolism, and secondly the energy for the microbial growth. The rate substrate utilization or consumption in equation (2.32 and 2.33) is then modified by Pirt to integrate the maintenance term as illustrated in equation 2.34. This concept of Pirt was first applied by Boon et al. (1995) to microbial ferrous-iron oxidation. The rate of microbial growth under substrate-limited conditions and balanced growth affects the observed biomass yield, as proposed by Pirt in Equation 2.34c

$$-r_{Fe^{2+}} = \frac{1}{Y^{\max}_{Fe^{2+}X}} r_X + m_{Fe^{2+}} C_X \qquad 2.34a$$

By simplification,

$$\frac{-r_{Fe^{2+}}}{r_X} = \frac{1}{Y^{\max}_{Fe^{2+}X}} + m_{Fe^{2+}} \frac{C_X}{r_X} \qquad 2.34b$$

Substituting equation 2.31 and 2.32 into 2.34b, yields equation 2.34c

$$\frac{1}{Y_{Fe^{2+}X}} = \frac{1}{Y^{\max}_{Fe^{2+}X}} + \frac{m_{Fe^{2+}}}{\mu} \qquad 2.34c$$

The following equations (2.34d and 2.34e) are obtained by substituting equation 2.31 into equation 2.34a.

$$-r_{Fe^{2+}} = \frac{1}{Y_{Fe^{2+}X}} \mu C_X + m_{Fe^{2+}} C_X \qquad 2.34d$$

$$q_{Fe^{2+}} = -\frac{r_{Fe^{2+}}}{C_X} = \frac{\mu}{Y^{\max}_{Fe^{2+}X}} + m_{Fe^{2+}} \qquad 2.34e$$

Where $Y_{Fe^{2+}X}$ is the observed biomass yield (e.g. g biomass per substrate consumed^{-1}), $Y^{\max}_{Fe^{2+}X}$ is the maximum microbial yield (e.g. g biomass per substrate consumed^{-1}), μ is the specific microbial growth (h^{-1}), $q_{Fe^{2+}}$ is the specific rate of substrate utilization (e.g. mol of substrate consumed per mol of biomass, per hour), and $m_{Fe^{2+}}$ represents the maintenance coefficient, which is the specific substrate uptake rate for maintenance activities (e.g. g substrate consumed (g biomass)$^{-1}$ hours^{-1}).

2.7 Yield maintenance

Subsequent to Pirt's concept, which stated that the substrate utilization rate is coupled with the microbial growth and cell maintenance. From equation 2.34c and 2.34e, the maximum biomass

yield and the maintenance coefficient is obtained from the graphs of $\frac{1}{Y_{Fe^{2+}}}$ vs $\frac{1}{\mu}$ or $q_{Fe^{2+}}$ vs μ as shown in figure 2.10a and b

$$q_{Fe^{2+}} = -\frac{r_{Fe^{2+}}}{C_X} = \frac{\mu}{Y^{\max}_{Fe^{2+}X}} + m_{Fe^{2+}} \qquad 2.34e$$

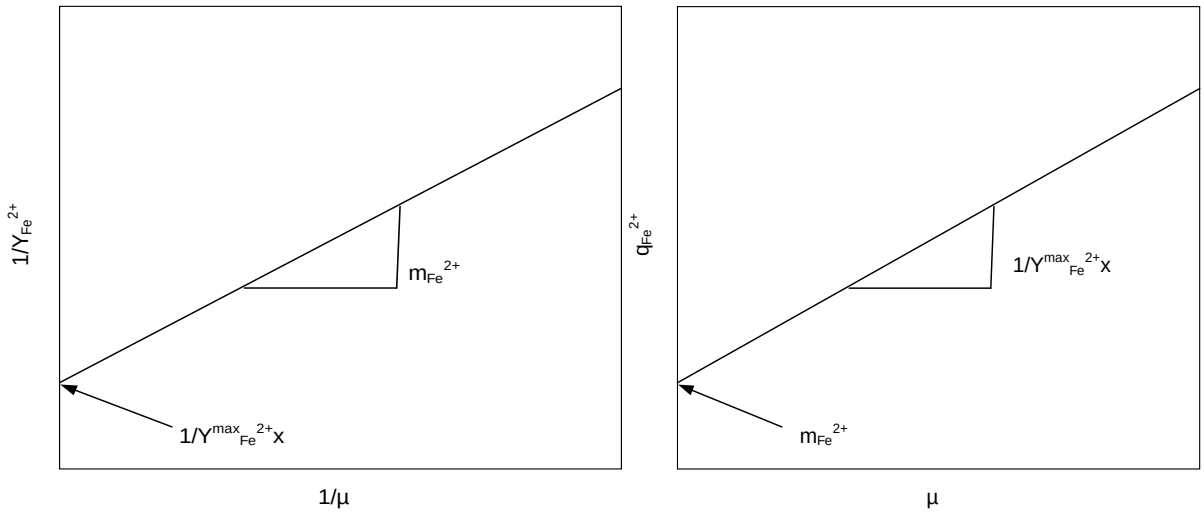

Figure 2.7: Graphs used to determine maximum biomass yield and the maintenance coefficient using a) Equation 2.34c and b) Equation 2.34e.

The linear relationship that exists between the specific ferrous-iron utilization, $r_{Fe^{2+}}$ and the specific growth rate, μ as well as the constant maintenance energy requirement has been established for various heterotrophic micro-organisms (Dempers, 2000). Due to the deviations from the constant maintenance equation (Equation 2.33e), when microorganisms are energy sufficient, it leads to the questioning of the validity of the relationship.

Researchers such as Ojumu et.al (2008) have challenged Pirt's concept that varying biomass yield maintenance at different conditions. It was suggested that the maintenance requirement was dependent on the specific growth rate (Ojumu et al., 2008, Dempers, 2000).

$$q_{Fe^{2+}} = \frac{\mu}{Y^{\max}_{Fe^{2+}X}} + m_{Fe^{2+}} + c\mu\, m_{Fe^{2+}} \qquad 2.35$$

Where *c* is a constant that defines the growth rate dependence of maintenance energy, the model developed by Neijssel and Tempest (1976) was modified on the assumption that the

maintenance energy term comprised of a portion that decreased with an increase in the specific growth rate.

$$q_{Fe^{2+}} = \frac{\mu}{Y^{\max}_{Fe^{2+}X}} + m_{Fe^{2+}} + m^{v}_{Fe^{2+}}(1 - k\mu) \qquad 2.36$$

The m_{Fe}^{2+} in Equation 2.36 represents the constant maintenance energy term and the growth rate dependent maintenance energy is represented by $m^{v}_{Fe^{2+}}(1 - k\mu)$. As the specific growth rate, μ, approaches the maximum value, μ^{max}, the growth rate dependent maintenance energy requirement decreased to zero (Pirt, 1965). This implies that

$$k = \frac{1}{\mu^{\max}} \qquad 2.37$$

As soon as the cells adapt to the environment, the microorganisms consume the available nutrients for digestion and energy provision to enable multiplication under balanced growth conditions during the exponential phase (Ngoma, 2015). The rate at which bacterial oxidation occurs is reported to be 500,000 times as fast as the rate of oxidation in the absence of bacteria (Boon, 1996). The growth rates of a mixed mesophilic consortium under conditions typical of a *Leptospirillum* dominated culture, based on their ferrous iron bioenergetics, have been reported in literature (Ingledew, 1982, Ngoma, 2015)**.** The growth rates for the range mesophilic temperatures and pH are shown in table 2.1. Various substrates in batch shake flasks under optimal conditions by *Acidothiobacillus ferrooxidans* have been acknowledged. The growth of pure and mixed bioleaching strains on low-grade chalcopyrite ore in batch shake flask experiments have been investigated (Ngoma, 2015). All strains indicated an increase in cell number with time. With decreasing temperature, in the study by Franzmann et al. (2005), a slower increase in cell number was observed.

Table 2: Growth rates of mesophilic microorganisms in various systems (Ngoma, 2015).

Microorganism	Substrate	System	Temperature	pH	Growth rate
Acidothiobacillus ferrooxidans	Low grade chalcopyrite containing ore	Glass column (0.4 m height, 160 mm inner diameter)	RT ± 23	1.7	0.0364 from day 16 to 22, 0.0005 from day 23 to 50
Acidothiobacillus ferrooxidans	Ferrous iron	Batch shake flask	Optimal	Optimal	0.19
Acidothiobacillus ferrooxidans	Sulphur	"	"	"	0.069

Acidothiobacillus ferrooxidans	Chalcopyrite	"	"	"	0.05
At. thiooxidans	Sulphur	"	"	"	0.046
At. thiooxidans	Low grade chalcopyrite containing ore	Glass column (0.4 m height, 160 mm inner diameter)	RT ± 23	1.7	0.083 from day 16 to 22, 0.0008 from day 23 to 50
At. caldus	"	"	"	"	0.0045, 0.0038
L. ferriphilum	"	"	"	"	0..0343,0.0051
Predominately L. ferrooxidans	Ferrous iron media	Continuous flow bioreactor (Height: Diameter ratio of 1.32, working volume of 1 L)	30	1.7	0.079
"	"	"	35	1.7	0.119
"	"	"	40	1.7	0.038
"	"	"	"	1.5	0.077
"	"	"	"	1.3	0.087
"	"	"	"	1.1	0.089
L. ferriphilum	"	"	40	1.1	0.1024
"	"	"	"	1.3	0.1043
"	"	"	"	1.5	0.1227
"	"	"	"	1.7	0.0952
L. ferrooxidans	Ferrous iron	Batch shake flask	Optimal	Optimal	0.069

2.8 Microbial ferrous iron oxidation rate equation

A number of kinetic models for bacterial oxidation by *Acidothiobacillus ferrooxidans* have been suggested (Breed et al., 1999). Various publications on the microbial ferrous iron kinetic have outlined the initial rates studies conducted in batch and continuos culture (Boon, 1996, Nemati et al., 1998, Ojumu et al., 2006, Van Scherpenzeel et al., 1998). These were performed in order to improve the efficiency of the recovery of metal, with the use of different models that were classified as empirical, Monod or Michaelis-Menten based. Most of the researchers have termed the oxidation of ferrous ions kinetics by the Monod Equation (Crundwell, 1997), which is given by

$$r_{Fe^{2+}} = \frac{r_{\max}\left[Fe^{2+}\right]}{K_s + \left[Fe^{2+}\right]} \qquad 2.38$$

Where r_{Fe}^{2+} is the oxidation rate of ferrous ions, r_{max} is the maximum rate of ferrous iron oxidation and K_S represents the substrate coefficient.

From equation 2.12, the microorganisms rely naturally on the reduced ferrous iron since it is the limiting reactant. It has been reported that success has been achieved in the optimum conditions using CSTR bioreactors, but much work still remains to be done on improving the kinetics (Wanjiya, 2013). Ojumu et al. (2006) did a review of published studies which were vital in attempting to detect a rate equation that is suitable for both combined and comprehensive, which also comprises substrate utilization, biomass synthesis and biomass maintenance as illustrated in table 2.2, that involves the use of substrate, biomass synthesis and biomass maintenance.

Table 3: Selected published kinetic models for ferrous-iron oxidation with Acidothiobacillus ferrooxidans.

Model	Conditions
$\mu = \frac{\mu_{max}\left[Fe^{2+}\right]}{Y_{SX} K_m \left[Fe^{2+}\right]}$	Batch STR, T = 25-30 ^oC, pH = 2-2.3, Fe_T = 6 g L^{-1}
$\mu = \frac{\mu_{max}\left[Fe^{2+}\right]}{K_m + \left[Fe^{2+}\right]}$	Continuous, T = 28 ^oC, pH = 2.2
$\mu = \frac{\mu_{max}\left[Fe^{2+}\right]}{\left[Fe^{2+}\right] + K_m\left(1 + \frac{\left[Fe^{3+}\right]}{K_i}\right)}$	Continuous, T = 30 ^oC, pH = 1.6, Fe_T = 5-400 mM
$\mu = \frac{\mu_{max}\left[Fe^{2+}\right] - \left[Fe^{2+}\right]_r}{K_m + \left(\left[Fe^{2+}\right] - \left[Fe^{2+}\right]_r\right)}$	Continuous, T = 22 ^oC, Fe_T = 5-22 mM, Isolate AK1

$\mu = \frac{\mu_{max}\left[Fe^{2+}\right]}{\left[Fe^{2+}\right] + K_S\left(1 + K_i\left[Fe^{3+}\right]\right)}$	Continuous, T = 35 ºC, pH = 1.8, Fe_T = 0.52-3.29 g L^{-1}
$-r_{O_2} = \frac{k_3'[X][Fe^{2+}]}{\left[Fe^{2+}\right] + K_m\left[1 + \frac{[X]}{K_i'} + \frac{\left[Fe^{3+}\right]}{K_{if}} + \frac{[X]\left[Fe^{3+}\right]}{\alpha K_i' K_{if}}\right]}$	Initial Rate, T = 29 ºC, pH = 1.8–2.0, Fe_T = 0.25-26 mM
$\mu = \frac{\mu_{max}\left[Fe^{2+}\right]}{\left[Fe^{2+}\right] + K_S + \left[Fe^{3+}\right]\frac{K_S}{K_i} + \frac{\left(\left[Fe^{2+}\right]\right)^2}{K_{Si}}}$	Continuous, T = 29 ºC, pH = 1.8-2.0, Fe_T =2-70.8 g L^{-1}
$-r_{Fe^{2+}} = a1\left(\frac{\rho o_2}{k_B + \rho o_2}\right)\left(\frac{\left[Fe^{2+}\right]}{\left[Fe^{2+}\right] + K_{Fe^{2+}}\left(1 + \frac{\left[Fe^{3+}\right]}{K'}\right)}\right)$	Continuous, T = 30 ºC, pH = 2.0, *Leptospirillum ferrooxidans*
$-r_{Fe^{2+}} = k\left(\frac{\left[Fe^{2+}\right]/\left[H^+\right]}{K_{Fe^{2+}} + \left[Fe^{2+}\right]/\left[H^+\right] + K_i\left[Fe^{3+}\right]}\right)^{0.5}\left(\frac{\rho o_2}{k_B + \rho o_2}\right)^{0.5}$	Theoretical, fitted to data from Huberts (1994)
$q_{Fe^{2+}} = \frac{q_{Fe^{2+}}^{max}}{1 + K_{Fe^{2+}}\frac{\left[Fe^{3+}\right]}{\left[Fe^{2+}\right]}}$	Only fitted to *Leptospirillum* data
$\frac{d\left[Fe^{2+}\right]}{dt} = \frac{K_0 e^{-\frac{E_a}{RT}}[X]\left[Fe^{2+}\right]}{\left(1 + \frac{\left[Fe^{3+}\right]}{K_i}\right)\left(K_m + \left[Fe^{2+}\right]\right)}$	Initial Rate, T = 30 ºC, pH =2.0, Fe_T = 0.45-31.5 kg m^{-3}
$q_{O_2} = \frac{q_{O_2}^{max}}{1 + \frac{K_s}{\left[Fe^{2+}\right] - \left[Fe^{2+}\right]_t} + \frac{K_S}{K_i}\cdot\frac{\left[Fe^{3+}\right]}{\left[Fe^{2+}\right] - \left[Fe^{2+}\right]_t}}$	Continuous, T = 30 ºC, pH = 1.8-1.9, Fe_T = 0.05-0.36 M
$q_{Fe^{2+}} = \frac{K_1^* \exp\left[\frac{nF}{2RT}\left(E^m - E_h^0\right)\right]\left\{1 - \exp\left[\frac{nF}{RT}\left(E^m - E\right)\right]\right\}}{1 + \frac{K_2^*}{\left[Fe^{2+}\right]} + K_3^* \exp\left[\frac{nF}{RT}\left(E_h - E_h^0\right)\right]}$	Electrochemical cell, T = 30 ºC, pH = 1.8, Fe_T = 0.05-1 M

Source: Adapted from Ojumu et al. (2006)

A simplified form of a previously used model for inhibited Michaelis-Menten kinetics that was developed (Breed and Hansford, 1999c, Hansford and Vargas, 2001) with respect to specific rate of ferrous-iron utilization, neglects the ferrous-iron saturation and threshold ferrous-iron concentration terms (Breed and Hansford, 1999b). This model (equation 2.39) was used to describe the kinetics within the range of ferric/ferrous-iron ratios found in bioleach systems (Breed et al., 1999).

$$q_{Fe^{2+}} = \frac{q_{Fe^{2+}}^{max}}{1 + K'_{Fe^{2+}}\frac{\left[Fe^{3+}\right]}{\left[Fe^{2+}\right]}} \qquad 2.39$$

Where $q_{Fe^{2+}}$ is the specific ferrous-iron oxidation rate, $q^{max}_{Fe^{2+}}$ represents the maximum specific ferrous-iron oxidation rate, and $K'_{Fe^{2+}}$ is the apparent affinity constant for the Hansford model. These parameters were determined by either fitting the experimental data to Equation 2.39, by using Equation 2.40 or by linearizing Equation 2.39.

$$\frac{1}{q_{Fe^{2+}}} = \frac{1}{q^{max}_{Fe^{2+}}} + \frac{K'_{Fe^{2+}}}{q^{max}_{Fe^{2+}}} \frac{[Fe^{3+}]}{[Fe^{2+}]} \qquad 2.40$$

The ferric/ferrous-iron or redox potential was recommended to be the principal factor governing ferrous iron oxidation kinetics in agreement with an electrochemical mechanism (Hansford and Vargas, 2001). The ferric/ferrous-iron ration in Equation (2.39) can be achieved from the solution redox potential through the use Nernst Equation, in the form

$$E_h = E'_h + \frac{RT}{nF} \ln \frac{[Fe^{3+}]}{[Fe^{2+}]} \qquad 2.41$$

E'_h and $\frac{RT}{nF}$ are obtained from the calibration curve

Where E_h is the potential of the solution (mV), E'_h is the standard potential of Fe^{3+}/Fe^{2+} couple (mV), *R* is the universal gas constant (kJ $K^{-1}mol^{-1}$), *T* is the absolute temperature (K), *n* is the number of electrons transferred per molecule, *F* is the kJ mV^{-1} $equiv^{-1}$, $[Fe^{3+}]$ is the ferric iron concentration (g L^{-1}), and $[Fe^{2+}]$ is the ferrous iron concentration, (g L^{-1}).

Previous research conducted on biological oxidation has focused on the practical aspects of improving the overall leaching rates from sulfide ores by studying the factors that influence bioleaching (Ojumu et al., 2008, Gómez and Cantero, 2003). However, the effectiveness of leaching is largely dependent on the microorganism efficiency and on the composition of chemical and mineralogy of the ore to be leached. Maximum yield of metal extraction can be achieved only when there is the correspondence of leaching conditions with the optimum growth conditions of the bacteria (Bosecker, 1997).

2.8.1 The effect of temperature

The effect of temperature on the oxidation rates of ferrous iron is a cardinal parameter for microorganisms which may populate a bioleaching operation. In chemical reactions, biological reactions appear to be temperature dependent, and the rate of the reactions decrease over a certain temperature. To maintain microorganisms, they must be subjected to temperatures,

not below their optimum operating temperature for their activeness (Chowdhury, 2012). As the microorganisms are destroyed quickly when subjected to a temperature above their optimum temperatures.

Although Optimum temperature and pH for *At.ferooxidans* have been reported by several authors (Jensen and Webb, 1995, Kupka et al., 2007, Halinen et al., 2009a, Daoud and Karamanev, 2006, Rawlings, 2002, Ojumu et al., 2009, Alemzadeh et al., 2009), however the optimum temperatures were held to be dependent on the variation of strains. Discrepancies arising from the optimal values for temperature and pH, suggests that the optimum temperature is pH dependent and decreasing the pH reduces the optimum temperature for growth and oxidation of iron (Ahonen and Tuovinen, 1989). The optimum temperature for ferrous iron and sulfide oxidation by *At.ferooxidans* is between 28 and 30^{o}C, and a decrease in metal extraction is due to lower temperatures (Bosecker, 1997, Tekin et al., 2013), but even at 4^{o}C, bacterial solubilisation of copper, cobalt, nickel and zinc was observed.

Studies by Ahonen and Tuovinen (1989) revealed that oxidation of iron has been demonstrated to occur at low temperatures of 5 to 6^{o}C, with an increase in maintenance energy requirement with lower temperatures in *At.ferooxidans*. Moreover, increasing the reaction temperature and the concentration of the cell bacteria resulted in a related increase in the rate of oxidation, with the largest increase recorded at a temperature between 10 and 20^{o}C and bacteria concentration between 0.25 and 0.5 mg/ml (Okereke and Stevens, 1991). Thermophilic bacteria can be applied for leaching purposes at higher temperatures of 50-60^{o}C. Franzmann et al. (2005) shows the relationship between oxidation rates of ferrous iron to a temperature of common bioleaching organisms using Ratkowsky equation. The application of Ratkowsky equation to iron oxidation data yielded estimated fundamental temperatures (T_{MIN}, T_{OPT}, and T_{MAX}) for activity to a greater accuracy than what was previously available (Ngoma, 2015).

The Ratkowsky Model was used to describe the temperature growth model (Ratkowsky et al., 1982) in Equation 2.42.

$$\sqrt{\mu_{\max}} = b(T - T_o) \qquad 2.42$$

Where *b* is the slope of the regression line, T_o represents the conceptual temperature of no metabolic significant.

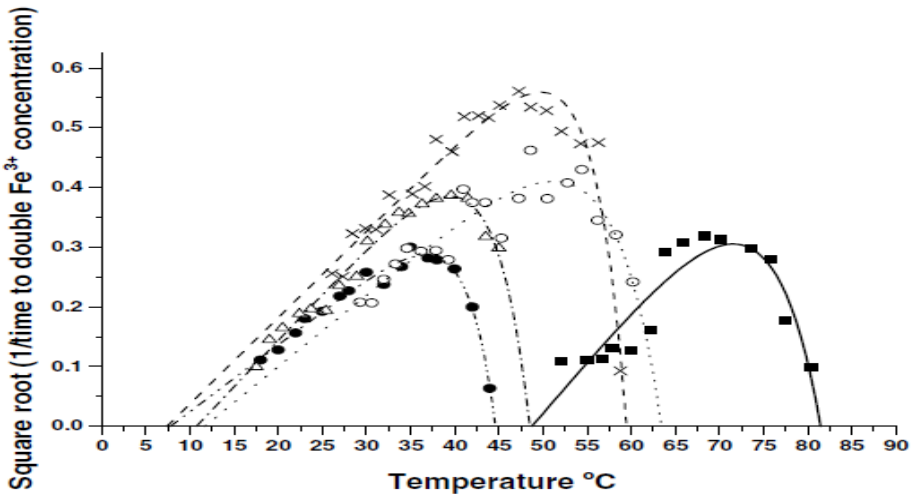

Figure 2.8: The relationship of oxidation of iron to temperature for a common range of bioleaching organisms using Ratkowsky plots (Franzmann et al., 2005)

The effect of temperature on the bioleaching rates of primary and secondary sulfides has been shown to be remarkable. (Franzmann et al., 2005) stated that at high temperatures, the rate of chemical reaction increases and the relationship that exist between reaction rate and the temperature is described by the Arrhenius Equation 2.43. Equation 2.44 describes the effect of temperature on the maximum oxidation rate (Chowdhury, 2012).

$$r_{Fe^{2+}}^{max} = K \exp\left(-\frac{E_a}{RT}\right) \qquad 2.43$$

$$\ln r_{Fe^{2+}}^{max} = -\frac{E_a}{R}\left(\frac{1}{T}\right) + \ln K \qquad 2.44$$

Where E_a is the activation energy (kJ/mol), *K* is the frequency factor, R is the universal gas constant (8.314 $J.K^{-1}$), and T is the temperature (K)

The activation energy and the frequency factor for microbial ferrous iron oxidation are obtained by plotting $\ln r_{Fe^{2+}}^{max}$ versus 1/T (inverse temperature), which yields a slope ($-E_a/R$) of the straight line and an intercept of ln K_o. The development of Arrhenius equation defines the effect of temperature on the rate of chemical reactions, and not biologically catalysed reactions that are exposed to enzyme denaturation with temperature increase. At temperatures above optimum,

fitting the Arrhenius Equation to oxidation rate data is not possible for microbial growth (Chowdhury, 2012). The effects of temperature on the growth of *Acidothiobacillus ferrooxidans* with its ability to oxidize ferrous iron, has been reported in literature with different values of activation energy which varies considering the operation conditions (Chowdhury, 2012, Kupka et al., 2007, Nemati and Webb, 1997). Moreover, values reported in literature also vary and these variations might be as a result of the different monitoring approach.

Limitation in the biochemical reaction occurs at low temperature, and this indicates higher activation energy values (Chowdhury, 2012, Ahonen and Tuovinen, 1989, Nemati and Webb, 1997), whereas diffusion control is associated with low activation energy values. An activation energy of 83 $kJ.mol^{-1}$ was suggested to be biochemical reaction limitation at a lower temperature, and an activation energy value of 49.82 $kJ.mol^{-1}$ was reported by Chowdhury (2012) in the temperature range of 5 to 18^{o}C. This is suggestive of chemical controlled reaction. On the contrary, another study carried out at a temperature ranging from 5 to 25^{o}C produced an activation value of 20.93 $kJ.mol^{-1}$ and this was reported to be diffusion controlled (Chowdhury, 2012). Franzmann et al. (2005) documented the activation energies of various strains of microbes at different temperature conditions and the activation energies on selected bioleaching microorganisms are shown in table 2.3

Table 4: Activation energies of some selected microorganisms studied on temperature effect

Organism	Temperature range studied (^{o}C)	Optimum Temperature (^{o}C)	Activation Energy, E_a ($kJ.mol^{-1}$)
A. brierleyi	45 – 95	71.5	Not recorded
S. thermosulfidooxidans	27 – 65	51.2	51
"F. cyprexacervatum"	35 – 65	55.2	65
Am. Ferroxidans	10 – 59	48.8	62
L. ferrooxidans	8 – 55	36.7	80
F.acidiphilum	12.7 – 47.2	39.6	79

L. ferriphilum	15 – 38	38.6	89
Acidothiobacillus ferrooxidans	10 – 55	29.6	32

Source: Adapted from (Ojumu et al., 2008)

2.8.2 The effect of pH

The optimization of pH is indeed a significant parameter for effective migration and active absorption in a heap bioleaching. The bacteria involved are chemolithotrophic and acidophilic in character. Heaps height are tens of meters and the irrigating solution pH nomadic through the heaps significantly differ (Ngoma, 2015). Solution pH, which is commonly determined through the balance between acid producing and acid consuming reactions, have a substantial effect on the microbial growth and ferrous iron oxidation during the leaching process. High solution pH inhibits the acidophilic microorganisms. The impact of pH on the microbial ferrous iron oxidation has been extensively studied (Özkaya et al., 2007, Ngoma, 2015, Nemati et al., 1998, Breed and Hansford, 1999a). These studies have revealed that the effect of pH variation on microbial growth and activity of bioleaching strain has profound implications for strain selection (Chowdhury, 2012) and has also led to the precipitation of ferric ion within the heap bed, which reduces the heap porousness.

Predominant metal sulfide dissolving microorganisms are extremely acidophilic, meaning that the organisms thrive at pH values below 3 (Rohwerder et al., 2003). Whereas, Smith et al. (1988), noted that acidophilic bacteria growth occurs at pH values between 1.0 to 4.5, with an optimum between 2.0 to 2.3. Moreover, similar optimum pH was also reported by Bosecker (1997).

At pH value less than 2.0, *Acidothiobacillus ferrooxidans* experiences considerable inhibition but could adapt to even lower pH values by addiction of acid (Bosecker, 1997). A study by Nemati et al. (1998) reveals that the activity of *Acidothiobacillus ferrooxidans* was independent of pH values between 1.9 to 2.4 and that the growth was strongly inhibited at pH values close to 1.0 and 4.0. A pH greater than 2.0, can possibly cause bacterial de-activation (Plumb et al., 2008, Van Aswegen et al., 2007, Penev and Karamanev, 2010). Lag periods were encountered for several months prior to the activity of *Acidothiobacillus ferrooxidans*, which was articulated at low pH value of 1.2 (Jensen and Webb, 1995).

It is imperative to maintain the iron in solution in order to prevent ferric precipitate from precipitating, (more on ferric iron precipitates is discussed in section 2.9.).Even though pH variation in the range of 1.5 to 3.5, was reported to have no influence on the growth of bacteria, but growth was unfavorable at pH less than 1.5 or greater than 3.5 (Nemati et al., 1998). Also, a pH range of 0.7 to 1.7 was reported as having no effect, not only on the microbial growth

(Chowdhury, 2012) but also on the ferrous iron oxidation by iron oxidizing microbes when operated under normal condition. Nevertheless, pH values between 1 to 6, with ferrous iron as an energy source, the growth of *Acidothiobacillus ferrooxidans* was able to occur (Jensen and Webb, 1995).

2.8.3 Significance of aeration

Most microbes are aerobic and chemolithotrophic (Nemati et al., 1998, Ngoma, 2015, Pradhan et al., 2008). Aeration is supplied in the form of oxygen (O_2) and carbon dioxide (CO_2). It is surprising that the implementation of forced aeration of heaps in order to optimize the activity of the microbes by meeting their physiological requirements for oxygen and carbon dioxide (Watling, 2006), only occurred in the mid-1990s, concurrently in Chile and Australia.

For biomass generation, sufficient CO_2 that serves as a source of carbon is of critical importance, since the bio-oxidation process depends on it for microbial growth (Petersen et al., 2010). As air is forced into the heap at the bottom of the pile, oxygen is close to saturation (Pradhan et al., 2008, Ngoma, 2015, Chowdhury, 2012), and the microbes that catalyses the oxidation of sulfide thereby consume O_2 as the air flows upward. As a result, the degree of O_2 depletion near the top of the heap prevails, thereby causing a gradual decline in both the population of microbes and the ferrous iron bio-oxidation rate.

A study by Lizama (2001) has shown that O_2 with the heap was anticipated to have come from the air fed at the bottom of the pile. Also, it has been stated that by aerating the bio heap, bio-oxidation reaction can be accelerated, thereby reducing the cycling time of leaching (Olson et al., 2003, Pradhan et al., 2008). This is an indication of the significance of oxygen supply for the possibility and activity of leaching microorganisms (Pradhan et al., 2008). Inhomogeneous aeration frequently results in areas of the heap being poorly aerated, with low CO_2 and O_2 (Bryan et al., 2012), thus requiring additional CO_2 in the aeration regime to improve the performance of the microbes.

The iron oxidation reaction by the microbes necessitates 0.07 g of O_2/g of ferrous iron and by considering the solubility of O_2, this amount cannot be available from the solution, requiring extra O_2 from external sources (Das et al., 1998, Wanjiya, 2013). This is because the solubility of O_2 in water is 8 g/m^3 at 35^{o}C, and with an increase of ionic concentration in the solution, the solubility decreases (Das et al., 1998). Again, if the interior of the heap is not properly aerated, it is susceptible to anaerobic conditions. The supply of O_2 is a requirement for growth and high activity of the leaching microorganisms. These O_2 and CO_2 are supplied to packed-bed bioreactors by aerating the system, while stirred in CSTR and shaking in flasks (Bosecker, 1997).

Consequently, the non- existence of an agitation in the packed-bed bioreactors, implies that microbes colonise on the packing rather than in the aqueous solution. Several studies (Chowdhury, 2012, Lizama, 2009) have substantiated oxygen requirement for microbial growth. During the oxidation of ferrous iron and sulfur, microbes essentially need O_2. Oxygen was observed not to be a limiting substrate for the growth of microbes in an experiment that was conducted in a 500 ml Erlenmeyer flasks containing 200 ml broth at 30^{o}C, shaken at 240 rev/min (Jensen and Webb, 1995).

Cultures of *Acidothiobacillus ferrooxidans* may perhaps be predicted to become limited by the availability of CO_2, with the observation of the limited solubility of CO_2, at the required pH for the optimum growth of *Acidothiobacillus ferrooxidans*. Limiting the CO_2 in the growing cultures of *Acidothiobacillus ferrooxidans* results in a shift of the exponential kinetics of ferrous iron oxidation to a linear relationship (Nemati et al., 1998). This is due to growth-uncoupled oxidation by a standing population of bacteria. O_2 and CO_2 consumption rates have shown the direct relationship in the sense that where there is little or no CO_2, the consumption of O_2 will proceed slowly. It was shown with a column reactor that a narrow peak of activity travels in the upper direction from the bottom over time (Petersen et al., 2011). CO_2 and O_2 are therefore other significant aspects that influence the metabolism of the bacteria (Nemati et al., 1998).

2.8.4 The effect of packing size

The size of packing in the reactor indeed has a significant effect on microbial growth and in ferrous iron oxidation, under normal conditions. Packed bed reactor consists of randomly arranged particles upon which cells are supported (Mazuelos et al., 2010). Also, in the study conducted by Mazuelos et al. (2001), which investigated glass spheres of range 1 to 7 mm particle size an increase in ferric iron productivity with an increased in particle size was reported. It was also documented that packed columns with glass spheres that are smaller than 4 mm experienced a rearrangement of the bed that fashioned the flow channeling that results in low production of ferric iron (Mazuelos et al., 1999). Poor flow channelling as a result of smaller particle size, slowed down the development of the biofilm and consolidation surrounded by the space between the particles (Mazuelos et al., 2001), due to the concentration of oxygen/carbon dioxide and nutrient solution limitations in the bioreactor (Nikolov et al., 1988).

2.8.5 Jarosite accumulation

Jarosite formation, which is pH dependent, affects the activity of acidophilic microorganisms. Additionally, the significance of jarosite formation has been reported in literature (Grishin et al., 1988, Wanjiya, 2013) It is regarded unwanted in this study due to its ability to inhibit the growth

of acidophilic microorganisms. (A more detailed explanation of jarosite formation was offered in section 2.9).

2.9 Precipitation of ferric iron

Ferric iron in acid solution is critical for the bacterial solubilisation of uranium from ores, it is also important in the dissolution of metal sulfide. Studies have also revealed that jarosite formation has an unfavourable effect on biological gas desulphurisation and metal bioleaching processes (Nemati et al., 1998). The precipitates slow the diffusion of reactants and products through the precipitate zone, thereby creating kinetics barriers. Ferric iron regeneration by bacterial re-oxidation of ferrous sulfates is deemed a step in the recycling of leach liquors in heap (Kelly and Jones, 1978). The precipitation of jarosite has been observed experimentally in various bacterial cultures (Jensen and Webb, 1995, Daoud and Karamanev, 2006, Nemati et al., 1998, Grishin and Tuovinen, 1988). It has been one of the main challenges in bio-hydrometallurgy, as it reduces the concentration of ferric iron in the leaching medium by occupying the space within the biomass carrier material (Özkaya et al., 2007). Precipitation of jarosite was reported to occur at higher pH where the solubility of ferric iron decreases, precipitating hydroxides, oxyhydroxide and hydroxy-sulphate compounds (Ojumu et al., 2008).

The hydroxy-sulphate precipitates are referred to as jarosite. The precipitation of jarosite on the mineral surface also inhibits bacterial access and limits the mass transfer of oxidant to the surface (Ozkaya et al., 2007). In applications that involve *At.ferooxidans,* minimization of jarosite formation is necessary for the increase in efficiency. When *At.ferooxidans* is grown on sulfate, the value of the initial pH increases as the removal of acid is achieved by the oxidation of ferrous iron (Jensen and Webb, 1995, Nemati et al., 1998). The overall reaction (equation 2.2) illustrates an important component in these biological leaching applications, which is the oxidation of ferrous iron. This is because an acidic environment is essential in ferrous iron oxidation. However, since there is hydrogen ions consumption, the initial pH of the media increases, which is counteracted by the hydrolysis of ferric iron (Liu et al., 2009, Daoud and Karamanev, 2006). The formation of insoluble hydroxyl compounds by the hydrolysis of ferric iron in water is shown in Equation 2.45.

$$Fe^{3+} + 3H_2O \leftrightarrow Fe(OH)_3 + 3H^+ \qquad 2.45$$

The extent of the type of ferric precipitate depends on the final value of the solution pH (Grishin and Tuovinen, 1988; Kupka et al., 2007; Nemati et al., 1998) of iron hydrolysis. The formation of these precipitates can be defined as either acid producing, leading to a decrease in solution pH or acid consuming that leads to an increase in solution pH (Plumb et al., 2008). The hydrolysis of ferric iron, that is, acid producing, reduces the pH in contrast to equations 2.2,

and it tends to stabilize at pH 2.4 approximately. The formation of the basic hydroxyl sulphates occurs in the presence of a suitable mono-valent cation, such as K^+ (potassium jarosite), Na^+ (natrojarosite), NH_4^+ (ammoniojarosite), or H_3O (hydronium jarosite), with the general formula $MFe_3(SO_4)_2(OH)_6$, which is a competing reaction for the hydrolysis (Daoud and Karamanev, 2006, Grishin and Tuovinen, 1988, Nemati et al., 1998), with M representing the mono-valent cation. The excess sulfate forms subsequent ferric hydroxy-sulphate;

$$3Fe^{3+} + M^{+} + 2HSO_4^{-} + 6H_2O \leftrightarrow MFe_3(SO_4)_2(OH)_6 + 8H^{+} \quad 2.46$$

$$8Fe^{3+} + SO_4^{-} + 14H_2O \leftrightarrow Fe_8O_8(OH)_6(SO_4)_2 + 22H^{+} \quad 2.47$$

The nature of precipitation of jarosite is dependent on pH, ionic composition and concentration of the medium (Jensen and Webb, 1995, Grishin and Tuovinen, 1988), If crystalline, the precipitates comprise various jarosite, and if absent, it yields amorphous compounds (Ojumu et al., 2008). Conversely, the study by Bigham et al. (2010) stated that the properties of these precipitates extend not only on the above-mentioned factors but also the precipitation rate and general chemistry. This is due to the abundance of NH_4^+ ions in the 9K mediums (Daoud and Karamanev, 2006). Moreover, Chowdhury (2012) and Ojumu et al. (2008) reported that at pH 1.6, ammonium jarosite was found predominately in ferrous iron oxidation by *Acidothiobacillus ferrooxidans*, and schwertmannite was observed at pH of 3.2. Maximum jarosite precipitation and increase in pH was observed in the study conducted by Daoud and Karamanev (2006), with an increase in operating temperature. At low-temperature oxidation of ferrous iron by *Acidothiobacillus ferrooxidans* in the study by Kupka et al. (2007), schwertmannite was found to be dominant.

There have been various studies on the significance of jarosite formation in bioreactors. The formation of jarosite precipitates is directly linked to the number of attached cells in the presence of glass beads by *Acidothiobacillus ferrooxidans* (Pogliani and Donati, 2000). The following table comprises of the type of precipitates on the number of studies on ferrous iron oxidation by *Acidothiobacillus ferrooxidans* at an applied pH.

Table 5: Nature of precipitate and the dependency of its formation on pH (Nemati et al., 1998)

pH	**Type of precipitates**
2.0 – 2.3	Jarosites
1.8 – 2.0	Yellowish-brown precipitate
2.3	Jarosites
2.2 – 5.0	Amorphous Fe^{3+} precipitate, crystalline jarosite
2.5	Fe^{3+} -hydroxy sulphates, jarosite

1.6	Free of precipitate
1.35	K-jarosite
1.9	Jarosites
2.2	Jarosites
1.8	Jarosites
1.9 – 2.2	Jarosites
2.3	NH_4^+ and K-jarosites
1.8 – 2.0	Yellowish-brown precipitate

2.10 Mass transfer in packed bed column reactor

The beds of sulfide minerals in heap bioleaching are irrigated by leaching solution, and also aerated with air (Lizama, 2009). When a mass transfer occurs from some interface into a well-mixed solution, it is expected that the transferred amount is relative to the difference in concentration and the interfacial area (Cussler, 1984). Due to the oxidative nature of bacteria, all chemical reactions that occur in the heap continue at a lower rate than the rate of oxygen mass transfer from gas-liquid phase (Lizama, 2009). The amount of mass transferred is proportional to the concentration difference and the interfacial area as shown in Equation 2.54.

$$\left(rate\ \ of\ \ mass\ \ transferrr\ \ ed\right) = k\left(\text{int}\ erfacial\ \ \ area\right)\left(concentrat\ \ ion\ difference\ \ \right) \qquad 2.54$$

Equation 2.54 can be written in a more acquainted symbols, describing the rate of oxygen mass transfer within the heap as in Equation 2.55, which can also be called Newton's law of cooling:

$$\frac{dC_{O_2}}{dt} = k_L a \left(C^*_{O_2} - C_{O_2}\right) \qquad 2.55$$

Where dC_{O_2}/dt is the oxygen mass transfer rate to the solution from the air, (mol.L^{-1}s^{-1}) $k_L\alpha$ is the oxygen mass transfer coefficient for the heap, (s^{-1}), $C^*_{O_2}$ is the equilibrium concentration of dissolved oxygen at the gas-liquid phase (mol.L^{-1}), and C_{O_2} is the bulk concentration of dissolve oxygen in the liquid phase (mol.L^{-1}).

Mass transfer profiles occur in heap bioleaching, where gas-liquid mass transfer can be rate controlling. (Lizama, 2009). The energy transported within the heap accounts for the temperature profiles that upsets the ascendancy of certain inhabitants of microbes (Naik, 2010). In a rapidly operating microbial oxidation system, the adsorption of oxygen may be gas-liquid mass transfer limited, thus, it rules the overall rate rather than the microbial oxidation

kinetics (Ojumu et al., 2008). The gas-liquid mass transfer is examined in order to determine the microbial oxidation rate of sulfide minerals (Naik, 2010).

Both physical and chemical factors influence the rate of oxygen transfer (Mazuelos et al., 2002). It can, therefore, affect either the value of the physical liquid-phase mass transfer coefficient (K_L), or the value of α, or the driving force for mass transfer $\left(C^{*}_{O_2} - C_{O_2}\right)$. Review of literature revealed that confident estimation of $k_L\alpha$ is critical in establishing the oxygen transport capacity of a heap. The molecules of the oxygen and carbon dioxide are transmitted from the gas bubble interior to the gas-liquid interface (Chowdhury, 2012). These molecules diffuse through a relatively stagnant liquid film that surrounds the gas bubble, which is then transported through the liquid phase.

2.11 Oxygen and carbon dioxide uptake rate in cells

It was noted in the study by Boon (1996) that the specific oxygen utilisation rate relates to the ferric-ferrous iron ratio.

$$q_{O_2} = \frac{q^{\max}_{O_2}}{1 + K'_{Fe^{2+}} \dfrac{\left[Fe^{3+}\right]}{\left[Fe^{2+}\right]}} \qquad 2.48$$

Harvey and Crundwell (1997) have described the energy for growth and maintenance obtained from the oxidation of ferrous-iron for bacteria, using the stoichiometric formula as shown in Equation 2.2

$$4Fe^{2+} + O_2\, 4H^{+} \rightarrow 4Fe^{3+} + 2H_2O \qquad 2.2$$

The oxidation of ferrous-iron is supplemented by the growth of bacteria, on which stoichiometric formula was assumed to have a composition $CH_{1.8}O_{0.5}N_{0.2}$ (Jones and Kelly, 1983, Roels, 1983). However, limiting the carbon and nitrogen sources to CO_2 and NH_4^+ yields the following formation of biomass:

$$CO_2, NH_4^{+}, H_2O \rightarrow CH_{1.8}O_{0.5}N_{0.2} \qquad 2.49$$

The carbon dioxide utilization rate may also be used in the estimation of both the bacterial concentration and growth rate (Boon, 1996, Chowdhury, 2012), assuming that the only carbon source is carbon dioxide (Dempers, 2000). The total quantity of biomass produced can be obtained directly from the total quantity of carbon dioxide consumed.

$$r_X = -r_{CO_2} \qquad 2.50$$

The oxidation rate of ferrous-iron $r_{Fe^{2+}}$ equals the production rate of ferric iron, $r_{Fe^{3+}}$ if it is assumed that jarosite precipitation was not formed (Boon, 1996) as shown in Equation 2.51:

$$-r_{Fe^{2+}} = r_{Fe^{3+}} \qquad 2.51$$

It is noteworthy to recall that the production rates are positive and the consumption rates are negative in the above equations. The cell concentration in batch culture may be determined from the initial bacteria concentration and the carbon dioxide utilization rate:

$$C_X = C_{X0} + \int_{t=0}^{t=t} -r_{CO_2}\,dt \qquad 2.52$$

By performing elemental and charge balance, it becomes possible to establish a relationship between the rate of microbial ferrous-iron oxidation and the rate of oxygen and carbon dioxide utilisation (Hansford, 1997).

$$-r_{Fe^{2+}} = -4r_{O_2} - 4.2r_{CO_2} \qquad 2.53$$

Where $-r_{Fe^{2+}}$ is the ferrous-iron oxidation rate (mol Fe^{2+} $.L^{-1}$ s^{-1}), $-r_{O_2}$ represents the oxygen consumption rate (mol O_2 $.L^{-1}$ s^{-1}), and $-r_{CO_2}$ is the carbon dioxide consumption rate (mol CO_2 $.L^{-1}$ s^{-1}).

2.12 Summary

Heap bioleaching is an established technology for extraction of valuable minerals from their sulfide ores, this is as a result of its design simplicity, the cost of operation, and it's applicability to low-grade ore. Studies on the mechanism of microbial ferrous-ion oxidation have been reported extensively in the various literature. The application of bioleaching in the industry involves tank and heap bioleaching, from which significant parameters were determined from the formulated models. In tank bioleaching, operating conditions (pH and temperatures) are manipulated close to optimum conditions. While the ferric to ferrous ratio predominant in the system is mainly governed by the interaction between the micro-organisms and mineral concentrates

Heap bioleaching, as discussed in section 2.2 showed significance recovery of metal as the process is designed for more efficiency. It may also be concluded that the process of bioleaching heap offers no control over the operating condition, unlike in tank operation. Moreover, poor mass transfer of oxygen and carbon dioxide to the heap may create diffusion since some ions will spontaneously mix, thereby, moving from a region of high concentration to lower concentration due to the heterogeneous nature of heap processes.

Microbial ferrous iron oxidation at moderate temperature has been studied extensively. Although recent studies on bioleach have investigated the effects of variations in operating conditions. Hence, the operating conditions for these studies were similar to those found in a typical heap situation. While studies on ferrous iron bio-oxidation conducted at moderate temperatures in a stirred tank bioreactors were reported by (Ngoma et al., 2015, Plumb et al., 2008), as showing that the kinetics may not represent those in the context of heap situation. However, with the temperature being a cardinal factor in the bioleaching processes, studies on the effect of low temperature were limited. Moreover, several studies that focused on temperatures lacked sufficient information in evaluating quantitatively the effects of temperature in the suboptimal range of <20^{o}C.

Although studies at low temperatures using shake flask have been reported in literature, however, the objective of these studies was to define the lower temperature limit for microbes that oxidize ferrous iron by characterizing the kinetics of bacterial ferrous-iron oxidation at suboptimal temperatures. A study (Dopson et al., 2007) that was carried out in a column bio-reactor at 7°C to simulate heap leaching have focused on the leaching rates at different temperatures. This study focused on the use of pure and mixed microbial cultures for low-temperature mineral and iron oxidation.

Several studies have reported and highlighted the effects and importance of ferric precipitate/ jarosite that were formed as a result of the loss of ferric iron. Jarosite formation has also been proven to be pH dependent. While the pH of the interior of the heap (unlike in tank) cannot be controlled directly, it can be maintained at the desired pH by controlling the pH of the feed using sulphuric acid. The increase in pH, as the oxidation of ferrous iron to ferric iron occurs, is facilitated by the consumption of protons, which then determines the extent of hydrolysis, while the type of the precipitates depends on the monovalent cations.

Studies were conducted using differing reactor (stirred tank bio-reactors, packed-bed bioreactors, and shake flasks) configurations to investigate the formation of jarosite at various operating conditions. With different reactor types, operating conditions, carrier matrix, and approach, determines the amount and the nature of jarosite formed. These studies specifically focused on the quantification of jarosite formed during microbial ferrous-iron oxidation.

Limited studies at low-temperature conditions also quantified the resulting jarosite formed during oxidation of ferrous-iron bio-oxidation. Therefore, it is imperative to investigate the kinetics of microbial ferrous-iron oxidation and also the kinetics of ferric precipitate at low-temperature conditions in the context that mimic real heap situation to fill the gaps identified in previous studies. The outcome of such investigation may provide an understanding of the kinetics of the oxidation and precipitation process under heap conditions, and it may also be used in the design of a typical heap bioleaching plant.

Chapter 3: Materials and methods

This chapter provides the detailed description of the materials used throughout the entire experiment. It also details the methodology as well as the logical techniques applied in the study. Finally, it reports the theoretical calculations applied to the experimental study for data analysis.

3.1.1 Growth medium

This section of work consists of all analytical reagents that were used in this experimental study. The ferrous iron media consists of 5 g/L of Fe^{2+} (added as $FeSO_4.7H_2O$), 2.65 g/L $(NH_4)_2HPO_4$, 5.55 g/L K_2SO_4, 9.15 g/L $(NH_4)_2SO_4$ and 50 mL Vishniac trace element solution (Chowdhury and Ojumu, 2014, Ojumu et al., 2009). The trace element solution contains 50 g/L EDTA ($C_{10}H_{14}N_2Na_2O_8.2H_2O$, M_w = 372.24 g/mol), which was dissolved in 200 mL of 6% (w/v) KOH solution (Chowdhury, 2012). In a separate container, the following chemicals were added, 22 g $ZnSO_4.7H_2O$, 9.24 g $CaCl_2.2H_2O$, 5.0 g $FeSO_4.7H_2O$, 5.06 g $MnCl_2.4H_2O$, 1.58 g $CuSO_4.5H_2O$, 1.1 g $(NH_4)_6Mo_7O_{24}.4H_2O$, 1.62 g $CoCl_2.6H_2O$, and the content in the container were successfully dissolved in a 400 mL of distilled water (H_2O). The EDTA solution was added to the container once, after the component in the container had completely dissolved, the Vishniac solution was added next and was made up to 1 L using H_2O (Chowdhury, 2012). An adjustment was made to the pH of the growth medium to the desired pH ($0.9 < pH < 1.3$) using concentrated (98%) H_2SO_4. It was noted not to attempt to preserve sterile conditions.

3.1.2 Bacteria culture and analysis of bacteria culture at 10°C

The mesophilic mixed cultures were obtained from the Centre for Bioprocess Engineering Research at the University of Cape Town, Cape Town (UCT) in South Africa. The mesophiles of UCT stock maintained at 35°C contains the various strains of microorganism as shown in Figure 3.1. The pre-dominant bacteria strain was *Leptospirrillum ferriphilum*, which is an iron oxidizing bacteria. The microorganisms were grown on pyrite concentrate in a 1 L batch stirred tank reactor at a temperature of 35°C and agitated at 550 rpm.

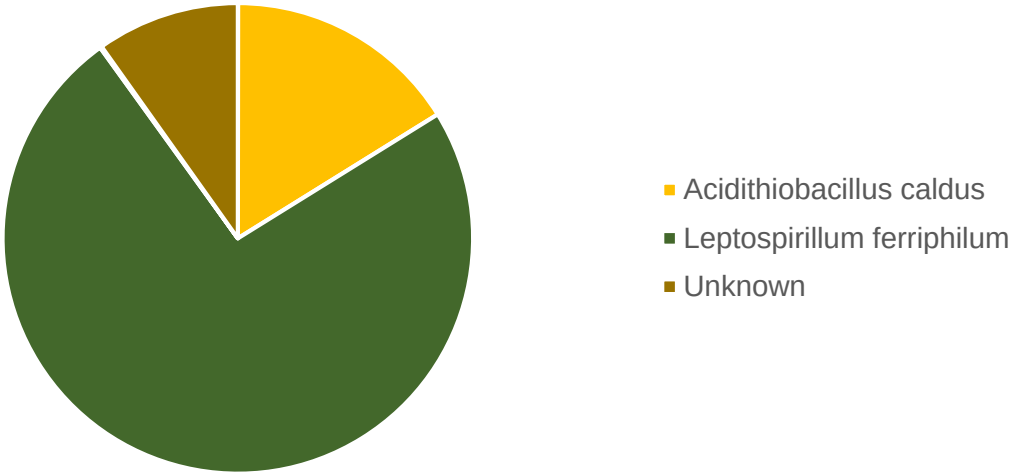

Figure 3.1: Distribution of the microbes in the mixed culture at 35°C.

The temperature mixed mesophiles in section 3.13 was maintained at 10^{o}C in 1 L stirred tank bioreactor. The stock was fed on with the ferrous iron substrate, supplied as 5 g/L of $FeSO_4.7H_2O$ of total iron. It was sub-cultured once the microorganisms were in their exponential phase to allow them to remain active. This was done by the removal of 200 mL stock and refilling it with 200 mL growth media. A known volume (100 mL) of the stock was analysed at the Centre for Bioprocess Engineering Research at the University of Cape Town in South Africa, for microbial speciation. At 10^{o}C, the predominant strain was seen to be *Acidothiobacillus ferrooxidans* as shown in Figure 3.2

Figure 3.2: Distribution of the microbes in the mixed culture at 10°C.

3.2 Methods

3.2.1 Experimental rig

The experimental setup for this study is shown in Figure 3.3. The experimental rig consists of two jacketed packed-bed bioreactors, made up of borosilicate glass with a total volume of 800 ml. The bioreactor has a dimension of height to diameter (H/D) of 12.5 approximately. The column was packed with an inert glass marble of diameter 15 mm to an equivalent height of 700 ml and was held in place with a stainless steel sieve of 1 mm. The working volume of the liquor inside the bioreactor was 550 ml, submerging about 40% of the glass marble bed in solution before sparging. During the operation, about 75% of the glass marble was submerged into the solution; the whole glass marble was not immersed to prevent flooding. Attached to the bioreactor was a refrigerator (Julabo, FL300) used to circulate cold water at a constant temperature to the bioreactor. The temperature of the bioreactor was maintained by circulating cold water at a constant temperature to the bioreactor from the bottom using the refrigerator. At the top of the bioreactor, a tube was connected to it through refrigerator where the water from the bioreactor is then cooled back to the desired temperature prior to circulating back to the bioreactor.

The feed containing 80% growth medium and 20% stock (v/v) was pumped into the bioreactor from the top using Master flex pump (Model no: 7520–47) with a variable speed drive. The liquor effluent from the bottom of the bioreactor was recycled back to the top of the bioreactor. Air was supplied to the bottom using an air pump (Hailipai, Aco: 9620) of six channels, while the off-gas leaving both the bioreactors was passed through a condenser, thereby minimizing evaporation. The solution redox potential was analysed using a CRISON GLP 21 pH and redox meters.

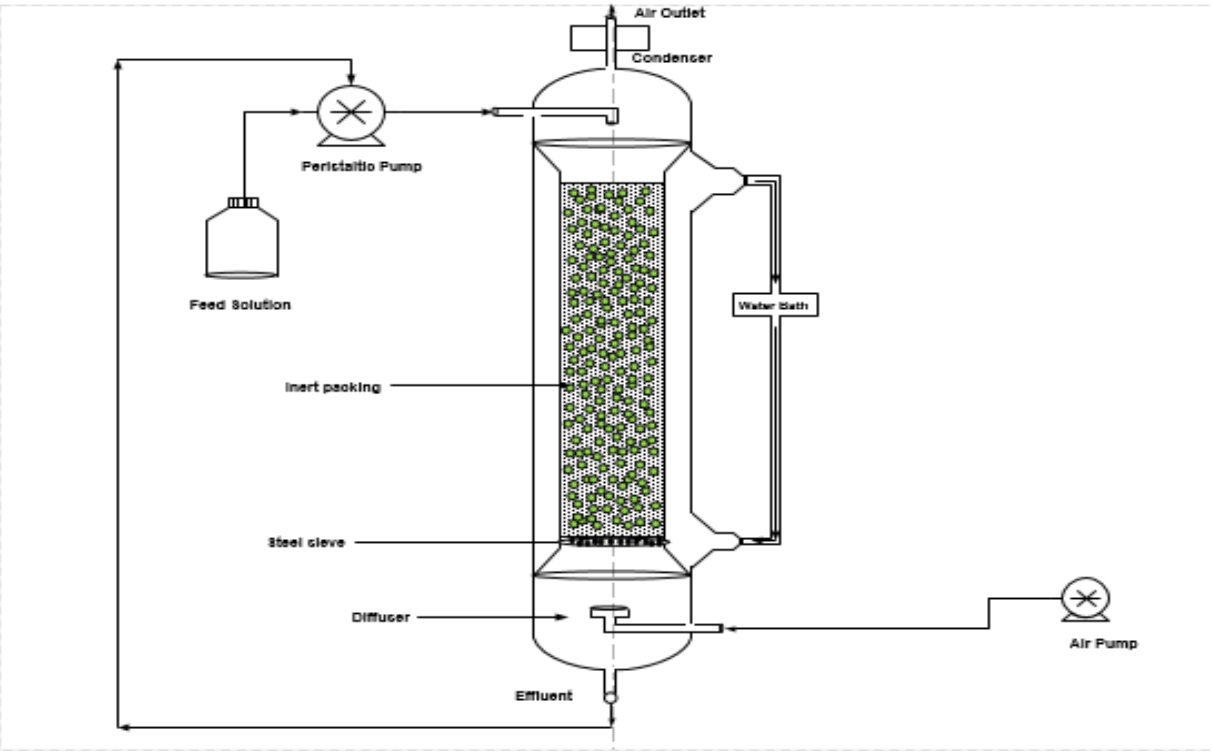

Figure 3.3: Schematic diagram of the experimental rig

3.2.2 Bio-oxidation of ferrous iron under batch culture

The experiments were conducted and repeated in identical packed-bed bioreactors, with 15 mm marble glass balls as the packing material with a working volume of 550 mL. A refrigerator was used to maintain the reaction in the bioreactor at a constant temperature. The diagram illustrating this phenomenon is shown in Figure 3.3. Dry air was used to aerate the cell suspension at a flow rate of 500 ml/min. The ferrous iron medium was fed to the bioreactor from the top at the start of the experiment, and the effluent was recycled back to the bioreactor from the top, while the off-gas from the bioreactor exit through a condenser to minimize liquor evaporation. The pH of the solution in the bioreactor was not controlled directly rather the feed solution was used as an alternative measure to control the pH in the bioreactor to the desired pH with 98% concentrated sulphuric acid (H_2SO_4). All the experiments were conducted at a pH and aeration rate of 1.35 ± 0.05 and 500 ml/min and the solution redox potentials were monitored with the aid of CRISON GLP 21 meter.

A new set of experiment was started with a total working volume of 550 mL (110 mL stock culture + 440 mL of growth medium), the pH of the solution of the feed to the bioreactor was again maintained at a fixed pH of 1.35 ± 0.05 and at a constant temperature. The solution in the column bioreactor was allowed to attain or reach a solution redox potential of 600 mV, before concluding the experiment. The ferric precipitate that precipitated clearly in solution was

determined through quantification and initial total iron and ferrous iron concentration were determined by means of titration.

Samples were collected through the recycling tube to the top for sampling. At every sampling time, solution redox potential was recorded and 5 ml of the liquor (sample) was analysed to determine the total iron concentration. This serves as a proxy to determine the concentration of both ferrous and ferric iron, with the aid of Nernst Equation. At the termination of each experiment, the total iron concentration was determined through titration method. The bioreactor was then washed with water followed by rising with distilled water, which neutralizes the pH in the reactor.

3.3 Analysis Procedures

3.3.1 Analysis of iron

The initial redox potential of the solution at the start was measured using redox electrode (Ag/AgCl), followed by titrating with potassium dichromate and barium diphenylamine sulphonate (BDS) as an indicator to determine both the concentration of ferrous iron and total iron. The redox and pH device were calibrated daily. At every sampling time of each experiment, total iron concentration, pH and the redox potential of the solution in the bioreactor were measured. Hence allowing for the determination of ferric to ferrous iron ratio in the bioreactor. The investigation of ferrous iron bio-oxidation was concluded at a redox potential of 600mV, and at this solution redox potential, the study to investigate the kinetics of ferric precipitates resumed. This Fe(III) study was operated for 36 hours for ferric iron. The difference between the initial total iron concentrations and the total iron concentration at maximum redox potential of the experiment facilitated the determination of ferric iron that precipitated in solution, which was used as an alternative to evaluate iron loss in the process at the end of each run. The ferrous iron concentration at maximum solution redox potential was also determined by titrating with both potassium dichromate and barium diphenylamine sulphonate (BDS). By subtracting the ferrous iron concentration from the total iron concentration we arrived at the ferric iron concentration. The following expression provides one of the important equation:

$$[Fe_T] = [Fe^{3+}] + [Fe^{2+}] \qquad 3.1$$

Where $[Fe^T]$ represents the total iron concentration (mmol Fe^{2+} L^{-1} h^{-1}), $[Fe^{3+}]$ represents ferric iron concentration (mmol Fe^{3+} L^{-1} h^{-1}), and $[Fe^{2+}]$ represents ferrous iron concentration (mmol Fe^{3+} L^{-1} h^{-1}).

The following expressions (3.2 & 3.3) show the ferrous iron oxidation equation and the Nernst Equation. The redox electrode (Ag/AgCl) calibration was performed against the half-life of ferrous to ferric iron oxidation, as shown in Equation 3.2. This helps in determining the ferric to a ferrous iron ratio within the bioreactor, as shown in Equation 3.3.

$$Fe^{2+} \rightarrow Fe^{3+} + e \qquad 3.2$$

$$E_h = E_h^{'} + \frac{RT}{nF} \ln \frac{[Fe^{3+}]}{[Fe^{2+}]} \qquad 3.3$$

Where the measured E_h represents standard redox potential, E'_h represents the solution potential measured, which accounts for the activity coefficient, formation of complexes, electrode type and fouling of the electrode. The values were obtained from the calibration plot of E_h versus, $\ln[Fe^{3+}/Fe^{2+}]$ with the intercept E'_h and the slope (RT/nF) been obtained from the plot.

3.4 Analysis of kinetic data

3.4.1 Microbial ferrous iron oxidation rate

The maximum overall ferrous-iron oxidation rate, $r_{Fe^{2+}}^{max}$ and apparent affinity constant for both Monod and Hansford model may be determined from equation 2.38 and 2.39. Equation 2.39 can be written in terms of $-r_{Fe^{2+}}$

$$r_{Fe^{2+}} = \frac{r_{max}[Fe^{2+}]}{K_s + [Fe^{2+}]} \qquad 2.38$$

$$r_{Fe^{2+}} = \frac{r_{Fe^{2+}}^{max}}{1 + K'_{Fe^{2+}} \frac{[Fe^{3+}]}{[Fe^{2+}]}} \qquad 2.39$$

These apparent affinity constants may be determined by fitting the experimental data to equations 2.38 and 2.39 using the least square method.

3.4.2 The effect of temperature

The maximum overall ferrous-iron oxidation rate, $r_{Fe^{2+}}^{max}$ and the operating temperature may be described by the Arrhenius Equation as shown in Equations 2.44 and 2.45.

$$r_{Fe^{2+}}^{max} = K \exp\left(-\frac{E_a}{RT}\right) \quad 2.44$$

$$\ln r_{Fe^{2+}}^{max} = -\frac{E_a}{R}\left(\frac{1}{T}\right) + \ln K \quad 2.45$$

The plot of $\ln r_{Fe^{2+}}^{max}$ versus $(1/T)$ should produce a straight line with a slope ($-E_a/R$) and an intercept ($\ln K$), and R is the universal gas constant. This provides information to determine the activation energy and the frequency factor for microbial ferrous-iron oxidation kinetics. The correlation factor (R^2), which was obtained inserted after plotting the experimental data, was determined. This accounts for the accuracy of the obtained experimental data. A correlation coefficient factor above 0.90 was accepted to be sufficient.

3.5 Conclusion

In this chapter, a detailed description of how the experimental study was carried out has been provided. A summary of the approaches is presented below:

- A description of the experimental rig used in measuring the kinetics of microbial ferrous-iron oxidation in a packed column reactor was given.
- A detailed description of the growth medium for the microorganism was presented.
- A detailed description showing the predominant bacteria obtained from the Centre for Bioprocess Engineering Research at the University of Cape Town, South Africa and the predominant bacteria used, was presented.
- Experimental procedures describing the effects of temperature and the precipitation of ferric iron were also discussed.
- The relevant techniques for conducting kinetics analysis and obtaining the desired parameters for microbial ferrous-iron oxidation were presented.

Chapter 4: The effect of temperature on the kinetics of microbial ferrous iron oxidation by *Acidothiobacillus ferrooxidans* in a packed-bed bioreactor

4.1 Introduction

Microbial ferrous iron oxidation is significant in hydrometallurgy, as it supplies the ferric ion reagent needed for the oxidation of sulfide minerals. The mechanism, involved in bio-oxidation, which is an essential sub-process of bioleaching of sulfide minerals, has been extensively researched (Silverman, 1967). Also, the kinetics of ferrous ion bio-oxidation sub-process has been investigated by several researchers (Gómez and Cantero, 2003, Hansford, 1997).

Early studies were conducted in shake flasks and stirred tank bioreactors with the view to provide an understanding of the kinetics and operating window for optimum performance (Boon et al, 1995; Breed et al., 1999; Meruane and Vargas, 2003). These studies have contributed to the success of tank bioleaching. Though, some studies were also conducted in reactor systems such as columns and packed bed (Chowdhury and Ojumu, 2014, Halinen et al., 2009b, Halinen et al., 2009a). However, it has been reported that results of studies conducted in these column systems may not be relevant to the real heap situation as these studies were conducted under flooded conditions which are contrary to the fluid dynamic in a typical bioleach heap situation (Chowdhury and Ojumu, 2014).

Although Chowdhury and Ojumu (2014) and Lizama et al. (2005) reported different kinetic parameters for ferrous ion bio-oxidation conducted in a bioreactor system that simulated heap solution flow dynamics when compared to flooded reactor systems. The studies were conducted at near microbial optimum temperature. However non-optimum conditions such as cold temperatures of less than 10^{o}C have been recorded to occur at internal zones of bioleach heaps, especially in regions where average weather condition may be freezing. It is important to understand the prevailing kinetics at these conditions (Ojumu et al., 2009, Ongendangenda and Ojumu, 2011). Available studies at low-temperature conditions by Kupka et al. (2007) and Ahonen and Tuovinen (1989) using shake flasks on investigating the kinetics of microbial ferrous iron oxidation do not mimic heap bioleach situation.

The objective of this study is to investigate the microbial oxidation of ferrous ion under cold conditions, in a packed column bioreactor system that is operated in a similar manner to bioleach heap. The result of the study will provide an understanding of the slow kinetic, by determining the parameters of the corresponding rate equation(s) that described the kinetics, which may be useful in design consideration of bio heap systems. Low-temperature iron oxidizing acidophiles iron (Ferroni et al., 1986, Ahonen and Tuovinen, 1989, Kupka et al., 2007) would be used in this study. Although Arrhenius equation has been used to determine

activation energy requirement for ferrous bio-oxidation, however, the studies were conducted at near microbial optimum temperature conditions (Ojumu et al., 2009, Chowdhury and Ojumu, 2014, Breed et al., 1999, Kupka et al., 2007, Ahonen and Tuovinen, 1989, Franzmann et al., 2005), and there is a dearth of studies conducted when temperatures become unfavourable for optimal performance. Hence, this study will determine the activation energy of microbial ferrous iron oxidation under cold conditions. This is to provide an understanding of the kinetics of microbial ferrous-iron oxidation by *Acidothiobacillus ferrooxidans* at cold conditions that are relevant to bioleach heap system.

4.2 Methodology

Batch culture experiments with *Acidothiobacillus ferrooxidans* were performed using a packed-bed column bioreactor at 6, 7, 8 and 10^{o}C. It should be noted that the coolant flow rate was adjusted such that a deviation of 0.5degrees was obtained in the bioreactor column. The initial solution pH of 1.35 ± 0.05 was achieved by adjusting with concentrated pH, the feed substrate that contains 5 g/L of total iron concentration. Section 3.2.2 described the experiment in detail.

4.3 Results and discussion

4.3.1 The rate of microbial ferrous iron oxidation, $r_{Fe^{2+}}$

The kinetics of microbial ferrous-iron oxidation were studied in a packed-column bioreactor, at an initial concentration of 5 g/L ferrous iron in the presence of *Acidothiobacillus ferrooxidans*. The Monod (Equation 2.38) and Hansford (Equation 2.39) were used to analyse the experimental data. These two models have been reported to describe ferrous bio-oxidation very accurately (Chowdhury, 2012, Ojumu et al., 2006).

$$-r_{Fe^{2+}} = \frac{r_{Fe^{2+}}^{max}[Fe^{2+}]}{K_{Fe^{2+}} + [Fe^{2+}]} \qquad 2.38$$

$$-r_{Fe^{2+}} = \frac{r_{Fe^{2+}}^{max}}{1 + K'_{Fe^{2+}}\frac{[Fe^{3+}]}{[Fe^{2+}]}} \qquad 2.39$$

The parameters in both Monod Equation $(r_{Fe^{2+}}^{max}, K_{Fe^{2+}})$ and Hansford Equation $(r_{Fe^{2+}}^{max}, K_{Fe^{2+}})$ were determined by fitting equations (2.38) and (2.39) to the experimental data, using Solver in Excel to minimize the sum of the square errors (SSE) between the measured and the predicted values of, $-r_{Fe^{2+}}$. This is shown in Figure 4.1a and b respectively. The maximum

ferrous-iron oxidation rate $r^{max}_{Fe^{2+}}$ was observed to increase when temperature increased within the range of temperature investigated (Table 4.1).

(a)

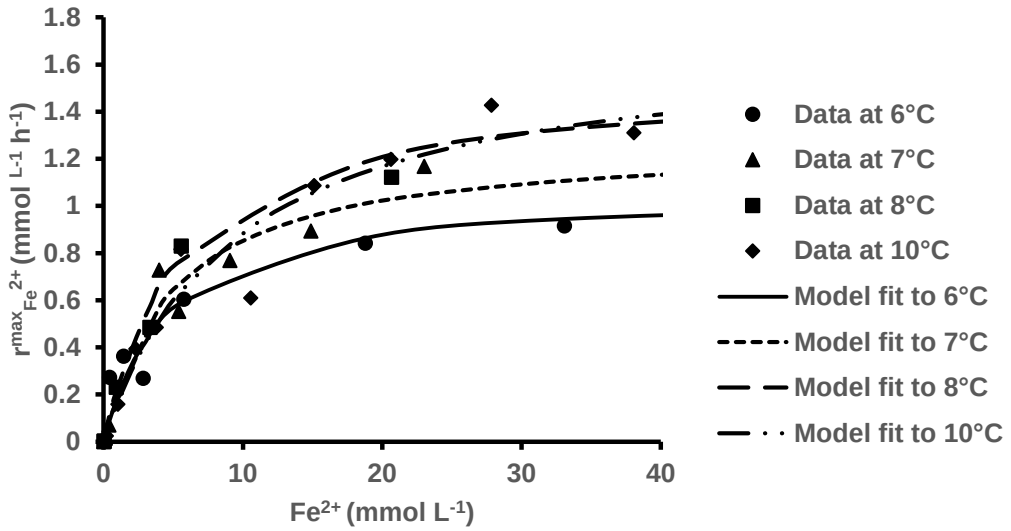

(b)

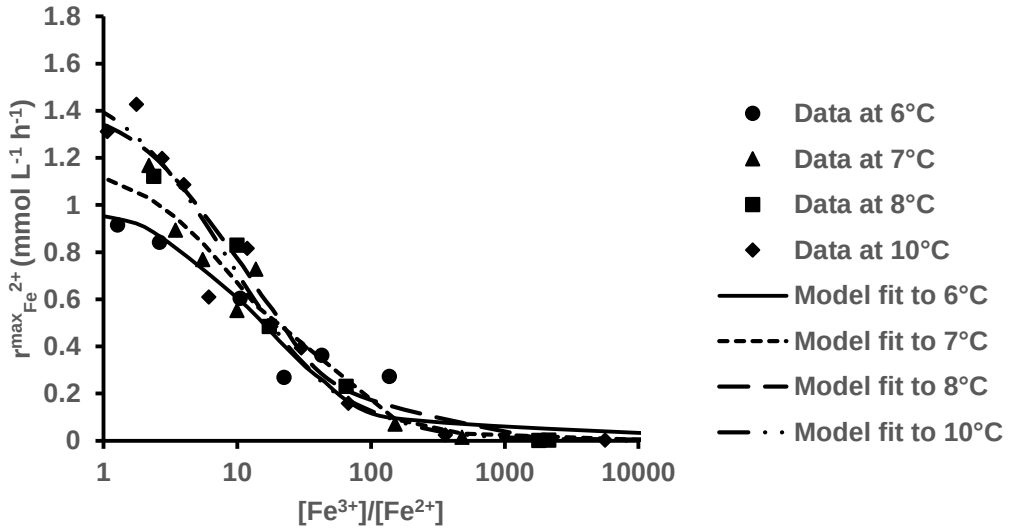

Figure 4.1: (a) The plot of ferrous-iron oxidation rate versus substrate concentration fitted to the Monod model; (b) The plot ferrous ion bio-oxidation rate versus ferric-to-ferrous ratio fitted to Hansford model.

Table 6: Maximum overall ferrous-iron oxidation and kinetic constant, determined by fitting the rate data to the Monod and Hansford models.

Temperature	Monod Model		Hansford Model		Average	Reference
	$r^{max}_{Fe^{2+}}$	$K_{Fe^{2+}}$	$r^{max}_{Fe^{2+}}$	$K'_{Fe^{2+}}$	$r^{max}_{Fe^{2+}}$	
6°C	1.08	4.67	1.02	0.0687	1.05	This study
Duplicate (6°)	1.31	4.67	1.23	0.0630	1.14	
7°C	1.27	4.83	1.21	0.0792	1.24	
8°C	1.41	4.95	1.46	0.0899	1.44	
10°C	1.65	7.16	1.53	0.0970	1.59	
4°C					0.0250	(Dopson et al., 2007)
20°C					4.30	(Lacey and Lawson, 1970)
30°C					5.55	(Alemzadeh et al., 2009)

Units: $r^{max}_{Fe^{2+}}$ (mmol/L.h); $K_{Fe^{2+}}$ (mmol/L); $K'_{Fe^{2+}}$ (dimensionless).

These results show the low activity of the microbes during the oxidation of ferrous ion within the temperature range investigated when compared to the oxidation rates reported in previous studies that were conducted at higher temperatures. Although it may be argued that there was no significant variation in the kinetics of the temperature studied, when compared with the studies by Chowdhury (2012) the significance may be apparent over a long period of time as may be the case in a typical bioleach heap operation, which may progress for months to years of continuous operation.

The study by Dopson et al. (2007), which was conducted at 4°C in a stirred tank bioreactor, reported maximum rate of oxidation of 0.025 mmol L^{-1} h^{-1}. This result shows that maximum ferrous iron oxidation rate was greater using a packed bed bioreactor when compared to stirred tank. Also, Kupka et al. (2007), reported an exponential pattern in the oxidation kinetics of ferrous iron oxidation conducted in shake flasks. The oxidation rate obtained in this study is small compared to the previous studies by Alemzadeh et al. (2009) and Lacey and Lawson (1970) with the maximum rate of 5.551 mmol L^{-1} h^{-1} and 4.30 mmol L^{-1} h^{-1}. The higher values of maximum oxidation rate found in previous studies as mentioned above may be as a result of different experimental conditions and/or temperature differences

The experiment at 6°C was repeated using the same column bioreactor as used during the course of experiments to ensure the validity of the data. The average maximum ferrous-iron oxidation rate was determined as shown in Table 6: Maximum overall ferrous-iron oxidation and kinetic constant, determined by fitting the rate data to the Monod and Hansford models.. The kinetic constants determined in this study using both Monod and Hansford models showed some increase with an increase in temperature. However, Monod Constant, as reported by

Chowdhury and Ojumu (2014), was higher relative to the values obtained in this study. A lower value is indicative of higher affinity, since the Monod Constant is an indication of microbial substrate affinity, in relation to cell growth and utilization of substrate. It is suggested that the Monod Constant values indicate that the energy obtained during oxidation process is directed towards cell maintenance in the packed bed column.

4.3.2 Determination of the activation energy of microbial ferrous iron oxidation

The effect of the increase in temperature with ferrous-iron oxidation rate may be described using the Arrhenius Equation (2.44). The equation was used to determine the activation energy of the investigated four temperatures, by plotting $\ln r_{Fe^{2+}}^{max}$ against $1/T$ which gives a straight line, from which the activation energy and frequency factor were determined. The values of the activation energy (E_a) and the frequency factor (K_o) for ferrous iron bio-oxidation kinetics were 67 kJ.mol^{-1} and 3.75 X10^9 mmol Fe^{2+}. L^{-1}. h^{-1}, respectively. These were average values obtained from the correlation of the experimental data to both Monod and Hansford Equations, as shown in Figure 4.2.

Several values of activation energy ranging from 33 to 96 kJ mol^{-1} on the effect of temperature on the growth of Acidothiobacillus ferrooxidans, with its ability to oxidize ferrous iron have been reported in literature (Ahonen and Tuovinen, 1989, Ferroni et al., 1986, Guay et al., 1977, Lacey and Lawson, 1970, Leduc et al., 1993, Lundgren, 1975, MacDonald and Clark, 1970). The value obtained from this study is within the range reported in the literature. The difference in reported values may have resulted from different monitoring approaches. However, differences in experimental conditions and reactor configurations may also be responsible for the variation. The activation energy determined from this study is comparable to the value of 68.4 kJ mol^{-1} obtained by (Nemati and Webb, 1997). Also, it should be noted that higher values of activation energy are indicative of a limitation in the biochemical reaction at low temperatures while lower values are associated to diffusion control.

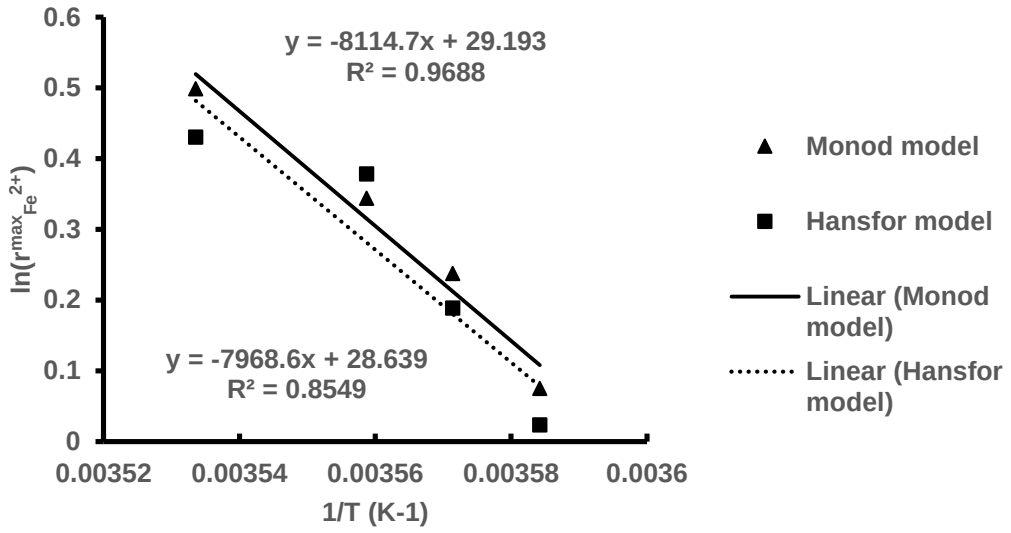

Figure 4.2: The effect of temperature on the maximum overall ferrous-iron oxidation rate using Arrhenius equation.

The relationship between apparent affinity constant ($K_{Fe^{2+}}$ and $K'_{Fe^{2+}}$) and temperature may be represented using a linear function (Equation 4.1 and 4.2), as shown in Figure 4.3.

Previous studies (Chowdhury, 2012, Breed et al., 1999, Ojumu et al., 2009) have reported this linear function.

$$K_{Fe^{2+}} = 6.33\ X\ 10^{-1} T - 172\ , \qquad R^2 = 0.85 \tag{4.1}$$

$$K'_{Fe} = 6.90\ X\ 10^{-3} T - 1.87\ , \qquad R^2 = 0.94 \tag{4.2}$$

(a)

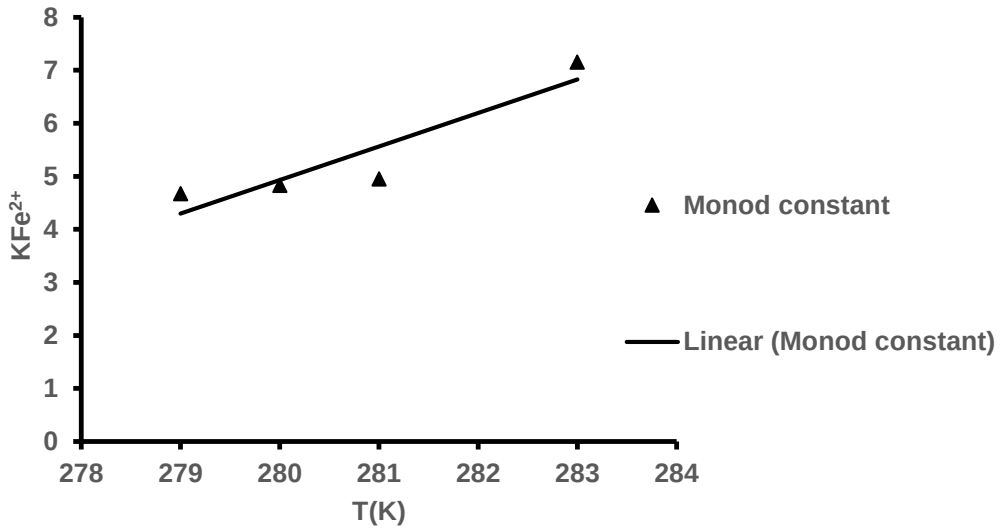

(b)

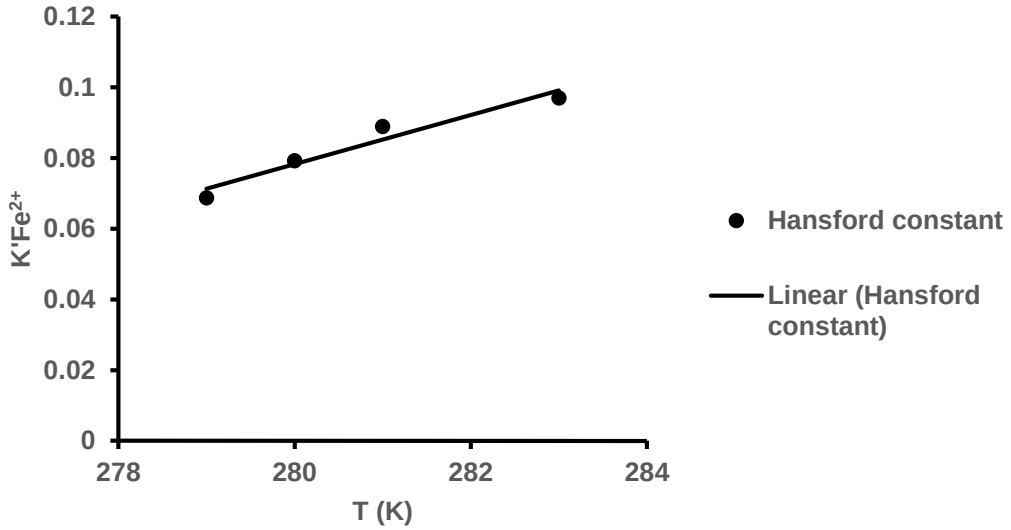

Figure 4.3: The effect of temperature on (a) the kinetic constant $K_{Fe^{2+}}$ of Monod equation and (b) the kinetic constant $K'_{Fe^{2+}}$ of Hansford Equation.

In order to obtain equation that predicts $r^{\max}_{Fe^{2+}}$ (maximum ferrous iron oxidation) as a function of ferric to ferric iron ratio ($[Fe^{3+}/Fe^{2+}]$) across a range of temperatures, the values of activation energy (E_a) and frequency factor K_o as well as the expression for $K_{Fe^{2+}}$ and $K'_{Fe^{2+}}$

(Equations 4.1 and 4.2) were substituted into the Monod and Hansford equations (2.38 and 2.39 respectively).

$$-r_{Fe^{2+}} = \frac{K_o \exp\left(-\frac{E_a}{RT}\right)\left[Fe^{2+}\right]}{\left(6.33\ X\ 10^{-1}T - 172\right) + \left[Fe^{2+}\right]} \qquad 4.3$$

$$-r_{Fe^{2+}} = \frac{K_o \exp\left(-\frac{E_a}{RT}\right)}{\left(6.90\ X\ 10^{-3}T - 1.87\right)\frac{\left[Fe^{3+}\right]}{\left[Fe^{2+}\right]}} \qquad 4.4$$

4.4 Conclusion

The Monod and Hansford equations were used to describe microbial ferrous-iron oxidation at low-temperature conditions in packed-bed bioreactors fairly accurately. The maximum ferrous iron oxidation was observed to increase with an increase in temperature in the range investigated. From the data obtained, the maximum rate of microbial ferrous iron oxidation in this study is low compared to previous studies conducted at higher temperatures. Even though, studies conducted at low temperatures used first order equation to describe results, thereby determining the rate constants of microbial ferrous iron oxidation. More so, both Monod and Hansford affinity constants increase with an increase in temperature. The value of the activation energy determined from the Arrhenius Equation indicated that the bio-oxidation reaction is biochemically limited at low temperatures. The rate of microbial ferrous-iron oxidation by *Acidothiobacillus ferrooxidans* is likely to be lower in stirred tank bioreactors than in packed bed columns if operated under the same condition. This study is expected to support the effort of predicting the performance of a heap bioleaching systems accurately at cold conditions.

Chapter 5: The effect of low temperature on ferric iron precipitate by *Acidothiobacillus ferrooxidans* in a packed column bioreactor

5.1 Introduction

The objective of various researchers on microbial ferrous iron oxidation has been to improve on the oxidation rate of ferrous iron oxidation. However, it was reported that ferric iron precipitate, which is solution pH dependent plays a key role in the rate of ferrous iron oxidation. The precipitation of ferric iron occurs as hydroxides, oxyhydroxides, and hydroxy-sulphate, with temperature being a dynamic that affects the precipitation (Kupka et al., 2007, Wang et al., 2006)

Ferric precipitates are known as a common and inevitable phenomenon as it may hinder the oxidation process. While its accumulation may enhance microbial bio-activity (Chowdhury and Ojumu, 2014), it has been shown that it can be managed by manipulating solution pH (Wanjiya et al, 2015). Slow precipitation of ferric iron observed at temperature, further reduces the decrease in the pH that accompanies Fe (III) oxyhydroxysulfate precipitation. It was observed in previous studies (Dopson et al., 2007, Kupka et al., 2007) that ferric ion precipitation was not significant during the bio-oxidation of ferrous ion to ferric ion at the cold condition. However, it was hypothesized that precipitation of ferric ion is continuous throughout the oxidation process or that it occurs only after the maximum potential has been reached.

The objective of this study is to investigate ferric ion precipitation with a view to understanding the kinetics of the precipitate formation under a cold condition in a packed-bed bioreactor. The result of this study will provide quantitative information about the slow kinetics of ferric precipitate in solution on one hand, and also provide an understanding of the trend of the formation be it continuous or preceded by bio-oxidation. These understanding may be useful in the design of bio-heap design.

5.2 Methodology

The study on the quantification of iron precipitate was carried out in a packed column at 6, 7, 8 and 10°C at pH 1.35 ± 0.05 with the feed substrate containing 5 g/L total iron concentration. The kinetics of ferric precipitation was investigated, starting at maximum solution redox potential. During the determination of ferric precipitate, the aqueous phase was sampled at 12-hour interval for 36 hours to determine the total iron concentration, starting at the maximum redox potential of the solution. The experimental approach was described in detail in Section 3.2.2.

5.3 Results and discussion

5.3.1 The effect of low temperature on the kinetics of ferric iron precipitation

The effect of ferric precipitate was observed to be increasing with increase in temperature within the range investigated. The maximum number of days taken for each experiment to attain its maximum redox potential, the conversion achieved and the iron precipitate is all shown in Table 7. The solution pH of ferrous iron oxidation increased at the start of the oxidation and decreased upon subsequent ferric iron precipitate, Kukpal et.al. (2007) reported observations similar to this. The redox potential of the solution decreased after it attained its maximum redox potential as observed during sampling, this indicates the depletion of ferrous iron which is a source of energy for the microbes. Despite all the available iron being in the form of Fe^{3+}, the solution in the bioreactor was clear of precipitate, with most of the ferric iron remaining in the solution.

Studies at low temperature with respect to ferric precipitate have also been reported, with the temperature being indicated to have a major effect on the formation of ferric iron precipitates (Ahonen and Tuovinen, 1989, Dopson et al., 2007, Kupka et al., 2007). The solution pH as shown in Figure 5.1 showed similarities in each of the temperatures investigated, showing high solubility of ferric iron, hence, a decrease in solution pH. Moreover, Kupka et al. (2007) showed that increase in solubility of ferric iron at low temperature helped a small amount of the precipitate in solution since ferric precipitates occur at higher pH. The amount of iron precipitate starting at the end of ferrous iron oxidation (maximum redox potential) to after 36 hours (during the ferric iron investigation) is shown in Table 7. The sum of ferric precipitate of all investigated temperature was insignificant compared to the mass of precipitate obtained in the study by Wanjiya et al. (2015).

Also, Liu et al. (2009) reported an amount of 3.73 g/L of ferric iron precipitate identified as jarosite obtained with an initial Fe^{2+} of 5 g/L, whereas, overall ferric iron precipitate obtained in solution in this study with an initial 5 g/L Fe^{2+} was 2.9 g/L. The difference between iron precipitate in the study by Liu et al. (2009) and this study is that the precipitate in the former was dried and quantified, while in this study, the formation of a precipitate was in solution.

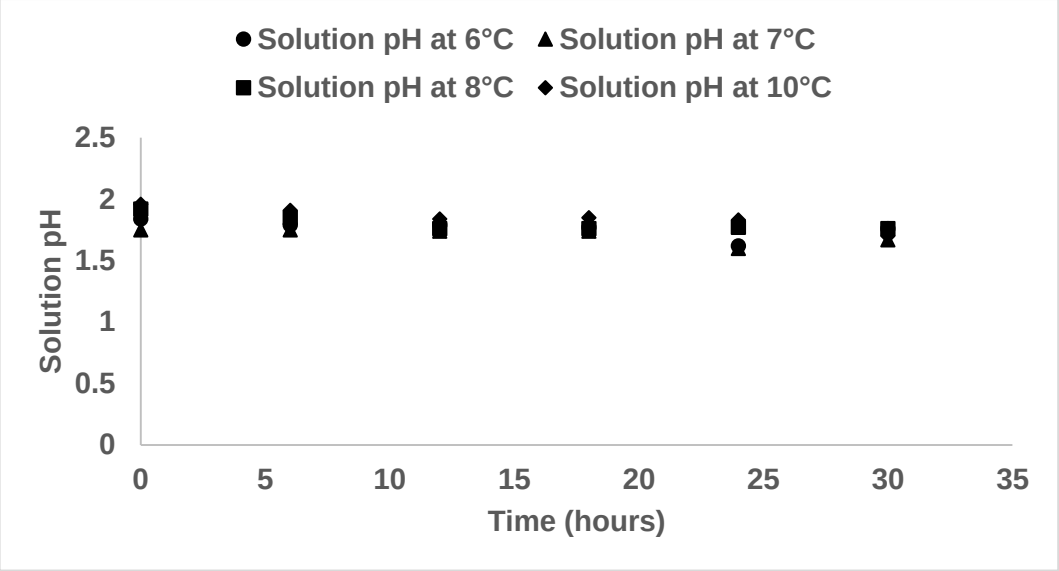

Figure 5.1: Solution pH during the investigation of ferric precipitate at maximum redox potential.

Table 7: Parameters obtained during the investigation of a ferric precipitate during 36 hours of operation.

Temperature	Max No of days	Max redox potential (mV)	pH (start to end)	Iron precipitate (g/L)	Conversion
6^{o}C	6	603	1.84 – 1.76	0.5991	99.9996
7^{o}C	6	603.8	1.75 – 1.67	0.6989	99.9957
8^{o}C	6	608.8	1.92 – 1.76	0.6989	99.9952
10^{o}C	5	617.2	1.96 – 1.70	0.8986	99.9987

This linear expression shows that despite depletion of ferrous iron, the rate of ferric iron precipitates increases as shown in Figure 5.2. If the experiments were to be allowed for a longer period, the rate would continue to increase. By arranging the overall data obtained at different temperatures in ascending order of % Fe precipitate, an overall plot of the data could be described in a single equation as shown in Figure 5.2. The region of Fe oxidation indicates the oxidation of ferrous iron at a conversion of 0.99. At this conversion, the maximum redox potential was achieved, further Fe precipitate continues to occur. Overall, the data suggests that ferric ion precipitate increased at the start of ferrous iron oxidation, and continued even after maximum redox potential was reached.

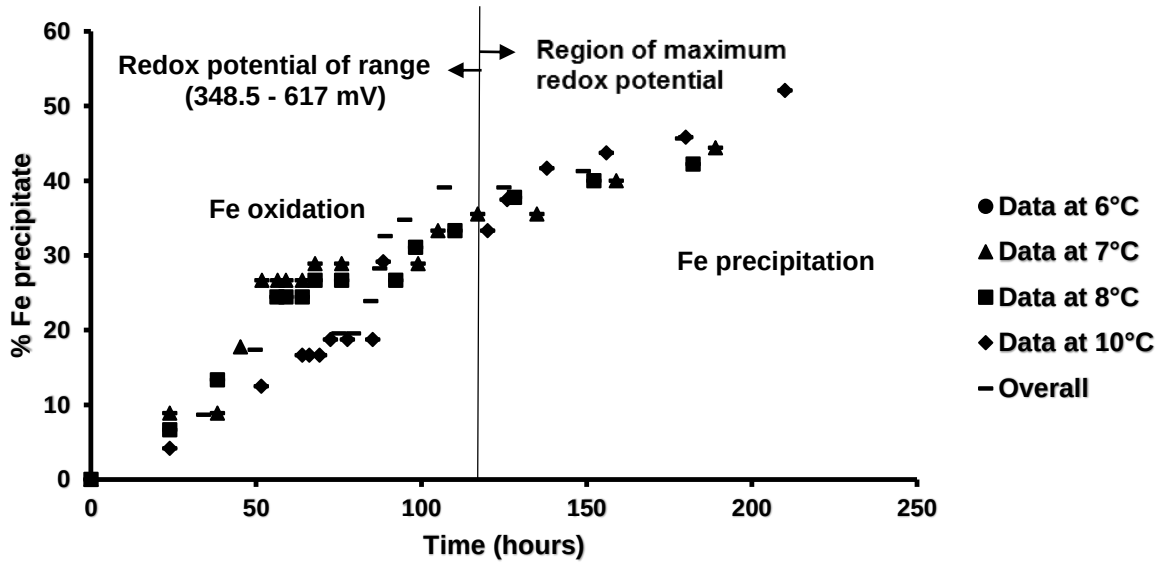

Figure 5.2: Fe precipitates at maximum redox potential

The experimental data in this study were described by both first and second-order differential equation with respect to total iron as shown in Figure 5.2 respectively. From the results, as shown in

Table *8*, first order was observed to have higher rate constants compared to second order. The values for rate constants of both orders increases with increase in temperature for ferric precipitate investigation. The R^2 values for the first order (Figure 5.3) and second order (Figure 5.4) were comparable to each other.

Table 8: Rate constants for first and second order of ferric iron precipitate

Temperature	**1st order (k_1) (h^{-1})**	**2nd order (k_2) ($m^{-1}\,h^{-1}$)**
6°C	0.0066	0.0024
7°C	0.0074	0.0026
8°C	0.008	0.0027
10°C	0.0106	0.0037

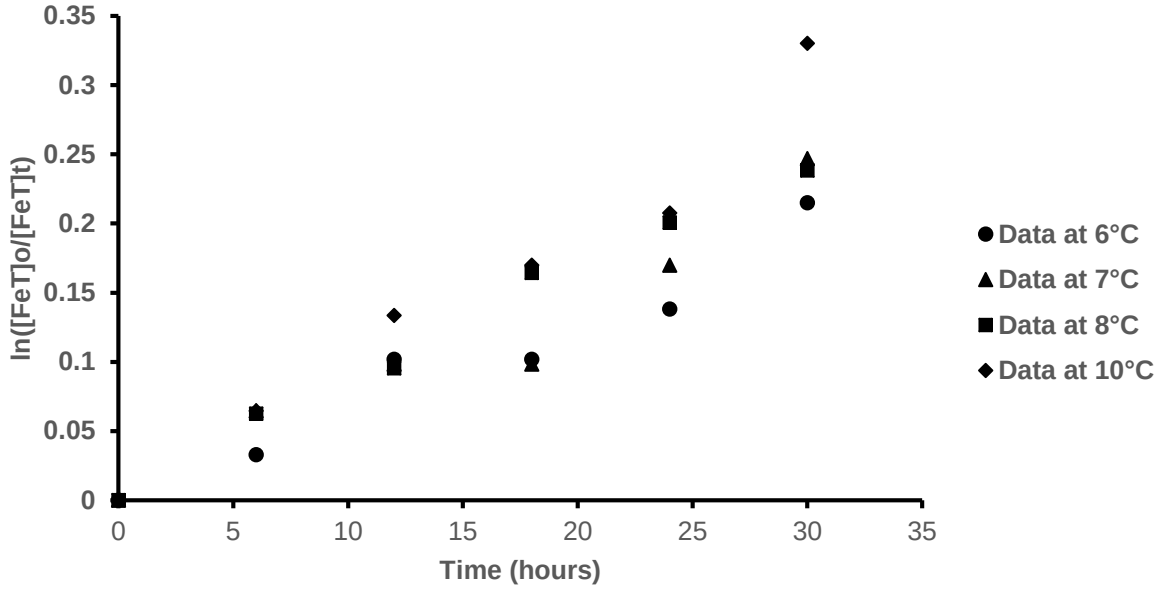

Figure 5.3: The plot of first order on the kinetics of ferric precipitate

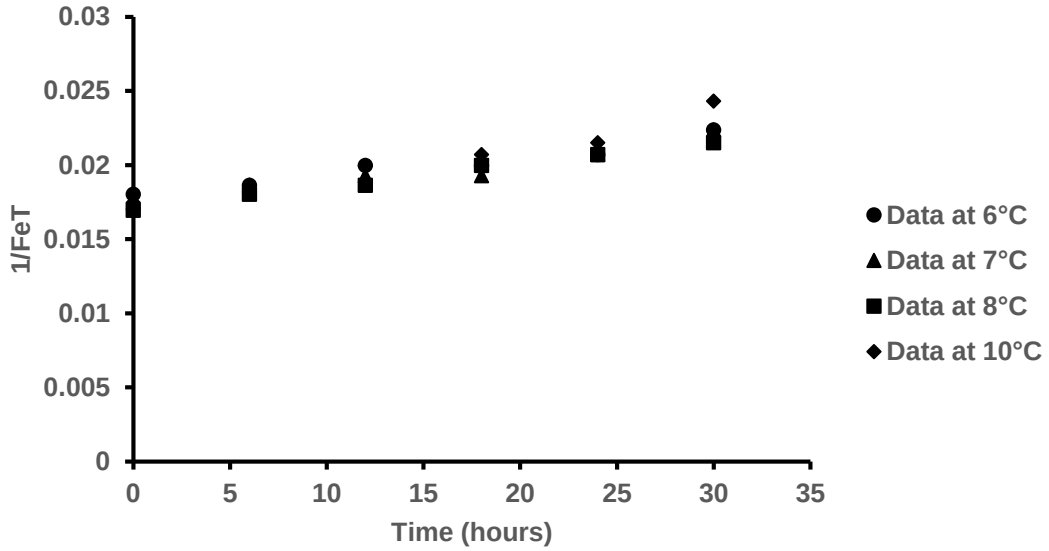

Figure 5.4: The plot of second order on the kinetics of ferric precipitate.

5.3.2 Determination of the activation energy of ferric precipitate at low temperature

The effect of low temperature on the ferric precipitate may also be described using Arrhenius Equation (2.44). The equation was used to determine the activation energy (E_a) in the range of temperature investigated, by plotting $\ln K$ against $1/T$, which gives a straight line. The

activation energy and the frequency factor (K_o) were determined from the above-mentioned graph. While the slope of the Arrhenius plot yielded a value of 77.1 kJ/mol for the activation energy for ferric precipitate based on the experimental data in the temperature range of 6 to 10°C respectively, this value was obtained from the correlation of the experimental data using first order differential equation.

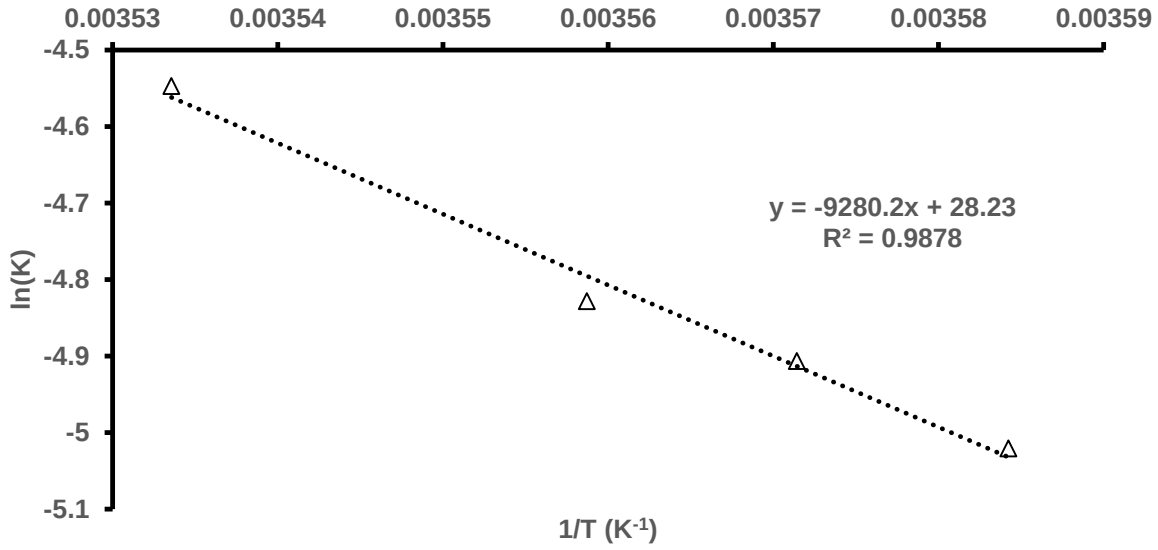

Figure 5.5: The effect of low temperature on the rate constant for ferric precipitate using Arrhenius Equation.

The value of activation energy (77.1 kJ/mol) and frequency factor (1.82 X10^9 mmol $Fe^{3+}.h^{-1}$) was obtained for ferric iron precipitate within the temperature range studied. It should be noted that although there are studies focusing on ferric precipitation in bioleach and/or bio-oxidation processes, the kinetics has not been investigated until now. This value of activation energy was obtained during the 36 hours of ferric precipitate investigation. Hence, when the maximum solution redox potential was attained.

5.4 Conclusion

The experimental data obtained during the investigation of the ferric iron precipitate in a packed-bed bioreactor was analysed. The solution in the bioreactor in the form of Fe^{3+} was clear of precipitate upon termination of each experiment. The maximum ferric iron precipitate in solution was observed at the highest operating temperature. The amount of ferric iron precipitate in a solution that precipitated between 7°C and 8°C shows that precipitation was higher at 7°C, whereas oxidation was higher at 8°C.

The rate constants at low-temperature conditions were described by both first and second order. The reaction is said to be first order, and higher rate constants were achieved in the first order. The value of activation energy determined from Arrhenius Equation for ferric iron precipitate was determined to be 77.1 kJ/mol. Further extension (for example 100 days) of the experiment will yield ferric iron precipitate within the bioreactor rather than only being in solution in the form of Fe^{3+}, which may explain the scenario currently encountered in bioleaching operations.

Chapter 6: Conclusions and Recommendations

6.1 Conclusions

The objective of this study was to investigate the kinetics of microbial ferrous iron oxidation by *Acidothiobacillus ferrooxidans* in a packed-bed bioreactor, with a view to providing some understanding of the effects of low temperatures and ferric iron precipitate on the kinetics that simulates a heap bioleach system. Similar studies using various simplified equations based on the Monod and Hansford models, which were developed to describe the rate of microbial ferrous iron oxidation by *Acidothiobacillus ferrooxidans, exist*. Moreover, the reported operating parameters in literature were similar to those which are promising in a real heap bioleaching operation.

This study investigated the microbial ferrous iron oxidation in a temperature controlled and well aerated packed bed reactor. The oxidation kinetics were monitored by measuring the redox potential during sampling. This allows for the determination of total iron concentration in the reactor. The rate of microbial ferrous iron oxidation was determined from the ferrous iron around the bioreactor.

This present study evidently shows that the microbial ferrous iron oxidation kinetics may be described by both Monod (Equation 2.38) and Hansford models (Equation 2.39).

$$r_{Fe^{2+}} = \frac{r_{\max}\left[Fe^{2+}\right]}{K_s + \left[Fe^{2+}\right]} \qquad 2.38$$

$$r_{Fe^{2+}} = \frac{r^{\max}_{Fe^{2+}}}{1 + K'_{Fe^{2+}}\dfrac{\left[Fe^{3+}\right]}{\left[Fe^{2+}\right]}} \qquad 2.39$$

Both models predicted the experimental data accurately. The effect of change in temperature on the system showed that the maximum overall oxidation rate increases exponentially with temperature as described by the Arrhenius Equation (Equation 2.44) and detailed in Chapter 4. The increase in the apparent affinity constant values for both Monod and Hansford models occurs with an increase in temperature. However, the apparent affinity constant values in the Hansford model are a combined parameter of ferric and ferrous inhibition on growth kinetics, hence limiting Hansford model as it does not predict the microbial activity. By utilizing all the kinetic parameters quantified into Equations 2.38 and 2.39, Equations 4.3 and 4.4 were obtained.

The investigation on the effect of ferric precipitation shows that ferric precipitates, as described in Chapter 5, increased with an increase in temperature and also increases in the kinetics

constant. The study showed that although ferric iron precipitate occurred at low-temperature range investigated, it remained in solution despite solution pH increase above 1.6. The amount of ferric precipitate obtained in solution is insignificant. Equation 2.38 and 2.39 were not capable of predicting the kinetics of ferric precipitate, however, the kinetic of ferric precipitate was predicted using both first- and second-order differential equation.

6.2 Recommendations

This study investigated the microbial ferrous iron oxidation kinetics that simulates heap bioleach operations. This study, however, does not represent the difficulties of a real heap leaching processes. Despite temperature changes and precipitation of ferric ions, various operating parameters within a heap operation (particle height, particle size, solution pH, etc.) also added to the limitations on the microbial kinetics. Several recommendations are suggested for future research.

Although the investigation into the effect of low temperature may not have revealed a real heap situation. However, it is important to note that the variation in temperature within a heap does not include a range promoting mesophilic growth only. The temperature in the industrial heap may range from a value as low as 10°C on the surface, in areas where low ambient temperature dominates, to values above 65°C within the heap that promotes the growth of extreme thermophiles. It is understood that this may decrease the efficiency of the heap operation by reducing the microbial ferrous iron oxidation rate, hence, the process becomes less economical. This study focuses only on a temperature range that promoted the mesophilic growth. Consequently, further studies relating to a wide temperature range is recommended, in order to contribute knowledge to the understanding of microbial ferrous iron oxidation that simulates a real heap situation.

The operating pH affects the microbial ferrous iron oxidation significantly. This study was carried out at a constant bioreactor pH of approximately 1.4. The pH was controlled by adjusting the pH of the feed stream. The optimum pH for *Acidothiobacillus ferrooxidans* growth is known to occur in a range between 2.0 to 2.3. Also, pH values close to 1.0 and 4.0 for *Acidothiobacillus ferrooxidans* strongly inhibit the growth. Ferric iron precipitate (jarosite) that is pH dependent is regarded as unwanted and cannot be eradicated completely, but it has been shown to facilitate the oxidation processes. Within the period of time covered, the solution was clear ferric precipitate, due to low-temperature ranges, but it is known that after several months of experiment, the precipitate will occur. It is therefore recommended that the management of ferric iron precipitate should be considered for further study.

Lastly, the packed bed bioreactor was operated at a constant particle height and size. Oxygen and carbon dioxide transfer may be rate controlling in the heap situation since oxygen is an electron acceptor in the microbial ferrous iron oxidation and carbon dioxide serves as a carbon source needed for cell generation. Oxygen and carbon dioxide are close to their saturation concentration at the bottom of the packed bioreactor, where the air is forced into the system. The bacteria catalysing the oxidation of ferrous iron and the continuous generation of new cells consume oxygen and carbon dioxide as the air flows upwards through the packing. This leads to a degree of oxygen and carbon dioxide depletion near the top of the packed-bed bioreactors. Understanding the effects of packing heights on the oxygen and carbon dioxide transfer is essential in a packed column bioreactor. This can be the focus of further investigation.

References

AHONEN, L. & TUOVINEN, O. H. 1989. Microbiological oxidation of ferrous iron at low temperatures. *Applied and environmental microbiology,* 55**,** 312-316.

ALEMZADEH, I., KAHRIZI, E. & VOSSOUGHI, M. 2009. Bio-oxidation of ferrous ions by Acidithioobacillus ferrooxidans in a monolithic bioreactor. *Journal of chemical technology and biotechnology,* 84**,** 504-510.

BIGHAM, J. M., JONES, F. S., ÖZKAYA, B., SAHINKAYA, E., PUHAKKA, J. A. & TUOVINEN, O. H. 2010. Characterization of jarosites produced by chemical synthesis over a temperature gradient from 2 to 40°C. *International Journal of Mineral Processing,* 94**,** 121-128.

BLANCH, H. W. 1981. Invited review microbial growth kinetics. *Chemical Engineering Communications,* 8**,** 181-211.

BOON, M. 1996. *Theoretical and experimental methods in the modelling of bio-oxidation kinetics of sulphide minerals*, TU Delft, Delft University of Technology.

BOON, M., HANSFORD, G. & HEIJNEN, J. 1995. Recent developments in modelling bio-oxidation kinetics. II. Kinetic modelling of the bio-oxidation of sulphide minerals in terms of the critical sub-processes involved. *Minerals Bioprocessing II***,** 63-82.

BOSECKER, K. 1997. Bioleaching: metal solubilization by microorganisms. *FEMS Microbiology reviews,* 20**,** 591-604.

BRANDL, H. 2008. Microbial leaching of metals. *Biotechnology Set, Second Edition***,** 191-224.

BREED, A., DEMPERS, C., SEARBY, G., GARDNER, M., RAWLINGS, D. & HANSFORD, G. 1999. The effect of temperature on the continuous ferrous-iron oxidation kinetics of a predominantly Leptospirillum ferrooxidans culture. *Biotechnology and bioengineering,* 65**,** 44-53.

BREED, A. & HANSFORD, G. 1999a. Effect of pH on ferrous-iron oxidation kinetics of Leptospirillum ferrooxidans in continuous culture. *Biochemical Engineering Journal,* 3**,** 193-201.

BREED, A. & HANSFORD, G. 1999b. Modeling continuous bioleach reactors. *Biotechnology and bioengineering,* 64**,** 671-677.

BREED, A. & HANSFORD, G. 1999c. Studies on the mechanism and kinetics of bioleaching. *Minerals engineering,* 12**,** 383-392.

BRIERLEY, C. 1999. Bacterial succession in bioheap leaching. *Process Metallurgy,* 9**,** 91-97.

BRIERLEY, C. 2010. Biohydrometallurgical prospects. *Hydrometallurgy,* 104**,** 324-328.

BRIERLEY, J. & BRIERLEY, C. 2001. Present and future commercial applications of biohydrometallurgy. *Hydrometallurgy,* 59**,** 233-239.

BRYAN, C., DAVIS-BELMAR, C., VAN WYK, N., FRASER, M., DEW, D., RAUTENBACH, G. & HARRISON, S. 2012. The effect of CO2 availability on the growth, iron oxidation and CO2-fixation rates of pure cultures of Leptospirillum ferriphilum and Acidithiobacillus ferrooxidans. *Biotechnology and bioengineering,* 109**,** 1693-1703.

CHOWDHURY, F. 2012. *The effect of temperature on the kinetics of microbial ferrous-iron oxidation in a packed column bioreactor.* Cape Peninsula University of Technology.

CHOWDHURY, F. & OJUMU, T. 2014. Investigation of ferrous-iron biooxidation kinetics by Leptospirillum ferriphilum in a novel packed-column bioreactor: Effects of temperature and jarosite accumulation. *Hydrometallurgy,* 141**,** 36-42.

CRUNDWELL, F. K. 1997. The kinetics of the chemiosmotic proton circuit of the iron-oxidizing bacterium Thiobacillus ferrooxidans. *Bioelectrochemistry and bioenergetics,* 43**,** 115-122.

CUSSLER, E. L. 1984. Fundamentals of mass transfer. *Diffusion: Mass Transfer in Fluid Systems***,** 237-273.

DAOUD, J. & KARAMANEV, D. 2006. Formation of jarosite during Fe 2+ oxidation by Acidithiobacillus ferrooxidans. *Minerals Engineering,* 19**,** 960-967.

DAS, T., AYYAPPAN, S. & CHAUDHURY, G. R. 1998. Factors affecting bioleaching kinetics of sulfide ores using acidophilic micro organisms.

DEMPERS, C. J. N. 2000. *An investigation into the use of batch experiments in the determination of the kinetics of ferrous-iron oxidation by Leptospirillum ferrooxidans.* University of Cape Town.

DOMIC, E. M. 2007. A review of the development and current status of copper bioleaching operations in Chile: 25 years of successful commercial implementation. *Biomining.* Springer.

DOPSON, M., HALINEN, A.-K., RAHUNEN, N., OZKAYA, B., SAHINKAYA, E., KAKSONEN, A. H., LINDSTROM, E. B. & PUHAKKA, J. A. 2007. Mineral and iron oxidation at low temperatures by pure and mixed cultures of acidophilic microorganisms. *Biotechnology and bioengineering,* 97**,** 1205-1215.

EHRLICH, H. L. 2001. Past, present and future of biohydrometallurgy. *Hydrometallurgy,* 59**,** 127-134.

FERRONI, G., LEDUC, L. & TODD, M. 1986. Isolation and temperature characterization of psychrotrophic strains of Thiobacillus ferrooxidans from the environment of a uranium mine. *The Journal of General and Applied Microbiology,* 32**,** 169-175.

FOGLER, H. S. 1999. Elements of chemical reaction engineering.

FRANZMANN, P., HADDAD, C., HAWKES, R., ROBERTSON, W. & PLUMB, J. 2005. Effects of temperature on the rates of iron and sulfur oxidation by selected bioleaching Bacteria and Archaea: application of the Ratkowsky equation. *Minerals Engineering,* 18**,** 1304-1314.

GÓMEZ, J. & CANTERO, D. 2003. Kinetic study of biological ferrous sulphate oxidation by iron-oxidising bacteria in continuous stirred tank and packed bed bioreactors. *Process Biochemistry,* 38**,** 867-875.

GRISHIN, S. I., BIGHAM, J. M. & TUOVINEN, O. H. 1988. Characterization of jarosite formed upon bacterial oxidation of ferrous sulfate in a packed-bed reactor. *Applied and environmental microbiology,* 54**,** 3101-3106.

GRISHIN, S. I. & TUOVINEN, O. H. 1988. Fast kinetics of Fe2+ oxidation in packed-bed reactors. *Applied and environmental microbiology,* 54**,** 3092-3100.

GUAY, R., SILVER, M. & TORMA, A. E. 1977. Ferrous iron oxidation and uranium extraction by Thiobacillus ferrooxidans. *Biotechnology and Bioengineering,* 19**,** 727-740.

HALINEN, A.-K., RAHUNEN, N., KAKSONEN, A. H. & PUHAKKA, J. A. 2009a. Heap bioleaching of a complex sulfide ore: Part I: Effect of pH on metal extraction and microbial composition in pH controlled columns. *Hydrometallurgy,* 98**,** 92-100.

HALINEN, A.-K., RAHUNEN, N., KAKSONEN, A. H. & PUHAKKA, J. A. 2009b. Heap bioleaching of a complex sulfide ore: Part II. Effect of temperature on base metal extraction and bacterial compositions. *Hydrometallurgy,* 98**,** 101-107.

HANSFORD, G. & VARGAS, T. 2001. Chemical and electrochemical basis of bioleaching processes. *Hydrometallurgy,* 59**,** 135-145.

HANSFORD, G. S. 1997. Recent developments in modeling the kinetics of bioleaching. *Biomining.* Springer.

INGLEDEW, W. Ferrous iron oxidation by Thiobacillus ferrooxidans. Biotechnology and bioengineering symposium, 1986. Wiley, 23-33.

INGLEDEW, W. J. 1982. Thiobacillus ferrooxidans the bioenergetics of an acidophilic chemolithotroph. *Biochimica et Biophysica Acta (BBA)-Reviews on Bioenergetics,* 683**,** 89-117.

JENSEN, A. B. & WEBB, C. 1995. Ferrous sulphate oxidation using Thiobacillus ferrooxidans: a review. *Process biochemistry,* 30**,** 225-236.

JONES, C. & KELLY, D. 1983. Growth of Thiobacillus ferrooxidans on ferrous iron in chemostat culture: influence of product and substrate inhibition. *Journal of chemical technology and biotechnology. B: biotechnology,* 33**,** 241-261.

KELLY, D. & JONES, C. 1978. Factors affecting metabolism and ferrous iron oxidation in suspensions and batch cultures ofThiobacillus ferrooxidans: relevance to ferric iron

leach solution regeneration. *Metallurgical applications of bacterial leaching and related microbiological phenomena.* Academic Press New York.

KIM, D.-J., PRADHAN, D., PARK, K.-H., AHN, J.-G. & LEE, S.-W. 2008. Effect of pH and temperature on iron oxidation by mesophilic mixed iron oxidizing microflora. *Materials transactions,* 49**,** 2389-2393.

KINNUNEN, P. H.-M. & PUHAKKA, J. A. 2005. High-rate iron oxidation at below pH 1 and at elevated iron and copper concentrations by a Leptospirillum ferriphilum dominated biofilm. *Process biochemistry,* 40**,** 3536-3541.

KUPKA, D., RZHEPISHEVSKA, O. I., DOPSON, M., LINDSTRÖM, E. B., KARNACHUK, O. V. & TUOVINEN, O. H. 2007. Bacterial oxidation of ferrous iron at low temperatures. *Biotechnology and bioengineering,* 97**,** 1470-1478.

LACEY, D. & LAWSON, F. 1970. Kinetics of the liquid-phase oxidation of acid ferrous sulfate by the bacterium Thiobacillus ferrooxidens. *Biotechnology and Bioengineering,* 12**,** 29-50.

LEDUC, L., TREVORS, J. & FERRONI, G. 1993. Thermal characterization of different isolates of Thiobacillus ferrooxidans. *FEMS microbiology letters,* 108**,** 189-193.

LIU, J.-Y., XIU, X.-X. & CAI, P. 2009. Study of formation of jarosite mediated by thiobacillus ferrooxidans in 9K medium. *Procedia Earth and Planetary Science,* 1**,** 706-712.

LIZAMA, H. 2009. Oxygen liquid-film mass transfer in heap leaching. *Hydrometallurgy,* 100**,** 29-34.

LIZAMA, H., HARLAMOVS, J., MCKAY, D. & DAI, Z. 2005. Heap leaching kinetics are proportional to the irrigation rate divided by heap height. *Minerals Engineering,* 18**,** 623-630.

LIZAMA, H. M. 2001. Copper bioleaching behaviour in an aerated heap. *International Journal of Mineral Processing,* 62**,** 257-269.

LUNDGREN, D. G. 1975. Microbiological problems in strip mine areas: Relationship to the metabolism of Thiobacillus ferrooxidans.

MACDONALD, D. & CLARK, R. 1970. The oxidation of aqueous ferrous sulphate by Thiobacillus ferrooxidans. *The Canadian Journal of Chemical Engineering,* 48**,** 669-676.

MAZUELOS, A., CARRANZA, F., ROMERO, R., IGLESIAS, N. & VILLALOBO, E. 2010. Operational pH in packed-bed reactors for ferrous ion bio-oxidation. *Hydrometallurgy,* 104**,** 186-192.

MAZUELOS, A., PALENCIA, I., ROMERO, R., RODRIGUEZ, G. & CARRANZA, F. 2001. Ferric iron production in packed bed bioreactors: influence of pH, temperature, particle size, bacterial support material and type of air distributor. *Minerals Engineering,* 14**,** 507-514.

MAZUELOS, A., ROMERO, R., PALENCIA, I., CARRANZA, F. & BORJAS, F. 2002. Oxygen transfer in ferric iron biological production in a packed-bed reactor. *Hydrometallurgy,* 65**,** 15-22.

MAZUELOS, A., ROMERO, R., PALENCIA, I., IGLESIAS, N. & CARRANZA, F. 1999. Continuous ferrous iron biooxidation in flooded packed bed reactors. *Minerals engineering,* 12**,** 559-564.

MONOD, J. 1942. Recherches sur la croissance des cultures bacteriennes.

MRWEBI, M. 2004. *Testing Monod: growth rate as a function of glucose concentration in Saccharomyces cerevisiae.* Stellenbosch: University of Stellenbosch.

MURR, L. & BRIERLEY, J. A. 1978. The use of large-scale test facilities in studies of the role of microorganisms in commercial leaching operations. *Metallurgical applications of bacterial leaching and related microbiological phenomena***,** 491-520.

NAIK, L. 2010. *The effect of carbon dioxide on the growth and activity of leptospirillum ferriphilum.* University of Cape Town.

NEIJSSEL, O. & TEMPEST, D. 1976. Bioenergetic aspects of aerobic growth of Klebsiella aerogenes NCTC 418 in carbon-limited and carbon-sufficient chemostat culture. *Archives of Microbiology,* 107**,** 215-221.

NEMATI, M., HARRISON, S., HANSFORD, G. & WEBB, C. 1998. Biological oxidation of ferrous sulphate by Thiobacillus ferrooxidans: a review on the kinetic aspects. *Biochemical engineering journal,* 1**,** 171-190.

NEMATI, M. & WEBB, C. 1997. A kinetic model for biological oxidation of ferrous iron by Thiobacillus ferrooxidans. *Biotechnology and Bioengineering,* 53**,** 478-486.

NGOMA, I. E. 2015. *Investigating the effect of acid stress on selected mesophilic bioleaching microorganisms.* Department of Chemical Engineering, Cape Peninsula University of Technology.

NGOMA, I. E., OJUMU, T. V. & HARRISON, S. T. 2015. Investigating the effect of acid stress on selected mesophilic micro-organisms implicated in bioleaching. *Minerals Engineering,* 75**,** 6-13.

NIKOLOV, L., VALKOVA-VALCHANOVA, M. & MEHOCHEV, D. 1988. Oxidation of high ferrous iron concentrations by chemolithotrophic Thiobacillus ferrooxidans in packed bed bioreactors. *Journal of biotechnology,* 7**,** 87-94.

OJUMU, T., PETERSEN, J., SEARBY, G. & HANSFORD, G. 2006. A review of rate equations proposed for microbial ferrous-iron oxidation with a view to application to heap bioleaching. *Hydrometallurgy,* 83**,** 21-28.

OJUMU, T. V., HANSFORD, G. S. & PETERSEN, J. 2009. The kinetics of ferrous-iron oxidation by Leptospirillum ferriphilum in continuous culture: the effect of temperature. *Biochemical Engineering Journal,* 46**,** 161-168.

OJUMU, T. V., PETERSEN, J. & HANSFORD, G. S. 2008. The effect of dissolved cations on microbial ferrous-iron oxidation by Leptospirillum ferriphilum in continuous culture. *Hydrometallurgy,* 94**,** 69-76.

OKEREKE, A. & STEVENS, S. E. 1991. Kinetics of iron oxidation by Thiobacillus ferrooxidans. *Applied and environmental microbiology,* 57**,** 1052-1056.

OLSON, G., BRIERLEY, J. & BRIERLEY, C. 2003. Bioleaching review part B. *Applied microbiology and biotechnology,* 63**,** 249-257.

ONGENDANGENDA, H. & OJUMU, T. 2011. The effect of initial pH on the kinetics of ferrous-iron biooxidation at low temperature. *African Journal of Biotechnology,* 10**,** 1679-1683.

OZKAYA, B., SAHINKAYA, E., NURMI, P., KAKSONEN, A. H. & PUHAKKA, J. A. 2007. Iron oxidation and precipitation in a simulated heap leaching solution in a Leptospirillum ferriphilum dominated biofilm reactor. *Hydrometallurgy,* 88**,** 67-74.

ÖZKAYA, B., SAHINKAYA, E., NURMI, P., KAKSONEN, A. H. & PUHAKKA, J. A. 2007. Kinetics of iron oxidation by Leptospirillum ferriphilum dominated culture at pH below one. *Biotechnology and bioengineering,* 97**,** 1121-1127.

PANDA, S., SANJAY, K., SUKLA, L., PRADHAN, N., SUBBAIAH, T., MISHRA, B., PRASAD, M. & RAY, S. 2012. Insights into heap bioleaching of low grade chalcopyrite ores—A pilot scale study. *Hydrometallurgy,* 125**,** 157-165.

PANTELIS, G. & RITCHIE, A. I. M. 1990. Macroscopic transport mechanisms as a rate-limiting factors in dump leaching of pyritic ores. *Applied Mathematical Modelling,* 16**,** 553-560.

PENEV, K. & KARAMANEV, D. 2010. Batch kinetics of ferrous iron oxidation by Leptospirillum ferriphilum at moderate to high total iron concentration. *Biochemical Engineering Journal,* 50**,** 54-62.

PETERSEN, J. & DIXON, D. 2004. Bacterial growth and propagation in chalcocite heap bioleach scenarios. *Biohydrometallurgy–a sustainable technology in evolution, IBS***,** 65-74.

PETERSEN, J. & DIXON, D. G. 2007. Modeling and optimization of heap bioleach processes. *Biomining.* Springer.

PETERSEN, J., MINNAAR, S. & DU PLESSIS, C. 2010. Carbon dioxide and oxygen consumption during the bioleaching of a copper ore in a large isothermal column. *Hydrometallurgy,* 104**,** 356-362.

PETERSEN, J., MINNAAR, S. & DU PLESSIS, C. Respirometry studies of the bioleaching of a copper ore in large columns—effect of changing temperatures. Proceedings of the 19th International Biohydrometallurgy Symposium (IBS2011), 2011. 53-58.

PIRT, S. 1965. The maintenance energy of bacteria in growing cultures. *Proceedings of the Royal Society of London B: Biological Sciences,* 163**,** 224-231.

PLUMB, J., MUDDLE, R. & FRANZMANN, P. 2008. Effect of pH on rates of iron and sulfur oxidation by bioleaching organisms. *Minerals Engineering,* 21**,** 76-82.

POGLIANI, C. & DONATI, E. 2000. Immobilisation of Thiobacillus ferrooxidans: importance of jarosite precipitation. *Process Biochemistry,* 35**,** 997-1004.

PRADHAN, N., NATHSARMA, K., RAO, K. S., SUKLA, L. & MISHRA, B. 2008. Heap bioleaching of chalcopyrite: a review. *Minerals Engineering,* 21**,** 355-365.

RATKOWSKY, D., OLLEY, J., MCMEEKIN, T. & BALL, A. 1982. Relationship between temperature and growth rate of bacterial cultures. *Journal of Bacteriology,* 149**,** 1-5.

RAWLINGS, D. E. 2002. Heavy metal mining using microbes 1. *Annual Reviews in Microbiology,* 56**,** 65-91.

ROELS, J. 1983. Energetics and kinetics in biotechnology.

ROHWERDER, T., GEHRKE, T., KINZLER, K. & SAND, W. 2003. Bioleaching review part A. *Applied Microbiology and Biotechnology,* 63**,** 239-248.

ROHWERDER, T. & SAND, W. 2007. Mechanisms and biochemical fundamentals of bacterial metal sulfide oxidation. *Microbial processing of metal sulfides.* Springer.

SAND, W., GEHRKE, T., JOZSA, P.-G. & SCHIPPERS, A. 2001. (Bio) chemistry of bacterial leaching—direct vs. indirect bioleaching. *Hydrometallurgy,* 59**,** 159-175.

SCHNELL, H. A. 1997. Bioleaching of copper. *Biomining.* Springer.

SILVERMAN, M. P. 1967. Mechanism of bacterial pyrite oxidation. *Journal of Bacteriology,* 94**,** 1046-1051.

SMITH, J. R., LUTHY, R. G. & MIDDLETON, A. C. 1988. Microbial ferrous iron oxidation in acidic solution. *Journal (Water Pollution Control Federation)***,** 518-530.

TEKIN, D., YÖRÜK, S. & BAYHAN, Y. 2014. The effect of temperature on rate of bacterial oxidation of Fe (II). *BULGARIAN CHEMICAL COMMUNICATIONS,* 46**,** 117-119.

TEKIN, D., YORUK, S. & BAYHAN, Y. K. 2013. The effect of temperature on rate of bacterial oxidation of Fe(II).

VAN ASWEGEN, P. C., VAN NIEKERK, J. & OLIVIER, W. 2007. The BIOX™ process for the treatment of refractory gold concentrates. *Biomining.* Springer.

VAN SCHERPENZEEL, D., BOON, M., RAS, C., HANSFORD, G. & HEIJNEN, J. 1998. Kinetics of ferrous iron oxidation by Leptospirillum bacteria in continuous cultures. *Biotechnology progress,* 14**,** 425-433.

VISHNIAC, W. & SANTER, M. 1957. The thiobacilli. *Bacteriological Reviews,* 21**,** 195.

WANJIYA, M. 2013. *Investigation of bacterial ferrous iron oxidation kinetics in a novel packed-column reactor: pH and jarosite management.* Cape Peninsula University of Technology, South Africa.

WANJIYA, M., CHOWDHURY, F. & OJUMU, T. V. Solution pH and Jarosite Management during Ferrous Iron Biooxidation in a Novel Packed-Column Bioreactor. Advanced Materials Research, 2015. Trans Tech Publ, 291-295.

WATLING, H. 2006. The bioleaching of sulphide minerals with emphasis on copper sulphides—a review. *Hydrometallurgy,* 84**,** 81-108.

YUJIAN, W., XIAOJUAN, Y., WEI, T. & HONGYU, L. 2007. High-rate ferrous iron oxidation by immobilized Acidithiobacillus ferrooxidans with complex of PVA and sodium alginate. *Journal of microbiological methods,* 68**,** 212-217.

ZENG, A.-P. & DECKWER, W.-D. 1995. A kinetic model for substrate and energy consumption of microbial growth under substrate-sufficient conditions. *Biotechnology progress,* 11**,** 71-79.

APPENDIX A: Statistical analysis

APPENDIX A

A.1 Sum of squares

Consider two quantities: y_i, the measured data and $\hat{y}_i$, the predicted data, which can be represented by regression line $\hat{y} = a + bx$, where a and b are the intercept and slope of the regression line respectively.

We define sum of squares due to error (SSE) as the sum of the square of the difference between the observed quantity and the predicted as shown in Equation A1.1

$$SSE = \sum \left(y_i - \hat{y}_i \right)^2 = \sum \left(y_i - a - bx_i \right)^2 \quad \text{A1.1}$$

This quantity will be small if the observed values y_i fall close to the regression line $\hat{y}_i = a + bx$, and will be large if they do not.

The term $y_i - \hat{y}_i$ is called the error for the observation. By substituting $a = \bar{y} - b\bar{x}$ into Equation A1.1, SSE can be expressed as follows:

$$SSE = \sum \left(y_i - \bar{y} + b\bar{x}_i \right)^2 = \sum \left(\left(y_i - \bar{y} \right) - b\left(\bar{x}_i - \bar{x} \right) \right)^2$$

$$= \sum \left(y_i - \bar{y} \right)^2 - 2b \sum \left(y_i - \bar{y} \right)\left(x_i - \bar{x} \right) + b^2 \sum \left(x_i - \bar{x} \right)^2 \quad \text{A1.2}$$

$$= SS_y + 2bSS_{xy} + b^2 SS_x$$

But $b = SS_{xy} / SS_x$, then SSE can written from Equation A1.2 as

$$SSE = SS_y - bSS_{xy} \quad \text{A1.3}$$

The first term on the right-hand side of Equation A1.3 is called total sums of squares and denoted by SST, such that SST = SS_y

The second term measures how much the total variability is reduced by the regression line $\hat{\gamma} = a + bx$. The term bSS_{xy}, which is denoted by SSR, is known as the sum of squares due to regression. By re-writing equation A1.3 becomes:

$$SSE = SST - SSR \quad \text{A1.4}$$

The importance of Equation A1.4 is that it reveals that SST may be decomposed into SSR and the error sums squares, SSE, the decomposition is explained by regression. Rewriting Equation A1.4 gives:

$$\frac{SSE}{SST} = 1 - \frac{SSR}{SST} \qquad \text{A1.5}$$

Where,

$$\frac{SSR}{SST} = \frac{bSS_{xy}}{SS_y} = \frac{SS^2_{xy}}{SS_{xy} SS_y} = R^2$$

$$SS_x = \sum x^2 - \frac{\left(\sum x\right)^2}{n}$$

$$SS_y = \sum y^2 - \frac{\left(\sum y\right)^2}{n}$$

$$SS_{xy} = \sum xy - \frac{\left(\sum x\right)\left(\sum y\right)}{n}$$

By using Equation A1.5, the error sum of squares (SSE) and the coefficient of regression (R^2) may be related, as shown in Equation A1.6

$$R^2 = 1 - \frac{SSE}{SST} \qquad \text{A1.6}$$

The relationship as described above will be applied in determining error analysis between the modelled and measured data that was obtained in this experiment.

A1.2 Error analysis between modeled and measured data

The regression coefficients as shown in Table A1.1 represent the predicted data using both the Monod and Hansford equations.

Table A1.1: Error analysis of experimental data.

Microbial ferrous-iron oxidation rate $r_{Fe^{2+}}$												
6°C			**7°C**			**8°C**			**10°C**			
Measured data	**a**	**a***	**Measured data**	**a**	**a***	**Measured data**	**a**	**a***	**Measured data**	**a**	**a***	
1.06	1.01	1.01	1.16	1.18	1.19	1.12	1.22	1.21	1.31	1.38	1.39	
0.915	0.945	0.942	1.13	1.13	1.13	0.829	0.769	0.776	1.43	1.31	1.31	
0.841	0.863	0.868	1.17	1.05	1.03	0.485	0.572	0.575	1.20	1.22	1.22	
0.605	0.595	0.595	0.893	0.957	0.947	0.231	0.216	0.215	1.09	1.11	1.11	
0.269	0.407	0.403	0.768	0.825	0.838	0.000658	0.00893	0.00909	0.816	0.712	0.715	
0.273	0.253	0.260	0.553	0.666	0.672	0.00167	0.00750	0.00765	0.484	0.562	0.563	
0.273	0.0904	0.0984	0.728	0.574	0.577				0.393	0.394	0.393	
SSR	0.0685	0.0632		0.0599	0.0662		0.0139	0.358		0.0377	0.0395	

A represents the predicted data using the Monod equation, while a* represents the Boon and Hansford equation.

APPENDIX B: Calibration

APPENDIX B

B.1 Theoretical aspect of the calibration using the Nernst Equation

The Nernst Equation (Equation C1.1) defines the relationship between the redox potential (E_h), the standard redox potential $(E^o{}_h)$ and the ferric to ferrous iron concentration $[Fe^{3+}]/[Fe^{2+}]$.

$$E_h = E^o{}_h + \frac{RT}{nF} \ln \frac{[a_{Fe^{3+}}]}{[a_{Fe^{2+}}]} \qquad \text{B1.1}$$

The standard redox potential $(E^o{}_h)$ for the half cell reaction $(Fe^{2+} \rightarrow Fe^{3+} + e)$ is 770 mV. This is derived from the thermodynamic data and applies to a situation where both activities of ferric, $a_{Fe^{3+}}$, and ferrous iron, $a_{Fe^{2+}}$, are equal, measured with a standard Hydrogen electrode. When the ionic strength is only zero, the activity of a compound *I*, a_i is equal to its concentration. With ionic strength greater than zero, $a_i = \gamma_i C_i$, where γ_i represents the activity coefficient. At equal ferric and ferrous iron concentrations, the actual value of E_h would change as the ionic strength increases as a result of the influence or other cations and anions. With the presence of complexing agents $(SO_4{}^{2-} OH^-)$ brings about a decrease of free ferrous and ferric ions (ref). By using Visual Minteq and HSC® Chemistry software that through simulation, that stronger complexes are formed with ferric reasonably than ferrous ions. Equation C1.1 may be written as:

$$E_h = E_h{}' + \frac{RT}{nF} \ln \frac{[Fe^{3+}]}{[Fe^{2+}]} \qquad 3.3$$

Where $E_h{}' = E_h{}^o + \frac{RT}{nF} \ln \frac{\gamma_{Fe^{3+}}}{\gamma_{Fe^{2+}}}$

The term $E_h{}'$ is referred as the solution potential that is measured at equal total ferric and ferrous-iron concentrations, and it accounts for activity coefficients Fe^{3+} and Fe^{2+}, the formation of complexes with Fe^{3+} and Fe^{2+} and the type of electrode. The adapted Nernst equation describes the measured redox (solution) potential, $E_h{}'$, the standard redox potential and the ratio between the total concentrations of ferric and ferrous ions. The intercept (E'_h) and slope (RT/nF) are then obtained from a plot of E_h versus $\ln([Fe^{3+}]/[Fe^{2+}])$.

Table B1.1: Values of parameters of calibration using Nernst equation

Temperature (°C)	E'_h (mV)	RT/nF (C J.mol^{-2})	R^2
6	397.35	17.004	0.9581
7	400.08	19.106	0.9855
8	399.15	17.345	0.9667
10	402.09	17.198	0.9642

APPENDIX C: Determination of Concentration of Iron Species

APPENDIX C

C.1 Reagent preparation

C.1.1 Spekker acid

Spekker acid solution was prepared my diluting equal volumes of 98% concentrated sulphuric acid and 85% of phosphoric acid with water in the ratio of 3:4 (acid: water), which is done by the following:

- Measure out 600 ml distilled water in a 2 L beaker
- Add 225 ml of 98% concentrated sulphuric acid and 225 ml of 85% phosphoric acid carefully and slowly into the walls of the beaker (Caution: heat of mixing usually result to localized boiling on rapid addition of the acids)
- Allow the solution to cool to room temperature before transferring into a storage bottle.

C.1.2 Stannous chloride solution

- Weigh out 30 g stannous chloride in a 200 ml beaker
- Add 100 ml of 32% concentrated hydrochloric acid and agitate at 50°C until it completely dissolves.
- Allow to cool to room temperature and dilute with 200 ml distil water.
- Add a small amount of granular tin to retard precipitation

C.1.3 Mercuric Chloride solution ($HgCl_2$)

- Weigh out 50 g mercuric chloride in a 2 L beaker
- Add 1 L of distilled water and agitate until completely dissolves (about 2 hours)
- Add a spatula tip of $HgCl_2$ and stir for further 2 hours before storage

C.1.4 Potassium Dichromate solution ($K_2Cr_2O_7$ – 0.0149 M)

- Dry about 10 g of $K_2Cr_2O_7$ (Mw = 294.2 g/mol) in an oven at 105 – 110 °C for 1 – 2 hours.
- Cool in a desiccator.
- Accurately weigh out 8.78 g of the dried $K_2Cr_2O_7$ into a 100 ml beaker.

- Transfer quantitatively into a 2 L standard using 1.5 L distilled water and agitate until completely dissolved.
- Transfer quantitatively into a 2 L standard flask and make-up to mark with distilled water.

C.1.5 Barium Diphenylamine Sulphonate (BDS) solution

(C24 H20BaN2O6S2)

- Weigh out 1 g of barium diphenylamine sulphonate in 250 ml beaker.
- Add 100 ml of 98% concentrated sulphuric acid. Agitate until completely dissolved.

C.2 Determination of ferrous-iron concentration by titration with potassium dichromate solution

- Pipette 5 ml of the aliquot solution into a 125 ml conical flask.
- Add 10 ml of the spekker acid solution.
- Add 2 – 3 drops of BDS indicator.
- Titrate with potassium dichromate solution until the first permanent colour change from yellow to intense purple is obtained.

Ferrous-iron concentration may be calculated using Equation B1.1:

$$\left[Fe^{2+}\right] = \frac{\left[K_2Cr_2O_7\right] \times V_T \times (55.84 \times 6)}{V_{Solution}}$$

Where,

$[Fe^{2+}]$ = Ferrous-iron concentration (g/L)

$K_2Cr_2O_7$ = Potassium dichromate concentration (i.e. 0.0149 M $K_2Cr_2O_7$)

V_T = Titration volume (ml) (amount of potassium dichromate added)

$V_{Solution}$ = Solution aliquot volume (ml)

C.3 Determination of total iron concentration by titration with potassium dichromate solution

- Filter 5 ml aliquot of sample solution
- Pipette the required amount of aliquot into a 125 ml conical flask
- Add 10 ml of spekker acid and heat to boil
- Add stannous chloride ($SnCl_2$) solution drop-wise until yellow colour completely disappears. Add one extra drop and record the amount of stannous chloride added.
- Allow the solution to cool to room temperature and add 10 ml of mercuric chloride ($HgCl_2$) solution. A silky-white precipitate should appear. If no precipitate forms, too little stannous chloride was added. If the precipitate is heavy and grey/black, too much stannous chloride was added. The experiment should be aborted and repeat in either case.
- Add 3 – 4 drops of barium diphenylamine indicator solution (BDS) and titrate with the potassium dichromate solution until the first permanent colour change from yellow to intense purple is obtained.

Total iron concentration may be calculated using Equation B1.1:

$$[Fe_T] = \frac{[K_2Cr_2O_7] \times V_T \times (55.84 \times 6)}{V_{Solution}}$$

Where,

$[Fe_T]$ = Ferrous-iron concentration (g/L)

$K_2Cr_2O_7$ = Potassium dichromate concentration (i.e. 0.0149 M $K_2Cr_2O_7$)

V_T = Titration volume (ml) (amount of potassium dichromate added)

$V_{Solution}$ = Solution aliquot volume (ml)

C.4 Vishniac Trace metal Solution

Vishniac trace metal solution was prepared according to the prescription by Vishniac and Santer (1957).

Weigh out accurately the following reagents and dilute to 500 ml volume with distilled water.

a) Prepare 6% KOH and dilute to 250 ml with distilled water
b) Dissolve 25 g EDTA in 100 ml of 6% KOH on a magnetic stirrer
c) In a separate 250 ml beaker, weigh the following and dissolve in 200 ml distilled water for 30 minutes on magnetic stirrer.

$ZnSO_4.7H_2O$	11 g
$CaCl_4.2H_2O$	4.62 g
$MnCl_2.4H_2O$	2.53 g
$FeSO_4.7H_2O$	2.50 g
$(NH_4)_6Mo_7O_{24}.4H_2O$	0.55 g
$CuSO_4.5H_2O$	0.79 g
$CoCl_2.6H_2O$	0.81 g

Transfer solution (c) into (b) and make up to 500 ml with distilled water by rinsing the 250 ml beaker with 200 ml distilled water (a deep greenish brown solution results)

APPENDIX D: Experimental Data

APPENDIX D

D.1 Iron Oxidation

6°C			7°C			8°C			10°C		
$[Fe_T]$	$[Fe^{2+}]$	% Fe precipitate	$[Fe_T]$	$[Fe^{2+}$	% Fe precipitate	$[Fe_T]$	$[Fe^{2+}]$	% Fe precipitate	$[Fe_T]$	$[Fe^{2+}]$	% Fe precipitate
82.25	70.61	0	80.45	66.94	0	80.45	73.08	0	85.82	81.53	0
75.10	33.10	8.696	73.30	39.31	8.889	75.09	47.20	6.667	82.24	57.56	4.167
67.94	18.79	17.39	73.30	23.03	8.889	69.73	20.68	13.33	75.09	15.11	12.5
66.16	5.763	19.57	66.15	14.89	17.78	60.79	5.570	24.44	71.51	5.557	16.67
62.58	2.830	19.57	59.00	9.057	26.67	60.79	3.317	24.44	71.51	3.789	16.67
59.00	1.431	23.91	59.00	5.382	26.67	60.79	0.9179	24.44	71.51	2.305	16.67
55.43	0.4278	28.26	59.00	3.312	26.67	59.00	0.03287	26.67	69.73	1.015	18.75
			59.00	1.558	26.67	59.00	0.027611	26.67	69.73	0.1930	18.75
			57.21	0.3752	28.89	59.00	0.00030	26.67	69.73	0.01237	18.75
			57.21	0.1192	28.89				60.79	0.003524	29.17
			57.21	0.001339	28.89				57.21	0.0002338	33.33

Units: $[Fe_T]$ (mmol L^{-1}); $[Fe^{2+}]$ (mmol L^{-1})

D.2 Iron Precipitation during ferric precipitate investigation

6°C			7°C			8°C			10°C		
Time (h^{-1})	**[Fe_T]**	**% Fe precipitate**	**Time (h^{-1})**	**[Fe_T]**	**% Fe precipitate**	**Time (h^{-1})**	**[FeT]**	**% Fe precipitate**	**Time (h^{-1})**	**[FeT]**	**% Fe precipitate**
0	55.43	32.61	0	57.21	28.89	0	59.00	26.67	0	57.21	33.33
6	53.64	34.78	6	53.64	33.33	6	55.42	31.11	6	53.64	37.50
12	50.06	39.13	12	51.85	35.56	12	53.64	33.33	12	50.06	41.67
18	50.06	39.13	18	51.85	35.56	18	50.06	37.78	18	48.27	43.75
24	48.28	41.30	24	48.27	40.00	24	48.27	40.00	24	46.48	45.83
30	44.70	45.65	30	44.70	44.44	30	46.48	42.22	30	41.12	52.08

Units: [Fe_T] (mmol L^{-1}):